

# **Direct and indirect effects of microorganisms on autophagy**

Ph.D. Thesis

**Zaid Isam Issa Al-Luhaibi**



**University of Szeged**

**Faculty of Medicine**

**Interdisciplinary Medical Sciences School**

**Supervisor:**

**Dr.habil. Klára Megyeri**

**Szeged, Hungary**

**2021**

## Table of Contents

Publications related to the subject of the Thesis: .....	4
Abstracts related to the subject of the Thesis: .....	4
Abbreviations .....	6
1. Introduction .....	9
1.1 The effect of cytokines and infectious agents on the autophagic process.....	9
1.1.1 Autophagy .....	9
1.1.2. Regulation of autophagy.....	11
1.1.3. Interaction between autophagy and pro-inflammatory cytokines .....	12
1.1.4. Autophagy facilitates IFN- $\gamma$ production.....	13
1.1.5. TNF- $\alpha$ activates and promotes autophagy.....	14
1.1.6. The impact of IL-17 on autophagy.....	14
Autophagy inhibits of IL-17 secretion .....	15
1.1.7. The IL-1 family and autophagy.....	16
Autophagy regulates the production of IL-1 $\beta$ , IL-18, and IL-1 $\alpha$ .....	16
1.1.8. IL-33 and IL-36 .....	17
1.1.9. Interleukin-36 $\alpha$ , $\beta$ , $\gamma$ , and IL-36Ra .....	18
1.1.10. Regulation of autophagy and pro-inflammatory cytokines in diseases.	19
1.1.11. Lipopolysaccharide of Gram-negative bacteria.....	21
1.2. COVID-19: SARS-CoV-2 and its cellular effects on GIT.....	22
2. Aims .....	28
3. Materials and Methods .....	29
3.1. Chemical compounds .....	29
3.2. Cell culture .....	29
3.3. Indirect Immunofluorescence assay .....	29
3.4. Western blot assays .....	30

3.5. Phospho-kinase array analysis.....	30
3.6. Statistical analysis .....	31
4. Results .....	31
4.1. The effects of IL-36 $\alpha$ and LPS on the subcellular localization of LC3B in the THP-1 cell line .....	31
4.2. The effects of IL-36 $\alpha$ and LPS on the levels of LC3B-I and LC3B-II .....	33
4.3. The effects of IL-36 $\alpha$ and LPS on the autophagic flux .....	34
4.4. The effects of IL-36 $\alpha$ and LPS on the level of Beclin-1 .....	35
4.5. The effects of IL-36 $\alpha$ and LPS on cellular signaling in the THP-1 cell line..	37
5. Discussion .....	39
5.1. IL-36 $\alpha$ and LPS cooperatively induce autophagy .....	39
5.2. The cellular effect of SARS-CoV-2 on GIT.....	42
6. Conclusion.....	45
7. Summary .....	46
8. Acknowledgements .....	48
9. References .....	49
10. Annexes .....	63

### **Publications related to the subject of the Thesis:**

1. Klara Megyeri, Áron Dernovics, **Zaid I I Al-Luhaibi**, András Rosztóczy. COVID-19-associated diarrhea

World J Gastroenterol 2021 Jun, Impact factor: 5.742, Q1

2. **Zaid I I Al-Luhaibi**, Áron Dernovics, György Seprényi, Ferhan Ayaydin, Zsolt Boldogkői, Zoltán Veréb and Klára Megyeri,\* IL-36 $\alpha$  and lipopolysaccharide cooperatively induce autophagy.

*Biomedicines* 2021 Oct, Impact factor: 6.081, Q1

### **Abstracts related to the subject of the Thesis:**

1. ESCCMID 30<sup>th</sup> 2020, Paris, France (Abstract only). **Zaid I.I Al-Luhaibi**<sup>1</sup>, Áron Dernovics<sup>1</sup>, Klára Megyeri<sup>1\*</sup> and György Seprényi<sup>2</sup>. *Investigation the pro-autophagic effect of IL-36 $\alpha$  and lipopolysaccharide in THP-1 cell line.*

2. MED-PÉCS 2021 (Abstract and Poster), **Zaid I.I Al-Luhaibi**<sup>1</sup>, Áron Dernovics<sup>1</sup>, Klára Megyeri<sup>1\*</sup> and György Seprényi<sup>2</sup>. *Investigation the pro-autophagic effect of IL-36 $\alpha$  and lipopolysaccharide in THP-1 cell line.*

**DEDICATION**

*I would like to dedicate this thesis to my family:*

*My parents: Father and Mother*

*My Brothers and Sister*

*My gorgeous Wife*

## Abbreviations

3- MA	3-Methyladenine
ACE2	angiotensin-converting enzyme type 2
AIM2	absent in melanoma 2 protein
Akt	serine/threonine protein kinase
Akt1/2/3	Ak strain transforming factor 1/2/3
AMPK $\alpha$ 1	adenosine monophosphate-activated protein kinase $\alpha$ 1
AP-1	activator protein 1
BCG	bacilli Calmette-Guerin
BCL2	B cell CLL/lymphoma 2
BFLA	bafilomycin A1
CCL	chemokine ligand
CD	cluster of differentiation
Con A	concanavalin A
COVID-19	coronavirus disease 2019
CREB	cAMP response element-binding protein
CSF	colony-stimulating factors
CXCL	C-X-C motif chemokine ligand
DCs	dendritic cells
EB	end-binding protein 1
eIF2a	eukaryotic translation initiation factor 2a
ERGIC	endoplasmic reticulum-Golgi intermediate compartment
ERK	extracellular signal-regulated kinase
ERs	endoplasmic reticulum stress
FAK	focal adhesion kinase

FLSs	fibroblast-like synoviocytes
GCN	general control nonderepressible
GIT	gastrointestinal tract
GSK3 $\beta$	glycogen synthase kinase 3 $\beta$
HLA-DR	human Leukocyte Antigen – DR isotype
Hsp90	heat shock protein 90
ICAM-1	intercellular adhesion molecule-1
IFN	Interferon
IKK	I $\kappa$ B kinase
IL-36Ra	IL-36 receptor antagonist
IL-36 $\alpha$	Interleukin-36 $\alpha$
IL-36 $\beta$	Interleukin-36 $\beta$
IL-36 $\gamma$	Interleukin-36 $\gamma$
IRAKs	IL-1 receptor-associated kinases
KFERQ	consensus peptide sequence
LBP	LPS-binding protein
LC3B	microtubule-associated protein 1 light chain 3B
LPS	lipopolysaccharide
MAPK	mitogen activated protein kinase
MEFs	mouse embryonic fibroblasts
MTOR	mechanistic target of rapamycin
MyD88	myeloid differentiation primary response 88
NF- $\kappa$ B	nuclear factor kappa-B cells
NLRP3	NOD-, LRR- and pyrin domain-containing protein 3
PAMP	pathogen-associated molecular pattern

PDI	protein disulfide isomerase
PI3P	phosphatidylinositol 3- phosphate
PIP <sub>2</sub>	Phosphatidylinositol 4,5-bisphosphate
PRAS40	proline-rich Akt substrate of 40 kDa
RA	rheumatoid arthritis
ROS	reactive oxygen species
SARS-CoV-2	severe acute respiratory syndrome coronavirus 2
SER	smooth endoplasmic reticulum
SHP2	Src homology region 2-containing protein tyrosine
SOCS	suppressors of cytokine signaling
Src	steroid receptor coactivator
STAT	signal transducer and activator of transcription
STAT	single transducer and activator of transcription
TGF	transforming growth factor
Th-17	T helper-17
THP-1	human monocytic cell line
TMPRSS2	transmembrane protease/serine subfamily member 2
TNF	tumor necrosis factor
TRAF-6	tumor necrosis factor receptor-associated kinase 6
TRAM	TRIF-related adaptor molecule
TRP	Transient receptor potential channels
VCAM-1	vascular cell adhesion molecule-1
WNK1	with no lysine kinase 1

## 1. Introduction

### 1.1 The effect of cytokines and infectious agents on the autophagic process

#### 1.1.1 Autophagy

Autophagy is an intracellular metabolic process in which cytoplasmic target molecules are transferred to the lysosome for degradation and recycling [1]. Depending on the type of cargo delivery, three different forms of autophagy can be distinguished: (i) macroautophagy, (ii) microautophagy, and (iii) chaperon-mediated autophagy. The difference among these types is how the constituents to be degraded are transported to the lysosome [1], [2]. Macroautophagy (hereafter referred to as autophagy) occurs under basal conditions and can be stimulated by environmental cues, nutrient starvation, growth factor depletion, various pathological conditions, infections, hypoxia, or pharmacological treatment [3], [4]. The major element in the regulation of autophagy is the mechanistic target of rapamycin (mTOR) pathway. The serine/threonine-protein kinase mTOR can be found in two distinct functional complexes, the mTOR complex 1 (mTORC1) and mTORC2. Only mTORC1 can directly govern autophagy [5]. Besides mTOR, mTORC1 is comprised of the regulatory-associated protein of mTOR (Raptor) and mammalian lethal with SEC13 protein 8 (mLST8) molecules. The non-core components associated with mTORC1 include proline-rich Akt substrate of 40 kDa (PRAS40) and DEP-domain containing mTOR-interacting protein (DEPTOR). Autophagy inducers inhibit mTORC1 activity, leading to consecutive activation of the ULK1 (autophagy-related gene 1 (atg1) homolog) complex and class III phosphatidylinositol 3-kinase (PI3KC3) complex, containing Beclin-1 protein [6], [7]. The activated PI3KC3 induces local production of phosphatidylinositol-3-phosphate (PI3P) at the endoplasmic reticulum membrane and thereby promotes the generation of an omegasome from which the isolation membrane is formed. PI3P attracts WD repeat domain phosphoinositide-interacting proteins (WIP1 and WIPI2), and WIPI2 then recruits a ubiquitin-like conjugation system, the ATG12-ATG5 ATG16L1 complex, to the omegasome [8]. A second conjugation system, consisting of ATG7 and ATG3, forms a covalent bond between the membrane-resident phosphatidylethanolamine (PE) and the ATG8 family member proteins, such as the microtubule-associated protein 1 light chain 3 (LC3) proteins [9]–[11]. The LC3B protein is essential for the elongation and closure of the phagophore membrane, trafficking of the autophagosomes, and their fusion with lysosomes. The autophagosomes eventually fuse with

lysosomes, the content of the autophagic cargo is degraded and made available for reuse [11]–[14].

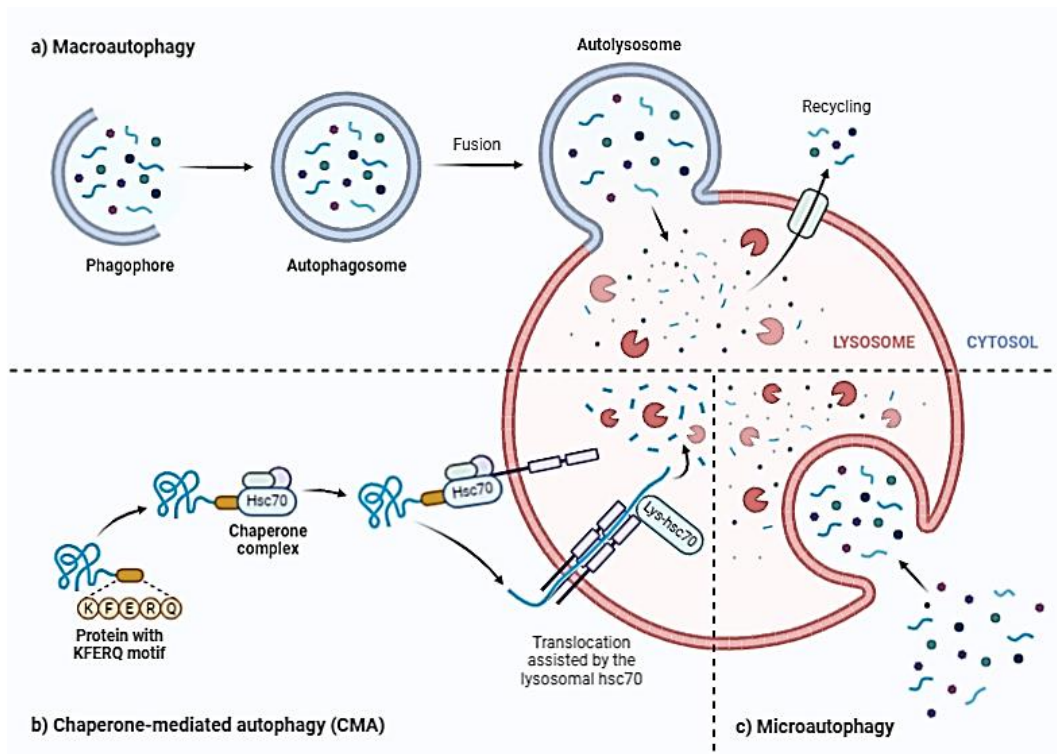


**Figure 1:** Types of autophagy. Source[15]

Autophagy is essential for the maintenance of cellular homeostasis and also plays a substantial role in pathological processes, including bacterial infections [4], [16]. Autophagic capture and delivery of bacteria to lysosomes function as a protective cellular antimicrobial defense mechanism known as xenophagy [17], [18]. Autophagy also controls bacterial infections indirectly via its multifaceted effects on the innate and adaptive immune responses [19]. The mTORC1 pathway affects the maturation, metabolic activity, activation, and differentiation of innate immune cells. Furthermore, mTORC1 regulates cytokine production by stimulating the production of type I interferons, interleukin-10 (IL-10), as well as transforming growth factor- $\beta$ , and downregulating the expression of IL-6, IL-12, IL-23, and tumor necrosis factor- $\alpha$  in monocytes, macrophages, and dendritic cells [20]. The autophagic machinery promotes the secretion of IL-1, IL-18, and high-mobility group protein B1, and facilitates antigen presentation to CD4<sup>+</sup> and CD8<sup>+</sup> T-cells [21].

### 1.1.2. Regulation of autophagy

Despite the many functions of autophagy in physiological and pathological processes, a deeper understanding of how autophagy is regulated in cells could assist in understanding how cells maintain homeostasis [7]. Autophagy is regulated by four major protein complexes, each of which is responsible for a specific stage. The ULK1 protein kinase, which is primarily made up of the ULK1, Atg13, and FIP200, plays a significant role in the early stages of autophagosome creation. The ULK1 complex controls autophagy initiation by determining the site of formation of the precursor membrane. Ser757, Ser317, and Ser556 are among the phosphorylation sites that can be phosphorylated by AMPK and mTOR [6]. The multiple phosphorylation sites on ULK1 can play different roles in autophagy, acting as either inhibitors or activators [22]. Second, the PI3KC3 complex, which includes VPS34, p150, Beclin-1, and Atg14, is essential for autophagosome nucleation and expansion. The complex can induce the production of PI3P, which acts as a landing pad for autophagy effectors. Third, the Atg12-coupled complex is mainly composed of the proteins Atg12, Atg5, and Atg16. Atg16 is noncovalently linked to Atg12–Atg5, which is essential for Atg5 and Atg12 localization to the pre-autophagosomal structure. The complex binds specifically to the precursor membrane's outer surface and mediates the final step of LC3 conjugation to PE, which is required for autophagosome formation. Finally, LC3 is cleaved by ATG4 to form LC3-I, which is conjugated to PE to form LC3-II, a reaction that requires the presence of Atg7 and Atg3. LC3-II is located in the inner and outer layers of the autophagosome, promoting expansion and closure of phagophores to form intact autophagosomes. The canonical signal transduction pathway associated with autophagy control is the PI3 K/Akt/mTOR pathway [23]. Despite the fact that this pathway is considered to control cell division and facilitate protein translation. The autophagic activity of cells can be inhibited by mTOR phosphorylation, and the mTOR inhibitor rapamycin has been shown to suppress mTOR phosphorylation and thereby activate autophagic activity. Ras/Raf/ERK, mTOR-independent inositol and calcium/calmodulin-dependent protein kinase-II (CaMK-II) are another signaling pathways that regulate autophagy [24]–[26]. Importantly, inability in precisely regulating these autophagic signaling networks may result in a number of diseases.

### 1.1.3. Interaction between autophagy and pro-inflammatory cytokines

The ubiquitous process of autophagy is strongly associated with immune and inflammatory activity. There is a two-way interaction between autophagy and pro-inflammatory cytokines; many cytokines modulate the autophagy process, and autophagy regulates many pro-inflammatory cytokines [27]. In face of a threat, pro-inflammatory cytokines, which are synthesized by adaptive and innate immune cells, play a key role in the functional responses of the immune and inflammatory systems, and the survival of the immune cells. The activity of the adaptive and innate immune systems might be regulated at a fundamental level by the relationship between autophagy and cytokines [28], [29]. The level of the autophagic activity is determined by several cytokines, such as interferon (IFN)- $\gamma$ , which initiates autophagic responses to kill pathogens, like *Chlamydia* and mycobacteria [30], [31]. Other cytokines that trigger autophagy include interleukin IL-1, IL-6, IL-17 and tumour necrosis factor (TNF)- $\alpha$ ; to counter these activators of autophagy, IL-4, IL-10, IL-13 and IL-33 inhibit the process. Autophagy simultaneously regulates the synthesis and secretion of some cytokines. The interactions between autophagy and pro-inflammatory cytokines and their significant effect upon the pathophysiology of disease, have become a point of research interest, with much being learned about the interactions. The pro-inflammatory cytokine, IFN- $\gamma$ , which plays a key role in adaptive and innate immunity, is secreted by activated CD4<sup>+</sup> and CD8<sup>+</sup> T cells, and natural killer cells [32], [33]. It achieves this by activating multiple immunomodulatory molecules; as such, IFN- $\gamma$  contributes to several inflammatory and autoimmune disorders [34]. Evidence suggests that autophagy is boosted by IFN- $\gamma$ , facilitating the presentation of antigens, the clearance of microbes and cellular proliferation. IFN- $\gamma$  secretion is stimulated by the activation of autophagy, initiating a positive feedback loop [35], [36]. Cell death can be triggered, and invading pathogens can be destroyed by IFN- $\gamma$ -stimulated autophagy. IFN- $\gamma$  promotes the autophagic elimination of intracellular pathogens by stimulating macrophages, which heightens the innate immune system's receptor-mediated phagocytosis and microbe-killing defensive processes [37], [38]. IFN- $\gamma$  may activate macrophages via a pathway involving the family M member 1 GTPase Irgm1/IRGM1, leading to maturation of mycobacteria-containing phagosomes. Studies of concanavalin A (Con A) in hepatoma cell lines show that cell death was increased by the IFN- $\gamma$  stimulation of autophagy. it has been reported IFN- $\gamma$  elevated concanavalinA (Con A)-induced autophagic flux in hepatoma cell lines. Inhibiting Irgm1 suppressed IFN- $\gamma$ /ConA-mediated lysosomal membrane permeabilization and hepatocyte death [39]. The pathway involved in IFN- $\gamma$ -

induced autophagy is dependent on mitogen-activated protein kinase (MAPK) 14 but does not require signal transducer and activator of transcription 1 (STAT1). In macrophages, the autophagy initiated by IFN- $\gamma$  involves JAK1/2, p38 MAPK and PI3K signaling [40].

The virulent strain H37Ra of *Mycobacterium tuberculosis* infects macrophages and stimulates autophagy. The co-localisation of LC3 and bacillus Calmette-Guérin (BCG) increased due to IFN- $\gamma$ -activation of macrophages prior to infection. The effect of IFN- $\gamma$  on the maturation of phagosomes containing BCG was completely absent in mouse macrophages deficient in Beclin-1; the inference of this is that autophagy is essential for IFN- $\gamma$  activity [41], [42]. Pathogens, such as *Burkholderia cenocepacia* (*B. cenocepacia*) and *Chlamydia trachomatis* (*C. trachomatis*), can rapidly be removed by IFN- $\gamma$  hastening the activation of autophagy. In human cystic fibrosis macrophages infected with *B. cenocepacia*, the formation of autophagosomes and lysosomal trafficking was improved in the presence of IFN- $\gamma$ , thereby successfully clearing the bacteria from the cells. Autolysosomes in mouse embryonic fibroblasts (MEFs) with knocked down immunity-related GTPase family member a6 (Irga6) were unable to detain *C. trachomatis*, which led to resistance to IFN- $\gamma$ -initiated death and enabled the pathogen to proliferate. This finding indicates that, Irga6 is key to IFN- $\gamma$ -instigated autophagy [43]. Apart from having a role in several infectious and systemic diseases, autophagy may also regulate normal cellular metabolism [44]. For example, the metabolism of tryptophan in human kidney epithelial cells might be regulated by IFN- $\gamma$ -mediated autophagy. Stimulating the metabolism of tryptophan in turn increased the expression of general control nonderepressible-2 (GCN2) kinase, which phosphorylates the autophagy activator, eukaryotic translation initiation factor 2a (eIF2a) [45]. Understanding how autophagy can encourage biosynthesis and contribute to the homeostasis of metabolism might yield insights into the relationship between autophagy and IFN- $\gamma$ .

#### **1.1.4. Autophagy facilitates IFN- $\gamma$ production**

In turn, the production of IFN- $\gamma$  is stimulated by autophagy, thereby enabling inflammatory responses [46]. For example, the creation of autophagosomes and IFN- $\gamma$ -induced LC3 conversion was significantly reduced in conditional knockdown of Atg5; this resulted in limited IFN- $\gamma$  secretion in CD4<sup>+</sup> T-cells. IFN- $\gamma$ -inducible inflammatory responses are noticeably improved by autophagy [47]. Also, the IFN- $\gamma$ -induced JAK2-STAT1 pathway was ineffective in Atg5 and Atg7-deficient MEFs, indicating the IFN- $\gamma$ -dependent pathway

requires the involvement of autophagy [48]. SHP2, SOCS1, and SOCS3 are known negative regulators of the IFN- $\gamma$  signaling pathway [49]. Certainly, phosphorylation of IFN- $\gamma$ -dependent STAT1 increased significantly when the expression of SHP2 was inhibited, suggesting that in Atg5<sup>-/-</sup> MEFs, SHP2 suppresses the IFN- $\gamma$  pathway [48]. Furthermore, without autophagy, the increased expression of SHP2 led to accumulation of reactive oxygen species (ROS), which inhibited STAT1. Simultaneously, the abundant ROS inhibited the JAK2-STAT1 signaling induced by IFN- $\gamma$ , in turn enabling activation of SHP2 [50], [51].

### **1.1.5. TNF- $\alpha$ activates and promotes autophagy**

TNF- $\alpha$  is a pleiotropic cytokine. It regulates various processes, including cell proliferation, differentiation, death, and proinflammatory responses. Mounting evidence indicates that TNF- $\alpha$  and autophagy are mutually obstructive [52]. The progression is hastened in several inflammatory diseases due to endotoxins stimulating the synthesis of TNF- $\alpha$ . Autophagy is primed by TNF- $\alpha$  in multiple cell types, including epithelial cells, osteoclasts, skeletal muscle cells, T-lymphoblastic leukaemic cells and vascular smooth muscle cells [52]–[57]. Through TNF- $\alpha$  modulation of the c-Jun aminoterminal kinase (JNK) pathway, the expression of LC3 and Beclin-1 is up-regulated in human atherosclerotic vascular smooth muscle cells; in the meanwhile, TNF- $\alpha$  also suppressed Akt activity [58]. Autophagy was increased in MCF-7 human breast cancer cells treated with TNF- $\alpha$ , which is attributed to the extracellular signal-regulated kinase (ERK) 1/2; meanwhile, in Ewing sarcoma cells, an abundance of ROS was generated by the down-regulation of TNF- $\alpha$ -mediated autophagy due to NF- $\kappa$ B stimulation [59], [60]. In intestinal epithelial cells of rats, TNF- $\alpha$  caused oxygen consumption to decline, increasing mitochondrial ROS production and causing the membrane potential of mitochondria to decrease. These effects promote autophagy [61]. In murine fibrosarcoma L929 cells, TNF- $\alpha$ -induced autophagy inhibited necroptosis by blocking the p38 MAPK-NF- $\kappa$ B pathway [62].

### **1.1.6. The impact of IL-17 on autophagy**

IL-17 cytokine is in fact a six-membered family of cytokines, identified as IL-17A to IL-17F. Inflammatory responses are mediated by IL-17, which is synthesised and secreted mainly by Th17 cells. In particular, IL-17A and IL-17F stimulate antibody synthesis, cytokine formation, the priming of T-cells and incite inflammation [63]. *In vitro* studies showed that B

cell autophagy increased along with the elevated IL-17 levels in experimental autoimmune myocarditis mice, which increased the activity of the ubiquitin-proteasome system and triggered ERK1/2 phosphorylation, which up-regulated p62 and Beclin-1 expression, and protected B cells from apoptosis [64]. These IL-17A-initiated changes were significantly inhibited by 3-methyladenine (3-MA). The accumulation of LC3-II was increased by IL-17A and IL-17F, which also encouraged autophagic flux, modulated the intracellular redistribution of LC3, and enabled autophagosomes and acidic vesicular organelles to form. IL-17A appears less effective than IL-17F in stimulating the autophagic cascade. *M. terrae* could be eliminated from macrophages through IL-17A and IL-17F-stimulated autophagy [63]–[65]. Besides modulating host defenses, IL-17 is implicated in the pathogenesis of rheumatoid arthritis (RA) as it causes the mitochondria in fibroblast-like synoviocytes (FLSs) to become dysfunctional, thereby increasing autophagy; FLSs invade cartilage and bone in RA [66]. The inflammation caused by IL-17 disrupts mitochondrial respiration, instigating Th17 cell infiltration. FLS survival might be enhanced by the subsequent stimulation of autophagy, which could limit apoptosis. On the other hand, the progression of pulmonary fibrosis was limited by blocking IL-17A, which initiated autophagy and reduced inflammation. The mechanisms by which IL-17A modulates autophagy have been highlighted in various studies. PI3K glycogen synthase kinase 3  $\beta$  (GSK3 $\beta$ ) signaling was initiated by IL-17A in lung epithelial cells. Activation of GSK3 $\beta$  limited B cell CLL/lymphoma 2 (Bcl-2) phosphorylation, which in turn reduced ubiquitination of Bcl-2, thus its degradation was diminished. Autophagy was inhibited by the subsequent interaction between Bcl-2 and Beclin-1. This indicates the presence of an IL17A-PI3K-GSK3B-Bcl-2 signaling cascade, which once activated, results in the downregulation of autophagy [67], [68].

### **Autophagy inhibits of IL-17 secretion**

Autophagy controls the Th1/Th17 balance in Crohn's disease and other inflammatory disorders. For example, treatment with the autophagy/lysosomal inhibitor chloroquine in human monocyte-derived Langerhans-like cells remarkably increased the IL-17A release by CD4<sup>+</sup> T cells while reducing IFN- $\gamma$  secretion. Chloroquine regulated the production of IL-17 in a p38 MAPK-dependent manner, possibly by triggering Th17 immunity. The production of IL-17 is regulated by chloroquine acting on p38 MAPK, which might stimulate Th17 immunity. Th17-cell differentiation is directed by release of IL-6 and transforming growth

factor (TGF)- $\beta$ , and IL-1. This suggests that the balance of Th1/Th17 is regulated through autophagy [69], [70].

### **1.1.7. The IL-1 family and autophagy**

Immune and inflammatory processes are regulated by pro-inflammatory interleukin cytokines (IL-1 $\alpha$ , IL-1 $\beta$ , IL-18, IL-33 and IL-36). Also known as “alarmins”, reflecting their ability to send out an alert calling for inflammatory responses, these cytokines are ‘first line responders’, being secreted in the earliest stages of inflammation. Acting in a self-regulatory manner, autophagy, which can be initiated by IL-1 $\alpha$  and IL-1 $\beta$ , regulates the secretion of IL-1 $\alpha$ , IL-1 $\beta$ , and IL-18 and their destruction [71]. Synthesized mainly by macrophages and monocytes, IL-1 $\beta$ , is considered the ‘master’ pro-inflammatory cytokine. Inflammatory cascades are initiated by the binding of IL-1 $\alpha$  and IL-1 $\beta$  to IL-1 receptor 1. Acting as the ‘master’, IL-1 $\beta$  can influence inflammatory responses by initiating the synthesis of IL-1 $\alpha$  and IL-23. IL-1 $\beta$  acts as a natural adjuvant, prompting antigen-specific immune responses. IL-1 $\alpha$  and IL-1 $\beta$  have also been identified as being capable of causing the formation of autophagosomes. Furthermore, these proinflammatory cytokines might limit inflammatory responses by stimulating autophagy as part of a negative feedback loop and support cytokine-mediated anti-microbial defence mechanisms [72]. ERS was activated by IL-1 $\beta$  in mouse pancreatic acinar cells, stimulating the release of Ca<sup>2+</sup> into the cytosol, culminating in autophagy [73]. It was noted that trypsin was activated by impaired autophagic flux, resulting in damage to the pancreas. However, protective effects were cast by mitochondrial signals stimulated by IL-1 $\beta$ -initiated autophagy [74].

### **Autophagy regulates the production of IL-1 $\beta$ , IL-18, and IL-1 $\alpha$**

Based on being localised to the autophagosomes’ intermembrane space, the secretion and degradation of IL-1 $\beta$  might be autophagic-dependent. The synthesis of IL-1 $\beta$ , which needs to be activated by caspase-1 and the formation of inflammasomes, is powerfully regulated by autophagy. To deliver IL-1 $\beta$  to autophagosomes requires two lysosome-targeting KFERQ sequences and the chaperone protein Hsp90 [73]. Autophagy helps the release of IL-1 $\beta$  by acting on alternative mechanism that involves the AIM2 inflammasome. The accumulation of AIM2 inflammasomes in an epithelial cell line, was linked to end-binding protein 1 (EB1) [75]. More research focusing on the inflammasomes and their interactions is

needed. Autophagy reduces IL-1 $\beta$  secretion indirectly by actively targeting pro-IL-1 $\beta$  to be degraded by lysosomes. In response to LPS stimulation, in mouse macrophages with knockdown of ATG16L1, the secretion of IL-1 $\beta$  increased [76]. It is hypothesised that macrophages and DCs in which Atg7 or Beclin-1 was deleted, or treated with 3-MA, synthesised IL-1 $\beta$  when challenged by TLR3 or TLR4 agonists. IL-1 $\beta$  localised to autophagosomes when macrophages were treated with TLR agonists [77]. Moreover, due to increased cleavage of pro-IL-1 $\beta$  in the liver, serum levels of the active form of IL-1 $\beta$  were considerably higher in mouse macrophages with knockdown of ATG5 [78]. The expression of IL-1 $\beta$  mRNA expression was significantly upregulated by LPS in ATG7-silenced mouse intestinal epithelial cells. Furthermore, autophagy targets in particular pro-IL-1 $\beta$  for lysosomal degradation and therefore indirectly reduces IL-1 $\beta$  secretion. The genetic knockdown of Atg16L1 in macrophages increased IL-1 $\beta$  release in response to LPS stimulation in mice [79]–[82]. In addition, down-regulation of autophagy enhanced the production of IL-18, which was processed by caspase-1 in an inflammasome-dependent manner. Treatment with 3-MA further increased the LPS-stimulated formation of IL-1 $\alpha$  via a mechanism independent of NLRP3 [83]–[85].

#### **1.1.8. IL-33 and IL-36**

The pro-inflammatory cytokines, IL-33 and IL-36, are the newest members of the IL-1 family to be discovered. These are present in particular immune cells and various tissues. The action of both IL-33 and IL-36 is to prompt natural killer cells to produce cytokines and chemokines, which modulate the innate immune system's responses to invading pathogens. In response to IL-33 and IL-36, Th1 cells upregulate their production of cytokines; however, the results of IL-33 and IL-36 activity is determined by the host's overall immune condition [71]. Until recently, there has been limited understanding of the relationship between these cytokines and autophagy. However, evidence from one murine study indicates that IL-33 reduces the inflammatory response and apoptosis. The effect was protective, defending the mice against collagenase-induced intracerebral haemorrhagic injury [86]. Likewise, due to IL-33 inhibiting apoptosis and autophagy, the neurons in neonatal rats were protected against deleterious consequences of recurrent seizures [87]. There are three subtypes of IL-36 cytokines: IL-36 $\alpha$  (IL-1F6), IL-36 $\beta$  (IL-1F8) and IL-36 $\gamma$  (IL-1F9). They activate MAPKs and NF- $\kappa$ B by acting on the same signaling cascade and by binding to the same heterodimeric receptors [88]. IL-36 contributes to the adaptive immune response by provoking the release

of chemokines and cytokines, which in turn recruits and activates CD4<sup>+</sup> T cells and DCs. As yet, research has not explored whether during the immune response the stimulation of IL-36 is modulated by autophagy.

### 1.1.9. Interleukin-36 $\alpha$ , $\beta$ , $\gamma$ , and IL-36Ra

IL-36 $\alpha$ , IL-36 $\beta$ , IL-36 $\gamma$ , and IL-36 receptor antagonist (IL-36Ra) belong in the IL-36 subfamily of the IL-1 cytokine family [89]–[91]. The IL-36 subfamily includes three agonist cytokines (IL-36 $\alpha$ / $\beta$ / $\gamma$ ) as well as the natural antagonist of IL-36 (IL-36Ra). Expression of IL-36 $\alpha$  can be observed at low levels in many different tissues most notably in the skin, esophagus, tonsil, lung, gut, and brain. IL-36 $\alpha$  can also be secreted by the immune cells including monocytes/macrophages and T cells [94]. IL-36 $\alpha$ / $\beta$ / $\gamma$  are highly induced in response to several stimuli including cytokines, Toll-like receptor agonists, bacteria, viruses, and various pathological conditions. The IL-36 subtypes are synthesized as precursor proteins. Cleavage of the precursor form of IL-36 $\alpha$  at a specific site located at nine amino acids N-terminal to a conserved A-X-Asp motif highly increases the affinity of the truncated cytokine to the receptor and enhances its biological activity [93], [94]. Proteases derived from neutrophil granulocytes such as cathepsin G, elastase, and proteinase-3 are involved in the processing and activation of IL-36 $\alpha$  by proteolytic cleavage [94], [95]. The truncated IL-36 $\alpha$ / $\beta$ / $\gamma$  bind to the IL-36R (IL-1Rrp2) and use the IL-1 receptor accessory protein (IL-1RAcP) as a co-receptor [90], [96], [97]. Following ligand binding, the Toll/IL-1 receptor (TIR) domain—located in the intracellular portion of the IL-36R:IL-1RAcP heterodimer—recruits myeloid differentiation primary response 88 (MyD88) adaptor protein, which in turn interacts with IL-1 receptor-associated kinases (IRAKs) and tumor necrosis factor receptor-associated kinase 6 (TRAF-6) [90], [98]. The MyD88/IRAK/TRAF6 platform activates activator protein 1 (AP-1), cAMP response element-binding protein (CREB) and nuclear factor- $\kappa$ B (NF- $\kappa$ B) transcription factors via I $\kappa$ B kinase (IKK), mitogen-activated protein kinases (MAPKs) including the extracellular signal-regulated kinases (ERKs), c-Jun N-terminal kinases (JNKs), and p38 [90], [91], [97].

IL-36 subtypes stimulate the production of several cytokines (IL-1 $\alpha$ , IL-1 $\beta$ , IL-2, IL-4, IL-6, IL-8, IL-10, IL-12, IL-17, IL-18, IL-22, IL-23, TNF $\alpha$ , HB-EGF, and IFN- $\gamma$ ), colony-stimulating factors (GM-CSF and G-CSF), chemokines (CCL1-3, CCL20, CXCL1-3, CXCL5, CXCL10, CXCL12), and cell adhesion molecules (VCAM-1, ICAM-1) in various

cell types [99]–[101]. Furthermore, IL-36 cytokines increase the intracellular level of antimicrobial peptides (beta-defensins 2 and 3, LL37, and protein S100-A7) and elevate the expression of major histocompatibility complex class 2 and clusters of differentiation 14 (CD14), CD40, CD80/CD86, and CD83 [100]–[102]. IL-36 $\alpha/\beta/\gamma$  thereby activate innate immune cells and induce inflammation. The pro-inflammatory IL-36 subfamily members also modulate the adaptive immune responses by stimulating TH-cell proliferation and promoting CD4<sup>+</sup> T lymphocyte differentiation toward TH1, TH17, and TH9 phenotypes. IL-36 $\gamma$  was shown to activate natural regulatory T-cells (Tregs) [103] and inhibit the generation of induced Tregs [104]. In acute resolving inflammation, IL-36  $\alpha/\beta/\gamma$  has been suggested to facilitate the elimination of pathogenic microorganisms, the resolution of tissue injury, and the restoration of tissue integrity. However, in chronic inflammatory processes, these IL-36 subtypes can exert a pathogenic effect by amplifying inflammatory processes [105]. IL-36 cytokines play important roles in various diseases including asthma, chronic obstructive pulmonary disease, ankylosing spondylitis, rheumatoid arthritis, psoriasis, systemic lupus erythematosus, glomerulonephritis, diabetes, and obesity [106], [107].

#### **1.1.10. Regulation of autophagy and pro-inflammatory cytokines in diseases**

Numerous infectious, autoimmune and inflammatory diseases could potentially be treated by therapeutically targeting autophagy [108], [109]. Cellular homeostasis is supported by autophagy modulating inflammatory and immune responses, which helps to eliminate bacterial, fungal, protozoan and viral pathogens [110]–[113]. Autophagy and immune processes are heavily influenced by proinflammatory cytokines, such as TNF- $\alpha$ , IL-1 $\beta$ , and IFN- $\gamma$ , which help to remove *M. tuberculosis* from host cells by stimulating autophagy [38], [114]. In that instance, autophagy activated T cells, promoted antigen presentation and triggered the fusion of lysosomes with autophagosomes containing the pathogen. Several pathogenic microorganisms, including *B. cenocepacia*, *C. trachomatis* and *Toxoplasma gondii*, can be eliminated with the assistance of autophagy stimulated by IFN- $\gamma$  [31], [43], [113]. The antigen presentation and phagocytic abilities of monocytes are enhanced by IFN- $\gamma$  priming. There is a strong relationship between restoring immune function and IFN- $\gamma$ -primed autophagy. Indeed, HLA-DR expression in the alveolar macrophages of trauma patients can be increased substantially by inhaling IFN- $\gamma$ , decreasing the risk of developing ventilator-associated pneumonia [115]. The treatment has been used in a number of patients

with severe infections; a notable response was observed in one septic patient with mucormycosis, whose condition improved very quickly following the administration of IFN- $\gamma$  in conjunction with nivolumab, an anti-PD1 antibody [116], [117]. Although autophagy can confer therapeutic benefits, excessive or unregulated autophagy may contribute to pathology. As described earlier, acute pancreatitis occurred in response to activated trypsinogen and autophagic flux being out of balance, due to IL-1 $\beta$  [73]. Based on this observation, treatment for this disease could potentially include interventions that modulate autophagy driven by IL-1 $\beta$ . Furthermore, in patients with RA, it was noted that osteoclast-oriented bone resorption and erosion was influenced by TNF- $\alpha$  dependent autophagy. The drugs, chloroquine and hydroxychloroquine, may be effective treatments for RA, as they inhibit autophagy, limiting bone loss [55]. Moreover, IL-17 caused mitochondrial dysfunction in FLSs in RA, and enhanced the formation of autophagosomes that showed anti-apoptotic properties and promoted FLS survival [66]. Based on the evidence garnered thus far about IL-17 and TNF- $\alpha$ , there is a potential therapeutic benefit to regulating these cytokines to alleviate RA. Also, the inhibition of inflammation, autophagy and apoptosis by IL-33 has been found to confer neurons with protection against deleterious effects of recurrent neonatal seizure and intracerebral haemorrhage [86], [87]. More research is required to establish whether IL-33 offers any therapeutic potential that could be exploited in clinical settings to treat a range of diseases.

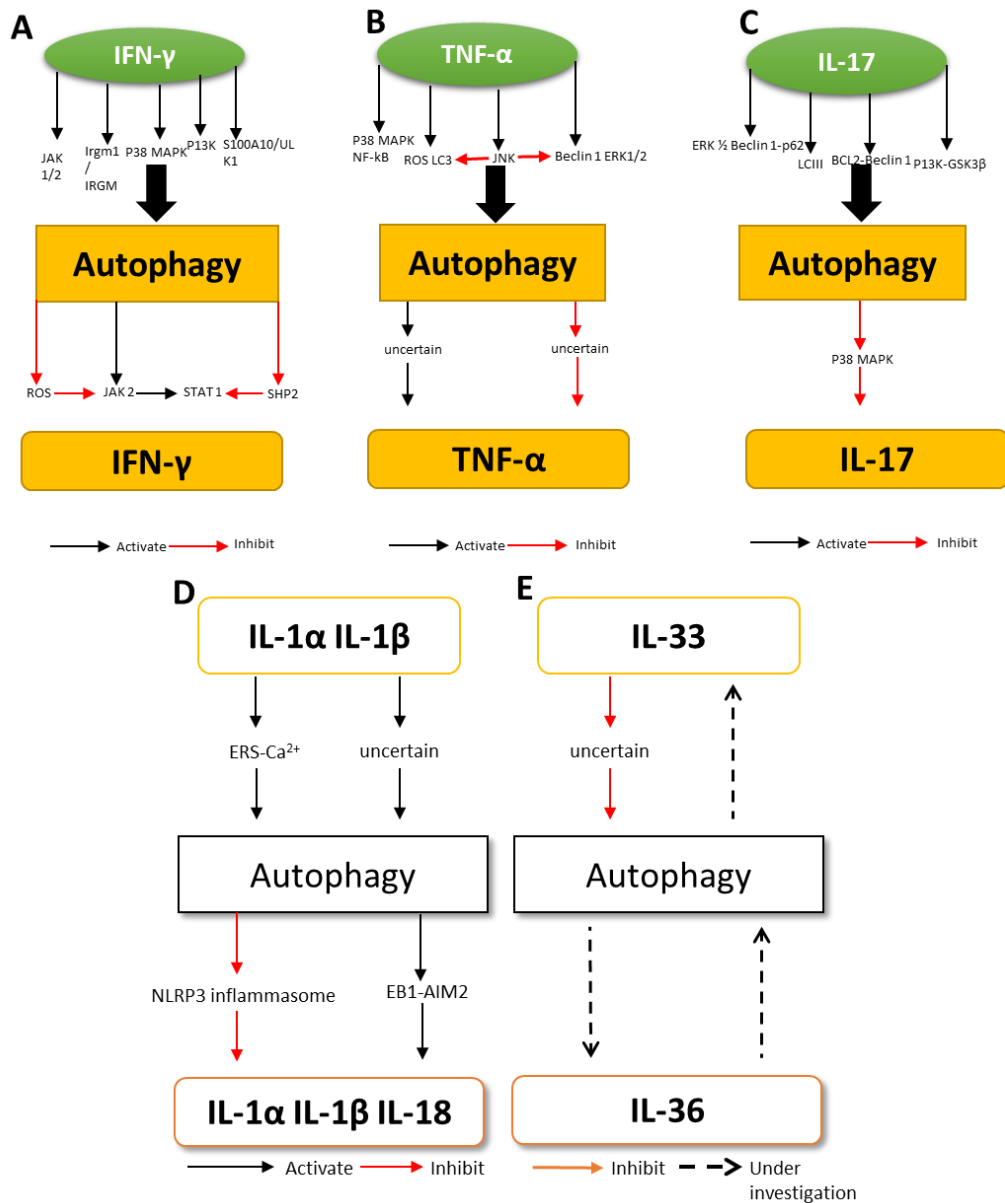


**Figure 2:** Mechanisms underlying the interplay between proinflammatory cytokines and autophagy. (a) IFN- $\gamma$  leads to autophagic activation via multiple mechanisms, including regulation of the JAK1/2, Irgm1/IRGM, p38 MAPK, S100A10/ULK1, and PI3K pathways. Autophagy, in turn, enhances IFN- $\gamma$  formation via the ROS/JAK2/STAT1 and SHP2/STAT1 signaling pathways. (b) TNF- $\alpha$  positively regulates autophagy through the ERK1/2, JNK, p38 MAPK-NF- $\kappa$ B, and ROS signaling pathways. Autophagy modulates TNF- $\alpha$  induction in a context-dependent manner. (c) IL-17 activates the ERK1/2-Beclin-1-p62 pathway leading to autophagy. On the other hand, IL-17 inhibits autophagy via the Bcl-2-Beclin-1 and PI3K-GSK3 $\beta$  pathways. Autophagy, in turn, down-regulates IL-17 production via p38 MAPK signaling. (d) IL- $\alpha$  and IL-1 $\beta$  activate endoplasmic reticulum stress (ERS) with subsequent autophagy, while autophagy enhances the formation of IL- $\alpha$ , IL-1 $\beta$ , and IL-18 in an NLRP3 inflammasome-dependent manner. (e) IL-33 has potential negative effects on autophagy. Source [27].

### 1.1.11. Lipopolysaccharide of Gram-negative bacteria

Lipopolysaccharide (LPS) is a powerful immunomodulatory molecule that contributes to the pathogenesis and clinical symptoms of infections caused by Gram-negative bacteria. LPS is the major structural component of the outer bacterial membrane and is composed of O antigen, poly/oligosaccharide core, and lipid A, termed endotoxin [118], [119]. LPS is a

pathogen-associated molecular pattern (PAMP) detected by sensor molecules located in the cytoplasmic and endosomal membranes as well as in the cytoplasm of cells [120]–[122]. Extracellular LPS is sensed and extracted from the bacterial outer membrane by the LPS-binding protein (LBP) and CD14 [120]–[122]. CD14 transfers monomeric LPS molecules to the Toll-like receptor 4 (TLR4)/myeloid differentiation factor 2 (MD-2) heterodimer leading to a conformational change and crosslinking of TLR4/MD2 receptor complexes [120]–[122]. In the cytoplasmic membrane, the dimerized TIR domain in the cytoplasmic portion of TLR4 consecutively recruits TIR domain-containing adaptor protein (TIRAP), MyD88, and IRAK proteins, thus leading to the assembly of a supramolecular complex termed the myddosome. The LPS-TLR4/MD2 complexes can also be internalized into endosomes. The TIR domain of endosomal TLR4 binds TRIF-related adaptor molecule (TRAM), which attracts TIR domain-containing adaptor-inducing interferon- $\beta$  (TRIF) resulting in the formation of another complex called the triffosome [121], [123]. Myddosomes and triffosomes recruit TRAF6 or TRAF3 and activate AP-1, NF- $\kappa$ B, CREB, and interferon regulatory factor 3 (IRF-3) via MAPKs, IKK, and class I PI3K [118], [120], [121]. The activated transcription factors turn on the expression of various cellular genes encoding inflammatory mediators including cytokines [118], [120], [121]. In addition to TLR4, another group of cytoplasmic membrane receptors—the transient receptor potential (TRP) cationic channels—can also bind LPS [118], [124]. TRP cation channel subfamily V members 2 and 4 (TRPV2 and TRPV4) and TRPM7 also contribute to the LPS-mediated activation of innate immune cells by triggering intracellular Ca<sup>2+</sup> mobilization and secretion of nitric oxide [125], [126]. Additionally, intracellular LPS within the cytoplasm of cells directly binds to the caspase activation and recruitment domains of caspase-4/5 in humans and caspase-11 in mice, which in turn leads to activation of inflammatory caspases, secretion of IL-1 $\beta$  and IL-18, as well as induction of pyroptosis [127]. In localized infections caused by Gram-negative bacteria, LPS-mediated activation of the immune response is protective by restricting bacterial invasion whereas the exaggerated inflammation seen in systemic infections is of pivotal pathogenetic and prognostic importance.

## **1.2. COVID-19: SARS-CoV-2 and its cellular effects on GIT**

Severe acute respiratory syndrome coronavirus 2 (SARS-CoV-2) recently emerged as a highly virulent respiratory pathogen that is known as the causative agent of coronavirus

disease 2019 (COVID-19) [128]. SARS-CoV-2 enters the human body through the airways and multiplies in the lungs. This novel coronavirus causes mild, severe, and critical respiratory disease in 81%, 14%, and 5% of cases, respectively [129]. It may also enter the bloodstream, which results in viremia and systemic spread throughout the body.

In addition to the airways, the virus can multiply in the gastrointestinal tract (GIT), urinary tract, and central nervous system. The infection elicits an intemperate immune response characterized by a life-threatening cytokine storm and a corrupted IFN system, which is unable to eliminate the pathogen effectively. As a result, a systemic inflammatory response syndrome occurs [130], [131]. In the severe and critical clinical manifestations of COVID-19, atypical pneumonia leading to progressive respiratory failure develops [129].

SARS-CoV-2 belongs to the genus *Betacoronavirus* of the family *Coronaviridae*, which comprises enveloped viruses with positive-sense single-stranded RNA genomes [132]–[134]. The spherical or elliptical virions are pleomorphic with diameters of 80-160 nm. The capsid has helical symmetry, which is built up by the nucleocapsid (N) protein. The spike (S), membrane (M), and envelope (E) proteins are located in the virion envelope [135], [136].

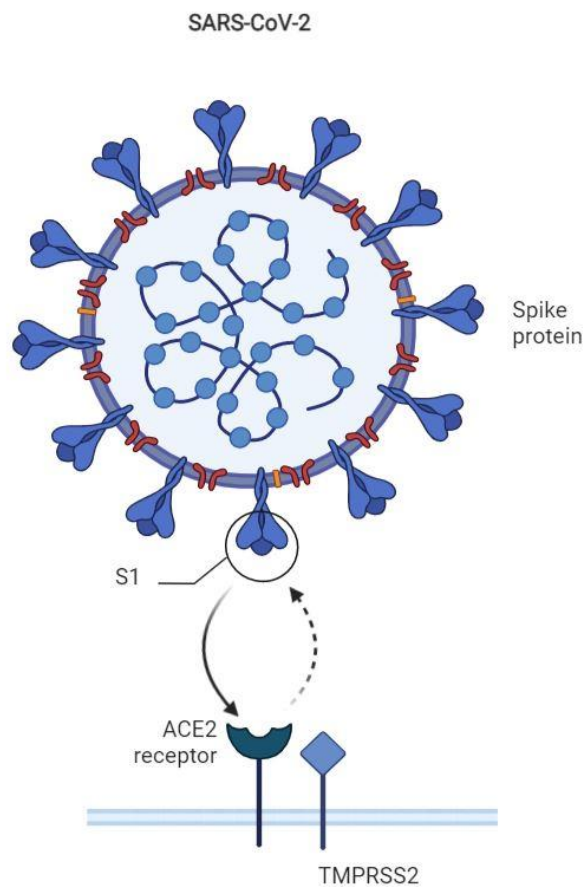


**Figure 3:** structure of SARS-CoV-2. Source[15]

Initially, the S protein of SARS-CoV-2 binds to its corresponding cell-surface receptor, angiotensin-converting enzyme type 2 (ACE2) [137], [138]. The S protein has two subunits: S1 and S2. The S1 subunit has a receptor-binding domain and is responsible for receptor engagement, whereas the S2 subunit is involved in the fusion process [138]–[140]. Following ACE2 binding, cellular proteases such as transmembrane protease/serine subfamily member 2 (TMPRSS2), TMPRSS4, and cathepsin L cleave S protein into S1 and S2 subunits, and the virus enters the host cell by receptor-mediated endocytosis [141]–[144]. These enzymes may also facilitate entry or expand the tissue tropism of SARS-CoV-2 [144]–[148].

The viral mRNAs are translated in the rough endoplasmic reticulum, leading to the formation of accessory proteins and structural proteins (N, M, E, and S). The M, E, and S proteins then become embedded in the endoplasmic reticulum, whereas the N proteins assemble with the newly synthesized full-length positive-sense RNA to form the nucleocapsid [149], [150]. After being transported to the ERGIC (endoplasmic reticulum-Golgi intermediate compartment), the nucleocapsids bud through the ERGIC membrane into its lumen. The mature virions reach the cytoplasm membrane *via* vesicular transport and are released from the cell [149], [150].

It has been determined that the symptoms of COVID-19 infection begin between 1-14 days after exposure to the virus. However, the scientists have classified the period of infection into 4 clinical phases [151], [152]. The infectious-virological phase (Phase 1) maximum duration 8 days. The presence of the virus in the upper airways and digestive tract stimulates usually specific symptoms, such as dry cough, fever, fatigue with normal peripheral oxygen saturation, diarrhea, headache, and conjunctivitis in the adults. As the humoral immune response is activated, plasma cells produce immunoglobulin (IgM and IgG antibodies). The infection triggers the synthesis of various inflammatory cytokines (IL-6). These responses especially if followed by reasonable pharmacological treatment, convert into an infective resolution in 80% of cases. The variety of responses in older patients in different categories (fit, frail, disable) is an important topic to be investigated [153] (Figure 4).

The pulmonary phase (Phase 2) usually begins after 10 days on average after the commencement of symptoms. During this phase the virus migrates to the lower respiratory tract and lung. The characteristic symptoms, such as shortness of breath, severe dyspnea and

fatigue can continue for 5 days or more. Low peripheral oxygen saturation ( $SpO_2 < 95\%$ ) characterizes this phase. Endothelial and initial cardiac damage may also occur [154]. Hospitalization in semi-intensive wards could be required at this stage. Clinical complications are more common in men than in women. This difference can be explained by a higher expression level of ACE2 receptors in adult human testes at the single-cell transcriptome level, indicating that this organ could be a possible target of SARS-CoV-2 infection and one of the causes of rapid spread of the disease [155] (Figure 4).

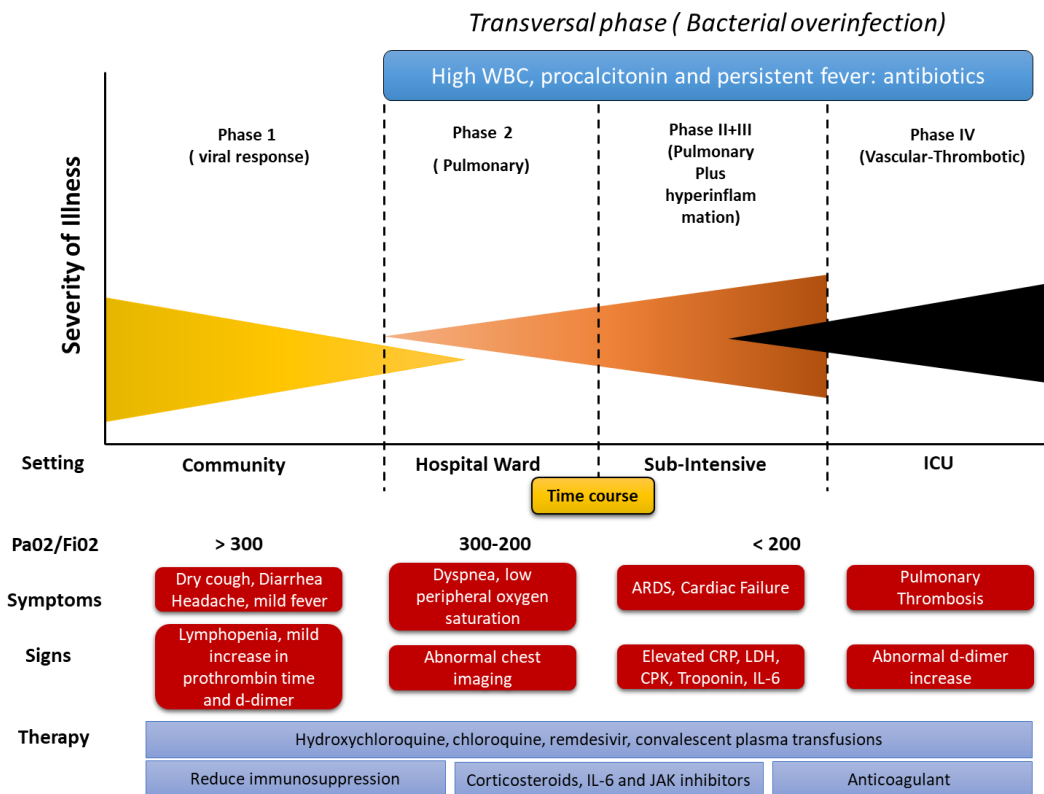


**Figure 4:** COVID 19 disease across different possible phases, therapeutic strategies, and settings. In Phase 1, viral response predominates, and respiratory and gastrointestinal symptoms can be treated at home with favipiravir. In Phase 2: pulmonary symptoms, fever and dyspnea worsen and rapid diagnosis by CT and hospitalization is required. In Phase 3, pulmonary and hyperinflammatory manifestations, clinically represented by ARDS, corticosteroids and IL-6 receptor antagonists should be started in sub-intensive wards. In Phase 4, thrombotic, anticoagulant therapy should be introduced and admission to ICU indicated. There is a transverse phase: bacterial superinfection, typically characterized by high fever, increased white blood cells and procalcitonin, where broad-spectrum antibiotic therapy is the choice treatment. Source: [152]

The Hyperinflammatory pulmonary phase ( Phase 3 ) is characterised by systemic symptoms with multi-organ involvement (ARDS SIRS/ Shock Cardiac Failure). It requires hospitalization in ICUs or respiratory intensive care units [156]–[158].

Endothelial damage, local and widespread thrombotic phenomena, and pulmonary hypertension are all indications of the vasculitic-thrombotic phase ( Phase 4 ) [159]. There is

an evidence to support the use of enoxaparin, which is well known for its antiviral effect, at high doses and dependent on weight and renal function, especially during this phase [160], [161]. The usual serum biomarker picture of this phase is characterized by normal WBC, extreme high levels of D-dimer, and troponin I that may indicate the possibility of thrombotic events in various organs.

GIT involvement is frequent in COVID-19 patients and includes anorexia, nausea, vomiting, diarrhea, and abdominal pain [162]–[170]. Among the specific GI symptoms, diarrhea is the most common. Based on different studies, the prevalence of diarrhea might range from 2% to 49.5% [169], [171], [172]. The reason why GI symptoms occur in only a subset of COVID-19 patients is currently unknown. There are no significant differences between the two patient groups in terms of demographics and certain coexisting conditions, such as pregnancy, cancer, chronic renal disease, chronic obstructive pulmonary disease, or immunosuppression. A study conducted by Jin *et al* [164] revealed that the rate of chronic liver disease in COVID-19 patients with GI symptoms is much higher than among those without GI symptoms. Moreover, the incidence of COVID-19 with GI symptoms displays familial clustering [164]. Based on these interesting observations, it is reasonable to infer that genetic, immunological, and epidemiological factors are involved in the development of COVID-19-associated diarrhea.

The treatment of COVID-19 is based on the phase of infection or the severity of the case. At the first phases, anti-inflammatory drugs are applied for 7-8 days such as chloroquine or hydroxychloroquine [173]. Although numerous antiviral medications have been considered, such as lopinavir/ritonavir and remdesivir have gained considerable attention. The first antiviral medication, lopinavir/ritonavir, was used to treat HIV and SARS in 2003 [174]. Another antiviral agent is remdesivir, which is a promising pharmaceutical drug and is currently being examined by several clinical trials as a possible COVID-19 medication [175]. On February 15, 2020, Favipiravir, an antiviral drug made by the Japanese pharmaceutical company Fujifilm Toyama Chemical, was authorized for the treatment of new influenza in China, and clinical studies are now underway. According to preliminary data from 80 individuals, favipiravir exhibited a more powerful antiviral impact than lopinavir/ritonavir and even had fewer adverse effects [176].

However, because no current definitive specific treatment for COVID-19 infection has been proven in a randomized clinical trial, WHO has now launched an efficacy study to investigate

four potential treatments: remdesivir, chloroquine/hydroxychloroquine, lopinavir and ritonavir, and lopinavir and ritonavir plus interferon $\beta$ -1. The major limitation of this study is that it will not be double blind; nevertheless, it will involve thousands of patients from many nations [177].

## 2. Aims

Our specific aims were:

**Aim 1: Investigation of the pro-autophagic effect of IL36 $\alpha$  and lipopolysaccharide in the THP-1 cells line.**

Our aim was to examine the (i) the levels of LC3B-I and LC3B-II, (ii) the autophagic flux, (iii) the subcellular localization of LC3B and Beclin-1 and (iv) the signaling pathways activated in THP-1 cells treated with IL-36 $\alpha$  and LPS alone or in combination.

**Aim 2: Collection of literature data on the main cellular effect of SARS-CoV-2 on GIT.**

In our review study, we aimed to summarize the effects of SARS-CoV-2 on the autophagic activity, viability, ion secretion, and inflammatory response of enterocytes. Furthermore, we also collected literature data on the role of the cellular effects exerted by SARS-CoV-2 in the development of COVID-19 gastrointestinal manifestation.

### 3. Materials and Methods

#### 3.1. Chemical compounds

Human recombinant IL-36 $\alpha$  (Biomol GmbH, Hamburg, Germany) was prepared in sterile distilled water and used at 10 ng/ml concentration in all experiments. Human recombinant IL-36Ra (Sigma–Aldrich, St. Louis, MO, USA) was prepared in sterile distilled water and used at 20-fold molar excess. A stock solution of autophagy inhibitor bafilomycin A1 BFLA (Santa Cruz Biotechnology, Dallas, TX, USA) was prepared in dimethyl sulfoxide. BFLA was used at a concentration of 100 nM in all experiments. LPS from *Escherichia coli* O111:34 (Sigma–Aldrich, St. Louis, MO, USA) used at 500 ng/ml in all experiments.

#### 3.2. Cell culture

The THP-1 human pro-monocytic cell line was grown in Dulbecco's modified Eagle's minimal essential medium (Sigma–Aldrich) supplemented with 10% fetal calf serum (Lonza, Verviers, Belgium) and 1% of an antibiotic/antimycotic (AB/AM) solution (Lonza) at 37 °C in a 5% CO<sub>2</sub> atmosphere.

#### 3.3. Indirect Immunofluorescence assay

Cytospin cell preparations were fixed in methanol acetone (1:1) for 10 minutes at -20 °C. The cells were treated with 1% bovine serum albumin in PBS for 30 min at 37 °C to block non-specific binding of the antibodies. To detect LC3B, the slides were stained with a 1:150 dilution of rabbit polyclonal antibody to LC3B (Sigma-Aldrich) for 1 h at 37 °C. To detect Beclin-1, the slides were stained with a 1:100 dilution of rabbit polyclonal antibody to Beclin-1 (Sigma-Aldrich) for 1 h at 37 °C. After washing with PBS, the samples were reacted with a 1:300 dilution of CF488A-conjugated anti-rabbit antibody (Sigma-Aldrich) for 1 h at 37 °C. The cells were visualized by confocal microscopy using an Olympus FV1000 confocal laser scanning microscope using UPLSAPO 60X (N.A. 1.35) oil immersion objective and 488 nm laser excitation with 500-600 nm detection range. LC3B-positive vacuoles were automatically quantified for each field after subtraction of the background level and establishment of an intensity threshold using ImageJ software (U.S. National Institutes of Health, Bethesda, MD, USA). The numbers of the LC3B-positive puncta were normalized by the numbers of cells in each field. An average of 500 cells was analyzed for each condition. The fluorescence intensity of LC3B was determined using the surface plot functions of the ImageJ software. The mean fluorescence intensity (MFI) method was used to quantify the fluorescent signal

intensities of cells. ImageJ software was used to draw an outline around each cell, and the MFI was measured. The corrected total cell fluorescence (CTCF) was calculated via the following formula:  $CTCF = \text{integrated density} - (\text{area of selected cell} \times \text{mean fluorescence of background readings})$ .

### **3.4. Western blot assays**

The cells were homogenized in CytoBuster lysis buffer (Merck KGaA, Darmstadt, Germany), and the mixture was then centrifuged at 10,000 g for 10 min to remove cell debris. Protein concentrations of cell lysates were determined using the Bio-Rad protein assay (Bio-Rad Laboratories Inc., Hercules, CA, USA). Supernatants were mixed with Laemmli sample buffer and boiled for 3 min. Aliquots of the supernatants were resolved by SDS-PAGE and electrotransferred onto Immun-Blot polyvinylidene difluoride (PVDF) membranes (Bio-Rad Laboratories Inc.). The membranes were blocked in PBS containing 0.05% Tween 20, and 5% dried non-fat milk (Difco Laboratories Inc., Detroit, MI, USA). The pre-blocked blots were probed with the appropriate antibodies for 4 h in PBS containing 0.05% Tween 20, 1% dried non-fat milk and 1% bovine serum albumin (Sigma-Aldrich). Rabbit anti-LC3B (Sigma-Aldrich) and rabbit anti- $\beta$ -actin (Sigma-Aldrich) primary antibodies were used at a 1:1000 dilution. Blots were then incubated for 2 h with peroxidase-conjugated anti-rabbit antibody (Sigma). Membranes were developed using a chemiluminescence detection system (GE Healthcare, Chicago, IL, USA). The autoradiographs were scanned with a GS-800 densitometer (Bio-Rad Laboratories Inc.), and the relative band intensities were quantified using ImageJ software [178].

### **3.5. Phospho-kinase array analysis**

A human phospho-kinase array (R&D Systems Inc., Minneapolis, MN, USA) was used to measure the relative phosphorylation levels of 43 signaling molecules. Control cells and cultures treated with IL-36 $\alpha$  and LPS alone or in combination for 30 min were homogenized in lysis buffer and centrifuged for five min at 14,000  $\times$  g. Protein concentrations of the supernatants were determined using a Bio-Rad protein assay (Bio-Rad Laboratories Inc.); after blocking, 300  $\mu$ g of protein was incubated with each array overnight at 4  $^{\circ}$ C. After washing, the arrays were reacted with a cocktail of phospho-site-specific biotinylated antibodies for two hours at room temperature, carefully washed again, and incubated with streptavidin–peroxidase for 30 min at room temperature. Signals were developed using a chemiluminescence detection system and recorded on autoradiography film. Spot densities of

phospho-proteins were quantified using ImageJ software [178] and normalized to those of positive controls on the same membrane after subtraction of background values.

### **3.6. Statistical analysis**

Statistical significance was analyzed by one-way ANOVA followed by Tukey's or Sidak's multiple comparison post-hoc tests. All statistical analyses were performed using GraphPad Prism 6 software (GraphPad Software Inc. San Diego, CA, USA). and P values less than 0.05 were considered statistically significant.

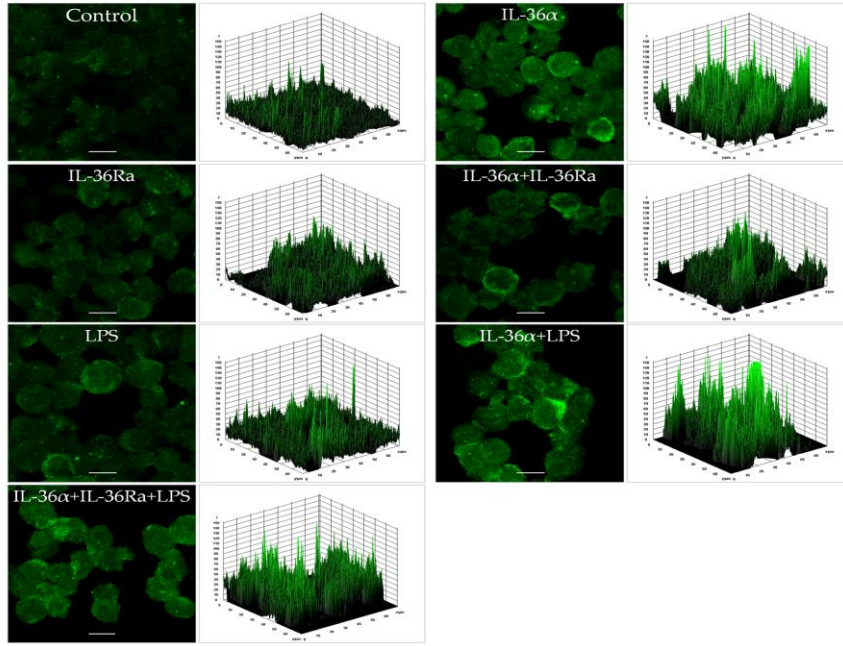
## **4. Results**

### **4.1. The effects of IL-36 $\alpha$ and LPS on the subcellular localization of LC3B in the THP-1 cell line**

To elucidate how IL-36 $\alpha$  and LPS affect the basal autophagy, we treated THP-1 cells with IL-36 $\alpha$  and LPS alone or in combination and measured the subcellular localization of LC3B.

Indirect immunofluorescence assays could determine the intracellular localization of LC3B at the 6-h time point and demonstrated that the control cells and the cultures treated with LPS have faint cytoplasmic LC3B staining (Figure 5A). Accordingly, the 3D surface plots revealed a few peaks of low height (Figure 5A). Cells treated with IL-36 $\alpha$  displayed staining patterns characterized by faint, punctate LC3B staining (Figure 5A). In contrast, the cells treated with the combination of IL-36 $\alpha$  and LPS displayed very bright LC3B staining, and the 3D surface plot consisted of numerous robust peaks (Figure 5A). This result indicates that IL-36 $\alpha$  and LPS cooperatively increased the accumulation of LC3B-positive vacuoles. IL-36 receptor antagonist (IL-36Ra) was used to investigate the role of IL-36 $\alpha$  in the synergistic activation of autophagy elicited by the combined treatment with IL-36 $\alpha$  and LPS. The cultures were pre-treated with IL-36Ra for 30 min, and then IL-36 $\alpha$  or a double combination of IL-36 $\alpha$  and LPS were added. The cultures treated either with IL-36Ra alone or in combination with IL-36 $\alpha$  displayed a faint cytoplasmic LC3B staining (Figure 5A). Cells treated with the triple combination of IL-36 $\alpha$ –IL-36Ra–LPS likewise displayed staining patterns characterized by faint, punctate LC3B staining (Figure 5A). Accordingly, the 3D surface plots revealed a few peaks of low height (Figure 5A).

A.



B.

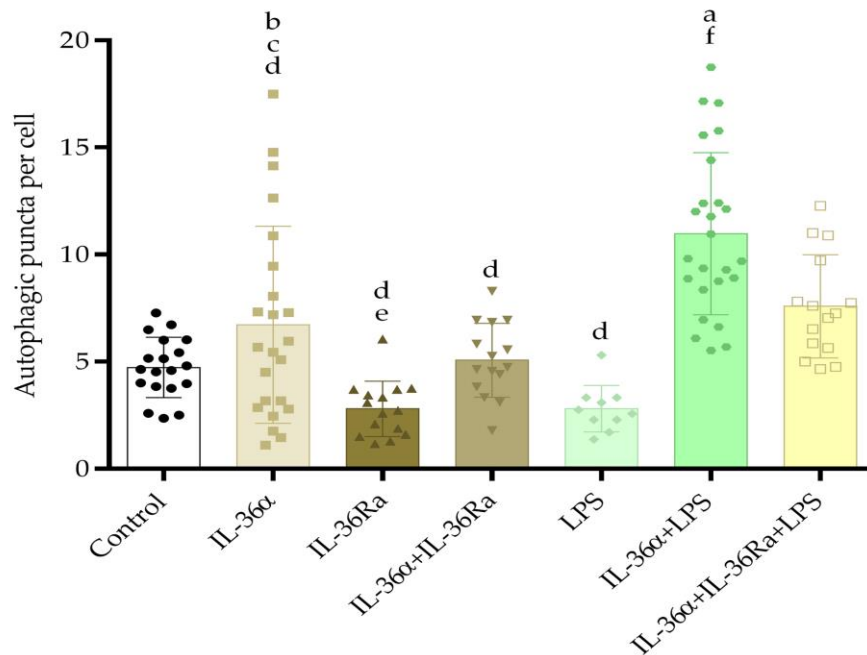


**Figure 5:** IL-36 $\alpha$  and LPS cooperatively increase the accumulation of LC3B-positive vacuoles. THP-1 cells were treated with 10 ng/ml IL-36 $\alpha$ , IL-36Ra, and 500 ng/ml LPS alone or in combination for 6 h, and the intracellular localization of LC3B was analyzed. Control cultures incubated in parallel were left untreated. (A) Immunofluorescence assays showing the fluorescence intensities of LC3B-positive vacuoles. The samples were stained for endogenous LC3B protein, and images were obtained by confocal microscopy. The images were subjected to fluorescence intensity analysis by using the Image J software. The 3D surface plots represent the intensity values of the whole image. The results are representative of two independent experiments. Scale bar, 10  $\mu$ m. (B) The average numbers of LC3B-positive autophagic vacuoles. The LC3B-positive autophagic vacuoles were automatically quantified with Image J software. The values on the bar graphs denote the means  $\pm$  SD of the results of two independent experiments. P values were calculated by the ANOVA test with the Tukey post-test. <sup>a</sup> $p < 0.0001$  vs Control; <sup>b</sup> $p < 0.01$  vs IL-36Ra; <sup>c</sup> $p < 0.05$  vs LPS; <sup>d</sup> $p < 0.001$  vs IL-36 $\alpha$ -LPS combination; <sup>e</sup> $p < 0.05$  vs IL-36 $\alpha$ -IL-36Ra-LPS combination; <sup>f</sup> $p < 0.001$  vs IL-36 $\alpha$ -IL-36Ra-LPS combination.

To investigate the effects of IL-36 $\alpha$  and LPS on autophagosome formation, the abundances of LC3B-positive vacuoles were determined at the 6-h time point. The average numbers of LC3B-positive vacuoles per cell in the control, IL-36 $\alpha$ -, or LPS-treated cultures were 4.72, 6.73, and 2.8, respectively (Figure 5B). The average numbers of LC3B-positive vacuoles per cell in cultures treated with a combination of IL-36 $\alpha$  and LPS were significantly higher than that observed in the control cultures (the average number of autophagosomes in the cultures treated with IL-36 $\alpha$ -LPS was 10.97 versus 4.72 in the control,  $p < 0.0001$ ) (Figure 5B). Moreover, the cells treated with the triple combination of IL-36 $\alpha$ -IL-36Ra-LPS exhibited significantly lower numbers of LC3B-positive vacuoles per cell than in the cultures treated with the IL-36 $\alpha$ -LPS combination: The average number of autophagosomes in the cultures treated with IL-36 $\alpha$ -IL-36Ra-LPS was 7.58 vs 10.97 in cells treated with IL-36 $\alpha$ -LPS,  $p < 0.05$  (Figure 5B). Thus, although IL-36 $\alpha$  and LPS alone do not cause a significant alteration in the number of LC3B-positive vacuoles, the combination of IL-36 $\alpha$  and LPS does significantly stimulate the accumulation of autophagosomes.

#### **4.2. The effects of IL-36 $\alpha$ and LPS on the levels of LC3B-I and LC3B-II**

The effects of IL-36 $\alpha$  and LPS on the levels of LC3B-I and LC3B-II were determined by western blot analysis. The control THP-1 cells displayed endogenous expression of both the lipidated and the non-lipidated forms of LC3B at each time point (Figure 6A, lanes 1–4). IL-36 $\alpha$ -treated cells exhibited slightly higher LC3B-II levels at the 0.5-, 2-, and 6-h time points than controls (Figure 6A, lanes 5–7). However, these alterations were not statistically significant (Figure 6B). Likewise, there were no significant alterations in LPS-treated cells versus controls (Figure 6). In contrast, the simultaneous treatment of cells with IL-36 $\alpha$  and LPS triggered a significant increase in the level of LC3B-II as compared with the controls (at the 0.5-, 6-, and 24-h time points the fold increases of LC3B-II levels in cells treated with IL-36 $\alpha$ -LPS combination were 3.52,  $p < 0.01$ , 3.0, and 3.02,  $p < 0.05$  for both, respectively) (Figure 6A, lanes 13, 15 and 16, and Figure 6B). These data suggest that IL-36 $\alpha$  and LPS alone do not increase the level of LC3B-II whereas combined IL-36 $\alpha$  and LPS treatment cooperatively stimulates the lipidation of LC3B.

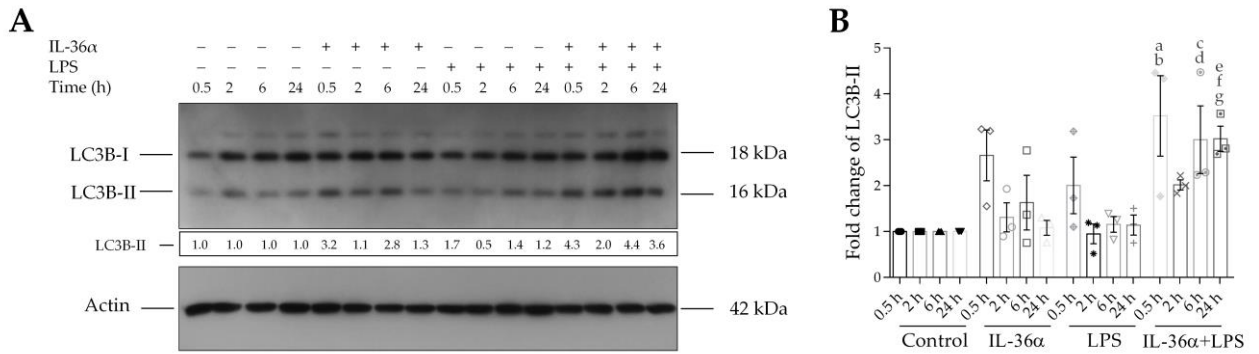


**Figure 6:** IL-36 $\alpha$  and LPS cooperatively increase the level of LC3B-II. **(A)** Western blot analysis showing the kinetics of endogenous LC3B-II expression. Total protein was isolated from controls (lanes 1-4), IL-36 $\alpha$ -treated cells (lanes 5-8), LPS-treated cells (lanes 9-12), and cells treated with IL-36 $\alpha$ -LPS combination (lanes 13-16) at the indicated time points. Samples were resolved on SDS-PAGE and transferred to PVDF filters. After incubation with the corresponding antibody, the levels of LC3B-I and LC3B-II were determined with a chemiluminescence detection system. Band intensities were quantified with ImageJ software. The ratios of the protein levels measured at 0.5, 2, 6, and 24 hours were compared to the corresponding time point controls and expressed as fold change (shown below each lane). The results are representative of three independent experiments. **(B)** The values on the bar graph denote the means  $\pm$  SD of the results of three independent experiments. P values were calculated by the ANOVA test with the Sidak post-test. <sup>a</sup> $p < 0.01$  vs the 0.5-h time point control, <sup>b</sup> $p < 0.05$  vs the 0.5-h time point LPS, <sup>c</sup> $p < 0.05$  vs the 6-h time point control, <sup>d</sup> $p < 0.01$  vs the 6-h time point LPS, <sup>e</sup> $p < 0.05$  vs the 24-h time point control, <sup>f</sup> $p < 0.01$  vs the 24-h time point IL-36 $\alpha$ , and <sup>g</sup> $p < 0.01$  vs the 24-h time point LPS.

### 4.3. The effects of IL-36 $\alpha$ and LPS on the autophagic flux

Bafilomycin A1 (BFLA) is an inhibitor of autophagosome-lysosome fusion and lysosomal hydrolase activity and was used to investigate the autophagic flux. The cultures were incubated with IL-36 $\alpha$  and LPS alone or in combination for 2 h and then treated with BFLA for another 4-h period just before the preparation of cell lysates. Compared with the control, BFLA increased the level of LC3B-II (Figure 7A, lanes 1 and 2, respectively). The elevated LC3B-II level of the BFLA-treated cells indicates that this drug efficiently blocked the autophagic flux under the experimental conditions used. In the presence of BFLA, IL-36 $\alpha$  triggered a higher increase in the level of LC3B-II than in the corresponding drug control (Figure 7A, lanes 4 and 2, respectively). However, this alteration was not statistically significant (Figure 7B). In contrast, compared with the BFLA control, LPS—acting singly or in combination with IL-36 $\alpha$ —elicited a significant increase in the levels of LC3B-II of cells incubated in the presence of BFLA (the fold increases of LC3B-II levels in cells treated either with LPS alone or the IL-36 $\alpha$ -LPS combination in the presence of BFLA were 6.22, and 6.47,  $p < 0.05$  for both) (Figure 7B). In the presence of BFLA, the cells treated with the IL-36 $\alpha$ -LPS combination exhibited higher increases in the level of LC3B-II than cultures stimulated only with LPS. These data indicate that combined IL-36 $\alpha$  and LPS treatment cooperatively stimulates the autophagic flux.

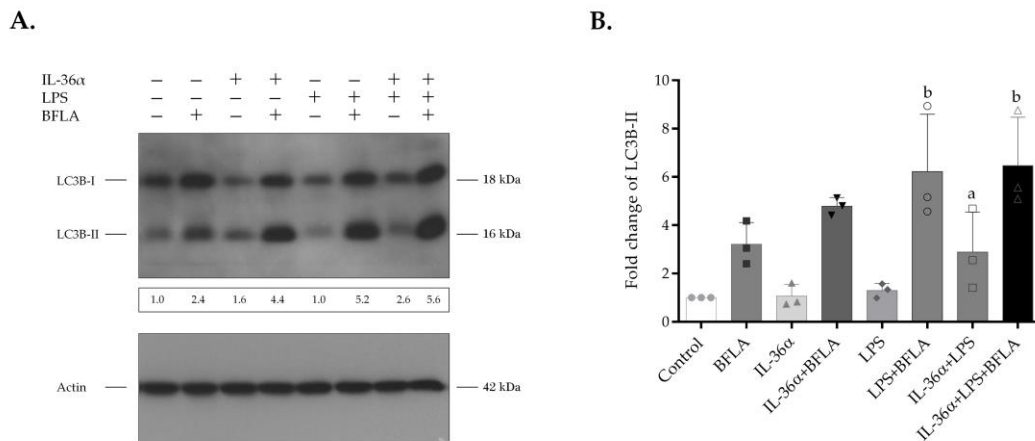


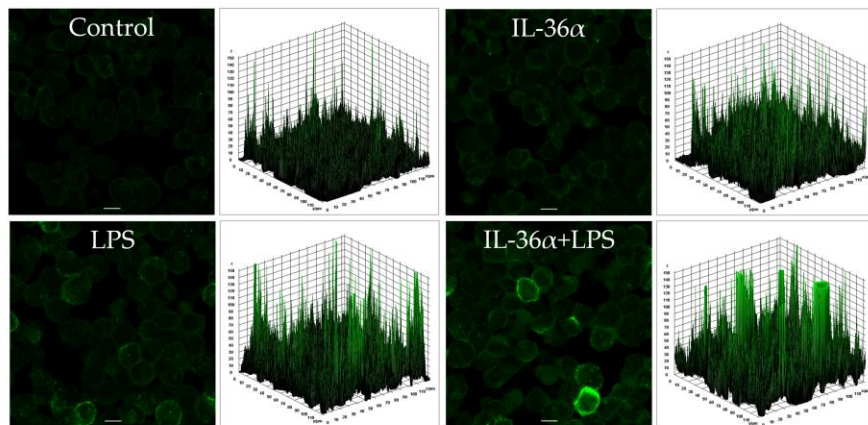
**Figure 7:** IL-36 $\alpha$  and LPS cooperatively stimulate the autophagic flux. THP-1 cells were treated with IL-36 $\alpha$ , and LPS alone or in combination for 2 h and then exposed to 100 nM bafilomycin A1 for another 4-h period. The total protein extracted was analyzed for LC3B expression by Western blot analysis. (A) Western blot analysis showing increased autophagic flux in cells treated with IL-36 $\alpha$ , and LPS alone, or in combination. The ratios of the protein levels were calculated, and expressed as fold change, shown below each lane. Results are representative of three independent experiments. (B) The values on the bar graph denote the means  $\pm$  SD of the results of three independent experiments. P values were calculated by the ANOVA test with the Sidak post-test. <sup>a</sup> $p < 0.05$  vs control, <sup>b</sup> $p < 0.05$  vs BFLA control. BFLA, bafilomycin A1

#### 4.4. The effects of IL-36 $\alpha$ and LPS on the level of Beclin-1

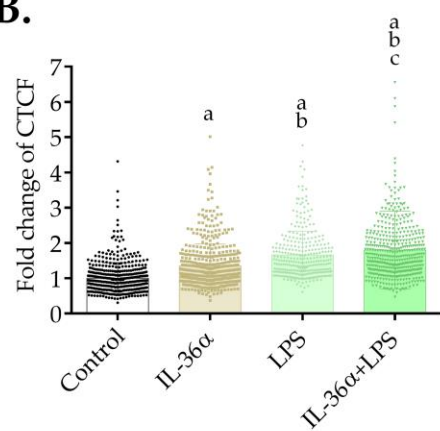
The effects of IL-36 $\alpha$  and LPS on the level and intracellular localization of Beclin-1 were determined by indirect immunofluorescence assay at the 6-h time point. The control cells showed a faint cytoplasmic Beclin-1 staining (Figure 8A).

Accordingly, the 3D surface plots revealed a few peaks of low height (Figure 8A). In contrast, the cells treated with IL-36 $\alpha$  and LPS alone or in combination displayed very bright Beclin-1 staining, and the 3D surface plots consisted of numerous robust peaks (Figure 8A). Measurement of the staining intensities showed that IL-36 $\alpha$  and LPS acting singly or in combination elicited significant increases as compared with the control (the CTCF values in cells treated with IL-36 $\alpha$ , LPS, or IL-36 $\alpha$ -LPS combination were 1.35, 1.66, or 1.8 vs 1.0 in the control,  $p < 0.0001$  for all, respectively) (Figure 8B). Measurement of the abundances of Beclin-1-positive vacuoles likewise revealed that IL-36 $\alpha$  and LPS acting singly or in combination triggered significant increases as compared with the control (the average numbers of Beclin-1-positive puncta in cells treated with IL-36 $\alpha$ , LPS or IL-36 $\alpha$ -LPS combination were 5.86, 8.18, or 13.55 vs 2.72 in the control,  $p < 0.01$ ,  $p < 0.0001$  and  $p < 0.0001$ , respectively) (Figure 8C). These data indicate that IL-36 $\alpha$  and LPS cooperatively elevate the level of Beclin-1.

A.



B.



C.

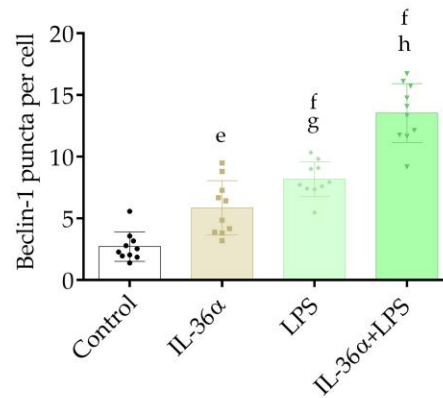
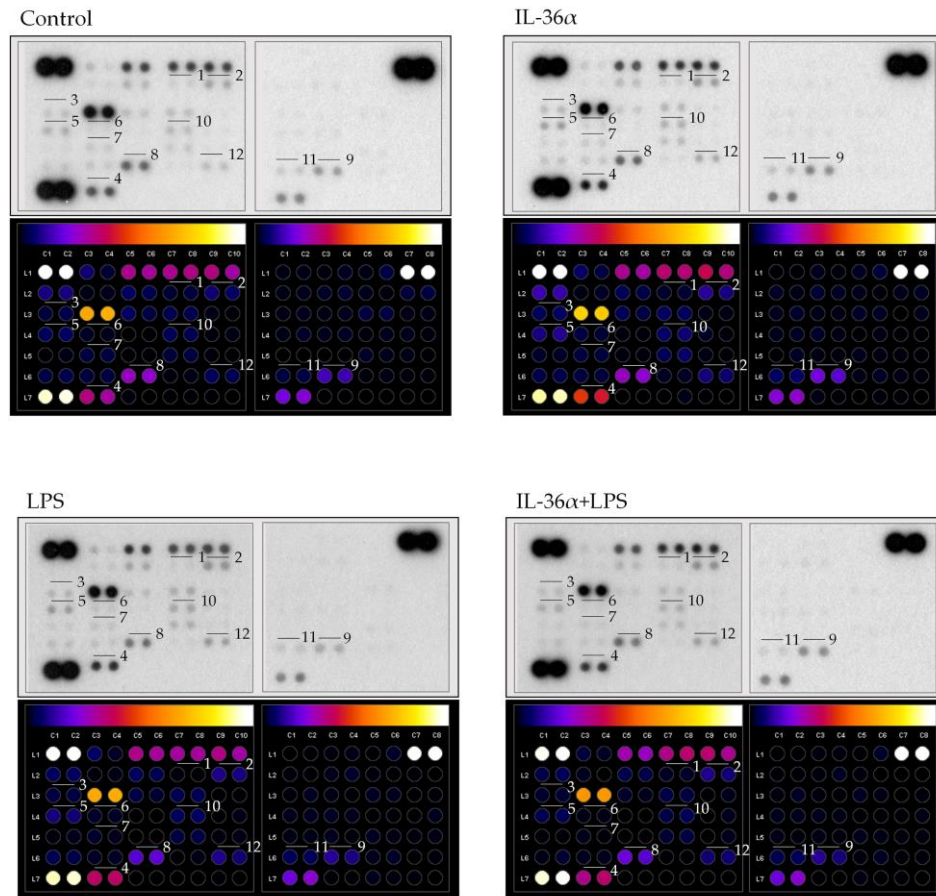


**Figure 8:** IL-36 $\alpha$  and LPS cooperatively increase Beclin-1 levels. THP-1 cells were treated with 10 ng/mL IL-36 $\alpha$ , IL-36Ra, and 500 ng/ml LPS alone or in combination for 6 h, and the level of Beclin-1 fluorescence was analyzed. Control cultures incubated in parallel were left untreated. (A) Immunofluorescence assay showing the fluorescence intensities of Beclin-1. The samples were stained for the endogenous Beclin-1 protein, and images were obtained by confocal microscopy. The images were subjected to fluorescence intensity analysis with ImageJ. The 3D surface plots represent the intensity values of the entire image. The results are representative of two independent experiments. Scale bar, 10  $\pm$  m. (B) Quantification of Beclin-1 fluorescence intensities. The fold changes of CTCF values were calculated as the CTCF of cells treated with 10 ng/mL IL-36 $\alpha$ , and LPS alone or in combination/CTCF of control cultures. The values on the bar graphs denote the means  $\pm$  SD of the results of two independent experiments. p values were calculated by the ANOVA test with the Tukey post-test. <sup>a</sup>p < 0.0001 vs. Control; <sup>b</sup>p < 0.0001 vs. IL-36 $\alpha$ ; <sup>c</sup>p < 0.05 vs. LPS. (C) Quantification of the intracellular abundances of Beclin-1 puncta. The Beclin-1-positive puncta were quantified with ImageJ software. The values on the bar graphs denote the means  $\pm$  SD of the results of two independent experiments. p values were calculated by the ANOVA test with Tukey post-test. <sup>e</sup>p < 0.01 vs. Control; <sup>f</sup>p < 0.0001 vs. Control; <sup>g</sup>p < 0.05 vs. IL-36 $\alpha$ ; <sup>h</sup>p < 0.0001 vs. IL-36 $\alpha$  and LPS.

#### 4.5. The effects of IL-36 $\alpha$ and LPS on cellular signaling in the THP-1 cell line

**A.**



**B.**

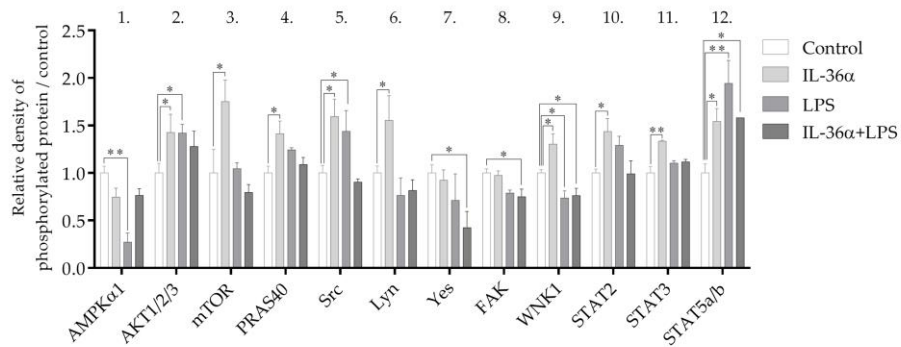


**Figure 9:** Differential phospho-kinase array profiles of cells treated with IL-36 $\alpha$  and LPS. **(A)** Phospho-kinase array analysis. Total protein was isolated from THP-1 cells treated with IL-36 $\alpha$ , and LPS alone or in combination for 30 min. Control cells were left untreated. The samples were hybridized with a phospho-kinase array kit. The labeled spots correspond to the phospho-proteins modulated by IL-36 $\alpha$  and LPS. **(B)** Quantification of phosphoproteins from the proteomic array (average of duplicate spots). Spot densities of phosphoproteins were quantified using Image J analysis software and normalized to positive controls on the same membrane. P values were calculated by the ANOVA test with the Sidak post-test. \*p < 0.05; \*\*p < 0.01.

A phospho-kinase array that detects the phosphorylation levels of 43 major protein kinases was used to investigate the effect of IL-36 $\alpha$  and LPS on the activation level of signaling pathways implicated in autophagy regulation. IL-36 $\alpha$  led to the activation of a subset of kinases (Figure 9). Compared with the control, the most significant effect was an increase in Akt strain transforming factor 1/2/3 (Akt1/2/3) (S473) phosphorylation. The phosphorylation levels of the proline-rich Akt substrate of 40 kDa (PRAS40) (T246) and mechanistic target of rapamycin (mTOR) (S2448)—two signaling molecules downstream of Akt1/2/3—were also increased (Figure 9). IL-36 $\alpha$  triggered phosphorylation of with no lysine kinase 1 (WNK1) (T60), some steroid receptor coactivator (Src) family kinases including Src (Y419) and Lyn (Y397), and signal transducer and activator of transcription (STAT) family members such as STAT2 (Y689), STAT3 (S727) and STAT5a/b (Y694/Y699). Compared with the control, LPS increased the levels of phospho-Akt1/2/3 (S473), phospho-Src (Y419), and STAT5a/b (Y694/Y699); it decreased phosphorylation of adenosine monophosphate-activated protein kinase  $\alpha$ 1 (AMPK $\alpha$ 1) (Figure 9). Compared with the control, IL-36 $\alpha$  and LPS combined treatment increased phosphorylation of STAT5a/b whereas the levels of phospho-Yes (Y426), phospho-focal adhesion kinase (FAK) (Y397), and phospho-WNK1 (T60) were decreased (Figure 9). Thus, IL-36 $\alpha$ , LPS, and the combined treatment elicit distinct phosphorylation patterns of signaling molecules.

## 5. Discussion

### 5.1. IL-36 $\alpha$ and LPS cooperatively induce autophagy

Compelling evidence indicates that cellular autophagic and immune processes are highly intertwined and that their coordinated functioning is essential for the efficient protection of the human body against pathogenic Gram-negative bacteria [4], [16], [18], [179], [180]. During infections, cytokines and molecules defined as pathogen-related molecular patterns (PAMP) act simultaneously to activate partially overlapping signaling pathways. The combined effect may differentially regulate cellular autophagic activity. Thus, this study investigated the impact of IL-36 $\alpha$  upon endogenous and LPS-induced autophagy.

To study the autophagic activity of THP-1 cells treated with IL-36 $\alpha$  and LPS alone or in combination, we determined the intracellular distribution of LC3B and measured LC3B lipidation as well as the autophagic flux [181]. These experiments demonstrated that the cells treated with IL-36 $\alpha$  alone displayed increased abundances of autophagic vesicles, elevated endogenous LC3B-II levels, and stimulated autophagic flux; these differences, however, were not statistically significant (Figures 5-7). Recent observations indicated that IL-36 $\beta$  and IL-36 $\gamma$  activate the autophagic process in primary murine CD4<sup>+</sup>CD25<sup>+</sup> Treg cells [182] and human macrophages [183], respectively. There may be several explanations for the weaker pro-autophagic effect of IL-36 $\alpha$  revealed in our present study such as differences between IL-36 subtypes and different sensitivities of various cell types to this cytokine. Consistent with previous findings [36], [184], [185]. Our results demonstrated that LPS significantly increased autophagosome synthesis (Figure 6). The combination of IL-36 $\alpha$  and LPS raised the intensity level of LC3B staining and cooperatively stimulated the translocation of this protein into autophagic vesicles (Figure 5). Supporting this observation, we found that IL-36Ra significantly inhibited the pro-autophagic effect of the IL-36 $\alpha$ /LPS combined treatment (Figure 6). The IL-36 $\alpha$ -LPS combination elevated LC3B-II and decreased LC3B-I levels indicating that the lipidation of LC3B is highly stimulated (Figure 6). Finally, our experiments showed that in cultures treated with the combination of IL-36 $\alpha$  and LPS, the autophagic flux is increased considerably by this cytokine/PAMP combination (Figure 7). These results suggest that IL-36 $\alpha$  and LPS cooperatively stimulate autophagy.

To investigate the effect of IL-36 $\alpha$  and LPS on the activation of some signaling pathways, we determined the phosphorylation levels of protein kinases implicated in autophagy regulation (Figure 9). Our studies have shown that IL-36 $\alpha$  increased the

phosphorylation of Akt1/2/3 (S473), PRAS40 (T246), mTOR (S2448), WNK1 (T60), and some Src as well as STAT family kinases such as Src, Lyn, STAT2, STAT3, and STAT5a/b. PRAS40 is a negative regulator of mTORC1 [186], [187]. Akt- and mTORC1-mediated phosphorylation of PRAS40 resulting in its dissociation from mTORC1 that in turn alleviates inhibition of mTORC1 and blocks induction of the autophagic cascade [186], [187]. An interesting recent study revealed that IL-36 $\beta$  stimulates mTORC1 via the PI3K/Akt, I $\kappa$ B kinase and MyD88 pathways [188]. Our experiments demonstrate that, like IL-36 $\beta$ , IL36 $\alpha$  activates mTORC1 via the PIK/Akt pathway. Moreover, we suggest that the Akt-mediated activation of mTOR involves PRAS40. Other previous studies indicated that WNK1 acts as an autophagy inhibitor by interfering with the activation of AMPK and PI3KC3 [189]. STAT3 has been shown to regulate autophagy in localization- and context-dependent manners and can elicit both pro-autophagic and anti-autophagic effects [190]. In light of these observations, our data suggest that in the early phase of IL-36 $\alpha$  signaling, both anti- and pro-autophagic pathways are activated. Our observations show that LPS increases phosphorylation of Akt1/2/3, Src as well as STAT5a/b and decreases the level of phospho-AMPK $\alpha$ 1 in THP-1 cells; this is fully consistent with previous reports [191], [192]. Interestingly, the phosphorylation pattern of cells incubated with IL36 $\alpha$  and LPS differed from the signatures detected either in IL36 $\alpha$ - or LPS-treated cells. We found that the IL36 $\alpha$ /LPS combined treatment increased phosphorylation of STAT5a/b, had minimal effect on the Akt/PRAS40/mTOR pathway, and reduced the levels of phospho-Yes, phospho-FAK, and phospho-WNK1. Thus, the combined treatment of IL-36 $\alpha$  and LPS appears to dampen PI3K/Akt/mTOR, FAK and WNK1 signaling. The TLR4 signal transduction network is known to be kept under strict control by multiple mechanisms including positive and negative crosstalk regulations that maintain the integrity of immune cells by preventing excessive inflammation [193]. The negative regulators acting through the activation of transcription play a primary role in the late phase of TLR and IL-36 signaling; their role in the early stage thus can be excluded. Important studies, however, revealed that PI3K has an essential role in the safety mechanism controlling the early-stage of TLR4-mediated signaling [194]. PI3K can suppress TLR4 signaling by altering the availability of phosphatidylinositol-(4,5)bisphosphate (PIP<sub>2</sub>) at the cytoplasmic membrane and hence can modulate the intracellular localization of adaptors, the magnitude of activation, and signal output [195]. Based on these observations, we suggest that the combinatorial effect of IL-36 $\alpha$ /LPS may exert an excessive PI3K activation, which—while not suspending the inhibition of

downstream events of autophagy—can significantly reduce it by decreasing the Akt-mediated activation of mTORC1.

Previous studies have demonstrated that Beclin-1 plays a pivotal role in the autophagic process. Beclin-1 was shown to interact with Bcl-2 and Bcl-X<sub>L</sub>, which suppresses autophagosome biogenesis. The release of Beclin-1 is a prerequisite for the formation of a functional PI3KC3 complex. Phosphorylation events and TRAF6-mediated ubiquitination of Beclin-1 may destabilize Beclin-1–Bcl-2/Bcl-X<sub>L</sub> association and abrogate Beclin-1-Bcl-2/Bcl-X<sub>L</sub> interaction. Some IL-36 $\alpha$  and LPS signaling intermediates have the potential to regulate the functional activity of Beclin-1. Thus, we investigated the effect of IL-36 $\alpha$  and LPS on Beclin-1 protein. Our results showed that IL-36 $\alpha$  and LPS acting singly or in combination elevated the staining intensities and increased the abundances of Beclin-1-positive vacuoles (Figure 8). The IL-36 $\alpha$ /LPS treatment was again more efficient than IL-36 $\alpha$  or LPS alone. These data further support the notion that IL-36 $\alpha$  and LPS cooperatively promote the autophagic process because increased Beclin-1 levels were shown to correlate with enhanced autophagy [181].

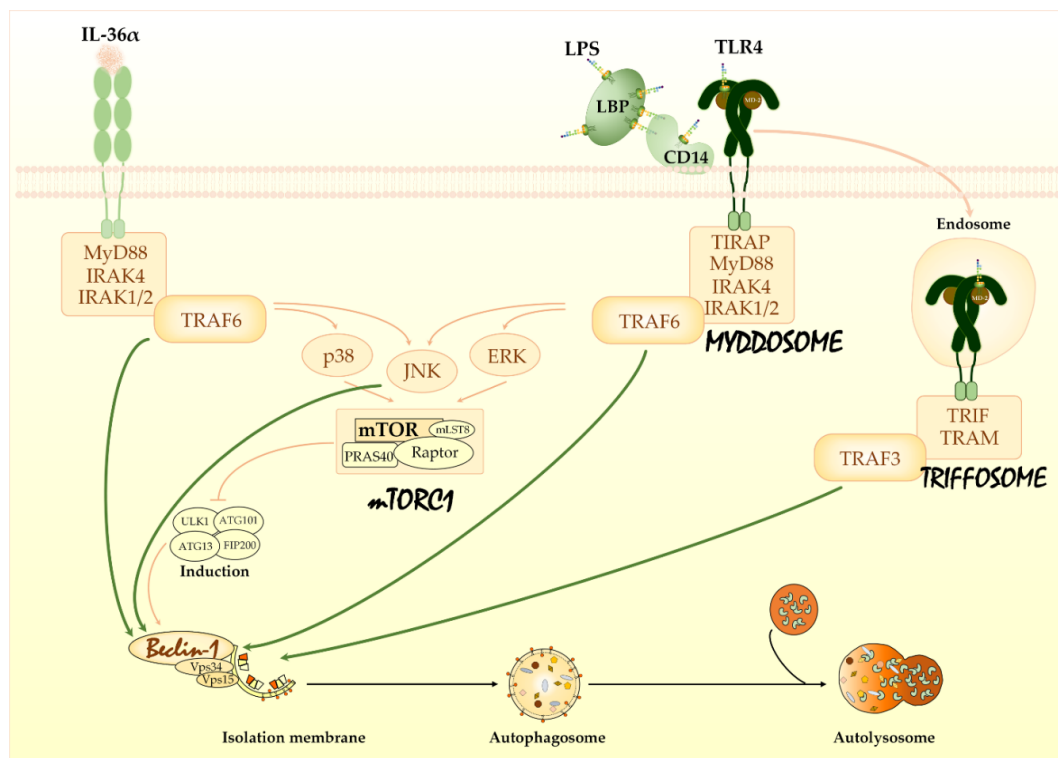


**Figure 10:** IL36 $\alpha$  and LPS cooperatively induced autophagy by multiple mechanisms. The IL-36 $\alpha$ /LPS combination reduces the activation level of the PI3K/Akt/mTORC1 axis by triggering rapid depletion of PIP<sub>2</sub> at the cytoplasmic membrane. As a result, mTOR-mediated inhibition of autophagy is alleviated. Additionally, the IL-36 $\alpha$ /LPS combination increases the activation level of PI3KC3 complex via the activation of MyD88, TRAF3, and TRAF6. As a result, autophagosome formation is stimulated. Thus, this cytokine/PAMP combination triggers pro-autophagic biased signaling by several mechanisms and thereby stimulates the autophagic cascade cooperatively.

Our results suggest a hypothetical model for the mechanism of the enhanced pro-autophagic effect observed in cells treated with IL-36 $\alpha$  and LPS simultaneously. The IL-36 $\alpha$ /LPS combination reduces the activation level of the PI3K/Akt/mTORC1 axis by triggering rapid depletion of PIP<sub>2</sub> at the cytoplasmic membrane. As a result, mTOR-mediated inhibition of autophagy is alleviated. Some components of the IL-36 $\alpha$  and LPS signaling networks are known to induce autophagy. MyD88 binds directly whereas TRAF3 and TRAF6 ubiquitinate the Beclin-1 protein, thus disrupting the interaction between Beclin-1 and Bcl-2 [36], [184]. This results in increased oligomerization of Beclin-1, activation of the PI3KC3 complex, and initiation of autophagosome formation [36], [184]. The IL-36 $\alpha$ /LPS combination increases the activation level of PI3KC3 complex directly and subsequently stimulates autophagy. Thus, this cytokine/PAMP combination triggers pro-autophagic biased signaling by several mechanisms and thereby cooperatively stimulates the autophagic cascade (Figure 10). Previous studies have shown that bacteria affect the autophagic cascade and, conversely, autophagy influences the infection process. The bacteria studied so far all interact with the autophagic machinery but in different ways. The structural components, PAMPs, and exotoxins of several bacteria induce autophagy. However, some bacteria can effectively prevent autophagic recognition, inhibit autophagy initiation and maturation of autophagosomes or block the fusion of lysosomes with autophagosomes, while others hijack the autophagic compartment to support their intracellular survival. Our data indicate that cytokines may modify the pro-autophagic effect of bacterial PAMPs. An increased xenophagic activity of innate immune cells exposed to IL-36 $\alpha$  and LPS—functioning as part of the cell-autonomous defense system—may play a protective role in the pathogenesis of infections caused by Gram-negative bacteria.

## **5.2. The cellular effect of SARS-CoV-2 on GIT**

During multiplication, SARS-CoV-2 modulates several cellular processes, including signaling, transcription, translation, cell division, the IFN system, autophagy, and apoptosis, as well as the biogenesis, function, and morphology of mitochondria and intracellular vesicles. Phosphoproteomic profiling has revealed that SARS-CoV-2 infection affects the activity of 97 kinases. The activities of several members of the p38 pathway and the guanosine monophosphate-dependent protein kinases are upregulated, while cell cycle kinases (CDK1/2/5), cell growth-related signaling pathway kinases (AKT1/2), and regulators of the cytoskeleton are down-regulated [196]. The functional changes in the signal transduction

pathways have been shown to play an important role in SARS-CoV-2-induced cytoskeletal damage, cytokine production, and slow-down in cell proliferation at the S/G2 transition phase [196]. Transcriptomic profiles of SARS-CoV-2-infected primary human bronchial epithelial cells, lung biopsy, and bronchoalveolar lavage fluid samples of COVID-19 patients have demonstrated upregulated expression of genes implicated in metabolism, immunity, and the stress responses of the endoplasmic reticulum and mitochondria [197]–[199]. It has been shown that the M protein, Nsp7, and ORF9c stimulate lipogenesis, while Nsp7, Nsp12, and ORF8 trigger endoplasmic stress response, and Nsp7 induces mitochondrial dysfunction [199]. Moreover, the M and E proteins, along with Nsp3a, Nsp6, Nsp8, Nsp10, and Nsp13, were shown to be able to modify the structure and function of the endomembrane system and vesicle trafficking, thereby facilitating several steps of viral multiplication [200]. Interestingly, the expression of genes involved in the humoral immune response and innate immune response-activating signal transduction are increased, whereas genes implicated in cytokine-mediated signaling pathways are down-regulated [198]. A multiplex gene expression analysis showed that the genes involved in type I IFN signaling were highly up-regulated, whereas the expression of IFN-stimulated genes (*ISGs*) was decreased in severe COVID-19 patients [201]. The levels of pro-inflammatory cytokines measured in sera of COVID-19 patients were highly increased in a pattern corresponding to a cytokine storm [202]–[204]. Consistent with this observation, transcriptional activation of pro-inflammatory cytokine genes was also detected in peripheral blood mononuclear cells and bronchoalveolar lavage fluid [205]. The sera and lung tissue samples of patients have shown IL-1 $\beta$ , IL-6, IL-10, IL-18, IL-33, transforming growth factor- $\beta$ , IFN- $\gamma$ , CSF2/GM-CSF, CSF3/G-CSF, CC chemokines [CCL2/MCP-1, CCL3/MIP-1A, CCL4/MIP-1B, CCL5/RANTES, CCL8, CCL3L1] and CXC chemokines [CXCL1, CXCL2 and CXCL10/IP10] [202], [204]–[206]. However, during SARS-CoV-2 infection, the production of type I and III IFNs is decreased [201], [207]. Thus, these data clearly demonstrate that SARS-CoV-2 infection alters both the transcriptional and translational patterns in cells profoundly [196], [207]. Other observations indicate that SARS-CoV-2 could trigger several cell-death processes, including apoptosis, necrosis, pyroptosis, and anoikis, depending on the type of cell. The death of infected cells may contribute to tissue damage and induce an inflammatory reaction [208]–[211].

It has also been revealed that SARS-CoV-2 Orf3a stimulates the formation of the autophagic Beclin-1-Vps34-Atg14 complex while simultaneously inhibiting the Beclin-1 complex containing the UVRAG adaptor protein [212]. Orf 3a thereby exerts a dual effect on

the autophagic process manifesting in the induction of the initial steps and a block in the fusion of the autophagosomes with lysosomes [212].

ACE2, the cellular receptor of SARS-CoV-2, is widely expressed in many types of cells and tissues of the GIT, including the esophagus, stomach, small intestine, colon, rectum, pancreatic exocrine glands and islets, and gallbladder [213]. The expression level of ACE2 in the GIT is highest in the ileum epithelial cells, especially in the absorptive enterocytes [214]. It has also been demonstrated that ACE2 is co-expressed with TMPRSS2/4 proteases in the GIT, with the highest level in the ileum [215]. These observations indicate that several cell types in the GIT are potentially susceptible to SARS-CoV-2 infection [132], [213]–[215]. SARS-CoV-2 infection in the lungs and GIT seems to display some different tissue-specific features. The production of type I and III IFNs is more efficient in the GIT than in the lungs. The antiviral IFNs may restrict viral replication in the GIT to some extent, which may allow the development of a less cytopathogenic or persistent form of infection in this anatomical region. SARS-CoV-2-mediated dysregulation of the ACE2:BOAT1 complex may modify the biological response of cells to the infection, and in enterocytes, it may contribute to the development of diarrhea by inducing amino acid starvation, which can decrease Na<sup>+</sup> uptake. These effects are not seen in the lungs, however, as ACE2 does not form a complex with BOAT1 in this organ.

SARS-CoV-2 infection of the GIT is of pivotal epidemiological significance, but further studies are needed to assess the extent of this risk.

## 6. Conclusion

Our results demonstrate that IL-36 $\alpha$  alone does not stimulate the cellular autophagic activity, whereas LPS increases autophagosome synthesis significantly. The IL-36 $\alpha$  and LPS combination synergistically elevate the level of LC3B-II, increase the autophagic flux and stimulate the intracellular redistribution of LC3B and Beclin-1. The phospho-kinase array results indicate that IL-36 $\alpha$ , LPS, and the combined treatment elicit distinct phosphorylation patterns of signaling molecules. The IL-36 $\alpha$ /LPS combination triggers pro-autophagic biased signaling by several mechanisms and thereby stimulates the autophagic cascade cooperatively in the THP-1 cell line. However, some limitations of this investigation, such as the need for additional experimental evidence that can corroborate the synergistic effect of this cytokine/PAMP combination in other cell types, have yet to be addressed. Moreover, further studies are needed to investigate the effect of increased autophagic activity on the functions of innate immune cells treated with IL-36 $\alpha$  and LPS simultaneously.

Severe acute respiratory syndrome coronavirus 2 (SARS-CoV-2) replicates in enterocytes, triggers ionic imbalances, activates the NLRP3 inflammasome pathway, induces apoptosis, and exerts a dual effect on the autophagic process. These effects of SARS-CoV-2 lead to the development of leaky gut. Increased permeability triggers the absorption of LPS into the circulation, further exacerbating inflammation induced by viral infection. In addition to drugs that affect the inflammatory response and viral replication, agents targeting autophagy and apoptosis appear to be potentially suitable for the treatment of COVID-19. The fecal-oral route of SARS-CoV-2 transmission calls for strict and more consistent adherence to hygiene rules to prevent the spread of COVID-19.

## 7. Summary

Autophagy is an intracellular catabolic process that controls infections both directly and indirectly via its multifaceted effects on the innate and adaptive immune responses. It has been reported that LPS stimulates this cellular process, whereas the effect of IL-36 $\alpha$  on autophagy remains largely unknown. We therefore investigated how IL-36 $\alpha$  modulates the endogenous and LPS-induced autophagy in THP-1 cells. The levels of LC3B-II and autophagic flux were determined by western blotting. The intracellular localization of LC3B was measured by immunofluorescence assay. The activation levels of signaling pathways implicated in autophagy regulation were evaluated by using a phosphokinase array. Our results showed that combined IL-36 $\alpha$  and LPS treatment cooperatively increased the levels of LC3B-II and Beclin-1, stimulated the autophagic flux, facilitated intracellular redistribution of LC3B, and increased the average number of autophagosomes per cell. The IL36 $\alpha$ /LPS combined treatment increased phosphorylation of STAT5a/b, had minimal effect on the Akt/PRAS40/mTOR pathway, and reduced the levels of phospho-Yes, phospho-FAK, and phospho-WNK1. Thus, this cytokine/PAMP combination triggers pro-autophagic biased signaling by several mechanisms and thus cooperatively stimulates the autophagic cascade. An increased autophagic activity of innate immune cells simultaneously exposed to IL-36 $\alpha$  and LPS may play an important role in the pathogenesis of Gram-negative bacterial infections.

SARS-CoV-2 can infect and replicate in esophageal cells and enterocytes, leading to direct damage to the intestinal epithelium. The infection decreases the level of angiotensin converting enzyme 2 receptors, thereby altering the composition of the gut microbiota. SARS-CoV-2 elicits a cytokine storm, which contributes to gastrointestinal inflammation. The direct cytopathic effects of SARS-CoV-2, gut dysbiosis, and aberrant immune response result in increased intestinal permeability, which may exacerbate existing symptoms and worsen the prognosis. By exploring the elements of pathogenesis, several therapeutic options have emerged for the treatment of COVID-19 patients, such as biologics and biotherapeutic agents. However, the presence of SARS-CoV-2 in the feces may facilitate the spread of COVID-19 through fecal-oral transmission and contaminate the environment. Thus, gastrointestinal SARS-CoV-2 infection has important epidemiological significance. The development of new therapeutic and preventive options is necessary to treat and restrict the spread of this severe and widespread infection more effectively.

**Considered novel findings**

- The IL-36 $\alpha$ /LPS combination significantly induces autophagy.
- IL-36 $\alpha$  activates mTORC1 via the PIK/Akt pathway, and the Akt-mediated activation of mTOR involves PRAS40.
- The IL-36 $\alpha$ /LPS combination triggers pro-autophagic biased signaling by several mechanisms and thus cooperatively stimulates the autophagic cascade.

## 8. Acknowledgements

I would like to express my sincere gratitude to my supervisor, **Dr. Megyeri Klára**, who has encouraged me since our first meet at the Airport and shared her thorough knowledge with me to inspire my research. My thesis would not have been possible without her unwavering support and belief in me.

My sincere appreciation and gratitude to our Head of Department **Dr. Burián Katalin** for her supported role during my PhD study.

I would like to thank **my fellow Ph.D. students** for creating great atmosphere at work.

**Staff members** at the Department of Medical Microbiology are gratefully thanked for creating a supportive and pleasant environment

I would also convey my honest thanks to my co-authors and other collaborators: Áron Dernovics , András Rosztóczy, György Seprényi , Ferhan Ayaydin , Zsolt Boldogkői and Zoltán Veréb for their essential contributions to complete the papers I and II.

I want to thank all lab mates past and present, especially **Áron Dernovics** in the Department of Medical Microbiology who helped and supported me during my project, for providing a good time and pleasant environment.

Special thanks to our secretary and the doctoral office coordinators past and the present especially Anikó Schillsong ,Edina Miklósne Bódi, Ildikó Német, Renáta Bódi, Ágnes Mester and Pleskó Andrea for the administrative support.

Special thanks to my colleagues from Iraq, Dr. Ahmed Mohsin , Dr. Ahmed Latif , Dr. Malik Hadi, Dr. Ahmed Saeed, Dr. Ahmed Jasim , Dr. Shwan Hariri, Dr. Sayif Mohammad , Dr. Islam Almsarrhad and Dr. Abdullah Alshammari for their care and support during the whole period of my study

I would like also to thank the Ministry of Higher Education and Scientific Research in Iraq especially the scholarships and the cultural relations office for offering this opportunity to study in Hungary.

I feel grateful to my dear wife, **Diar Daood**, for her love , patience , during my PhD studies and who has always encouraged and believed in me.

I want to acknowledge the Tempus and Stendium Programme for providing this opportunity and financial support for the funding of my doctoral studies.

Lastly, but not least, I would like to extend my special thanks to the whole of my **family** and **friends**, for their continuous encouragement and supporting.

## 9. References

---

- [1] K. R. Parzych and D. J. Klionsky, “An Overview of Autophagy: Morphology, Mechanism, and Regulation,” *Antioxidants & Redox Signaling*, vol. 20, no. 3, pp. 460–473, Jan. 2014, doi: 10.1089/ars.2013.5371.
- [2] M. A. Hayat, Ed., *Autophagy: cancer, other pathologies, inflammation, immunity, infection, and aging*. Amsterdam: Boston : Elsevier, Academic Press, 2016.
- [3] C. Tukaj, “The significance of macroautophagy in health and disease,” *Folia Morphologica*, vol. 72, no. 2, Art. no. 2, 2013, doi: 10.5603/FM.2013.0015.
- [4] R. Khandia *et al.*, “A Comprehensive Review of Autophagy and Its Various Roles in Infectious, Non-Infectious, and Lifestyle Diseases: Current Knowledge and Prospects for Disease Prevention, Novel Drug Design, and Therapy,” *Cells*, vol. 8, no. 7, p. 674, Jul. 2019, doi: 10.3390/cells8070674.
- [5] Y. C. Kim and K.-L. Guan, “mTOR: a pharmacologic target for autophagy regulation,” *J Clin Invest*, vol. 125, no. 1, pp. 25–32, Jan. 2015, doi: 10.1172/JCI73939.
- [6] J. Kim, M. Kundu, B. Viollet, and K.-L. Guan, “AMPK and mTOR regulate autophagy through direct phosphorylation of Ulk1,” *Nat Cell Biol*, vol. 13, no. 2, pp. 132–141, Feb. 2011, doi: 10.1038/ncb2152.
- [7] J. Yang, S. Carra, W.-G. Zhu, and H. H. Kampinga, “The Regulation of the Autophagic Network and Its Implications for Human Disease,” *Int. J. Biol. Sci.*, vol. 9, no. 10, pp. 1121–1133, 2013, doi: 10.7150/ijbs.6666.
- [8] R. Roberts and N. T. Ktistakis, “Omeasomes: PI3P platforms that manufacture autophagosomes,” *Essays in Biochemistry*, vol. 55, pp. 17–27, Sep. 2013, doi: 10.1042/bse0550017.
- [9] Y. Ichimura *et al.*, “A ubiquitin-like system mediates protein lipidation,” *Nature*, vol. 408, no. 6811, pp. 488–492, Nov. 2000, doi: 10.1038/35044114.
- [10] N. Mizushima *et al.*, “A protein conjugation system essential for autophagy,” *Nature*, vol. 395, no. 6700, pp. 395–398, Sep. 1998, doi: 10.1038/26506.
- [11] N. Mizushima, “The ATG conjugation systems in autophagy,” *Current Opinion in Cell Biology*, vol. 63, pp. 1–10, Apr. 2020, doi: 10.1016/j.ceb.2019.12.001.
- [12] D. J. Klionsky and B. A. Schulman, “Dynamic regulation of macroautophagy by distinctive ubiquitin-like proteins,” *Nat Struct Mol Biol*, vol. 21, no. 4, pp. 336–345, Apr. 2014, doi: 10.1038/nsmb.2787.
- [13] S. Nakamura and T. Yoshimori, “New insights into autophagosome-lysosome fusion,” *Journal of Cell Science*, vol. 130, no. 7, pp. 1209–1216, 2017, doi: 10.1242/jcs.196352.
- [14] H. Nakatogawa, Y. Ichimura, and Y. Ohsumi, “Atg8, a Ubiquitin-like Protein Required for Autophagosome Formation, Mediates Membrane Tethering and Hemifusion,” *Cell*, vol. 130, no. 1, pp. 165–178, Jul. 2007, doi: 10.1016/j.cell.2007.05.021.
- [15] “BioRender.” <https://app.biorender.com/> (accessed Sep. 23, 2021).
- [16] B. Levine, N. Mizushima, and H. W. Virgin, “Autophagy in immunity and inflammation,” *Nature*, vol. 469, no. 7330, pp. 323–335, Jan. 2011, doi: 10.1038/nature09782.
- [17] I. Nakagawa *et al.*, “Autophagy defends cells against invading group A Streptococcus,” *Science*, vol. 306, no. 5698, pp. 1037–1040, Nov. 2004, doi: 10.1126/science.1103966.

- [18] V. Sharma, S. Verma, E. Seranova, S. Sarkar, and D. Kumar, "Selective Autophagy and Xenophagy in Infection and Disease," *Front Cell Dev Biol*, vol. 6, p. 147, 2018, doi: 10.3389/fcell.2018.00147.
- [19] M. Qian, X. Fang, and X. Wang, "Autophagy and inflammation," *Clin Transl Med*, vol. 6, no. 1, p. 24, Dec. 2017, doi: 10.1186/s40169-017-0154-5.
- [20] T. Weichhart, M. Hengstschläger, and M. Linke, "Regulation of innate immune cell function by mTOR," *Nat Rev Immunol*, vol. 15, no. 10, pp. 599–614, Oct. 2015, doi: 10.1038/nri3901.
- [21] Y. Ge, M. Huang, and Y. Yao, "Autophagy and proinflammatory cytokines: Interactions and clinical implications," *Cytokine & Growth Factor Reviews*, vol. 43, pp. 38–46, Oct. 2018, doi: 10.1016/j.cytogfr.2018.07.001.
- [22] D. Egan, J. Kim, R. J. Shaw, and K.-L. Guan, "The autophagy initiating kinase ULK1 is regulated via opposing phosphorylation by AMPK and mTOR," *Autophagy*, vol. 7, no. 6, pp. 643–644, Jun. 2011, doi: 10.4161/auto.7.6.15123.
- [23] V. Nikolettou, K. Sidiropoulou, E. Kallergi, Y. Dalezios, and N. Tavernarakis, "Modulation of Autophagy by BDNF Underlies Synaptic Plasticity," *Cell Metabolism*, vol. 26, no. 1, pp. 230–242.e5, Jul. 2017, doi: 10.1016/j.cmet.2017.06.005.
- [24] A. Mahli *et al.*, "ERK activation and autophagy impairment are central mediators of irinotecan-induced steatohepatitis," *Gut*, p. gutjnl-2016-312485, Jan. 2017, doi: 10.1136/gutjnl-2016-312485.
- [25] F. Sun, X. Xu, X. Wang, and B. Zhang, "Regulation of autophagy by Ca<sup>2+</sup>," *Tumour Biol*, vol. 37, no. 12, pp. 15467–15476, Nov. 2016, doi: 10.1007/s13277-016-5353-y.
- [26] M. Schiebler *et al.*, "Functional drug screening reveals anticonvulsants as enhancers of mTOR-independent autophagic killing of Mycobacterium tuberculosis through inositol depletion," *EMBO Molecular Medicine*, vol. 7, no. 2, pp. 127–139, Feb. 2015, doi: 10.15252/emmm.201404137.
- [27] Y. Ge, M. Huang, and Y. Yao, "Autophagy and proinflammatory cytokines: Interactions and clinical implications," *Cytokine & Growth Factor Reviews*, vol. 43, pp. 38–46, Oct. 2018, doi: 10.1016/j.cytogfr.2018.07.001.
- [28] D. J. Klionsky, "Autophagy: from phenomenology to molecular understanding in less than a decade," *Nat Rev Mol Cell Biol*, vol. 8, no. 11, pp. 931–937, Nov. 2007, doi: 10.1038/nrm2245.
- [29] S. B. Singh *et al.*, "Human IRGM regulates autophagy and cell-autonomous immunity functions through mitochondria," *Nat Cell Biol*, vol. 12, no. 12, pp. 1154–1165, Dec. 2010, doi: 10.1038/ncb2119.
- [30] Y.-P. Chang *et al.*, "Autophagy facilitates IFN-gamma-induced Jak2-STAT1 activation and cellular inflammation," *J Biol Chem*, vol. 285, no. 37, pp. 28715–28722, Sep. 2010, doi: 10.1074/jbc.M110.133355.
- [31] M. A. Al-Zeer, H. M. Al-Younes, P. R. Braun, J. Zerrahn, and T. F. Meyer, "IFN-gamma-inducible Irga6 mediates host resistance against Chlamydia trachomatis via autophagy," *PLoS One*, vol. 4, no. 2, p. e4588, 2009, doi: 10.1371/journal.pone.0004588.
- [32] L. Wang, F. Du, H. Wang, and C. Xie, "Cooperation of CD4<sup>+</sup> T cells and CD8<sup>+</sup> T cells and release of IFN- $\gamma$  are critical for antileukemia responses of recipient mice treated by microtransplantation," *Experimental and Therapeutic Medicine*, vol. 15, no. 2, pp. 1532–1537, Feb. 2018, doi: 10.3892/etm.2017.5541.
- [33] J. Bresseit *et al.*, "Divergent Roles of Interferon- $\gamma$  and Innate Lymphoid Cells in Innate and Adaptive Immune Cell-Mediated Intestinal Inflammation," *Front. Immunol.*, vol. 9, 2018, doi: 10.3389/fimmu.2018.00023.

- [34] R. Mulder, A. Banete, K. Seaver, and S. Basta, “M(IL-4) Tissue Macrophages Support Efficient Interferon-Gamma Production in Antigen-Specific CD8+ T Cells with Reduced Proliferative Capacity,” *Front. Immunol.*, vol. 8, 2017, doi: 10.3389/fimmu.2017.01629.
- [35] S. P. Tu *et al.*, “Interferon- $\gamma$  inhibits gastric carcinogenesis by inducing epithelial cell autophagy and T cell apoptosis,” *Cancer Res*, vol. 71, no. 12, pp. 4247–4259, Jun. 2011, doi: 10.1158/0008-5472.CAN-10-4009.
- [36] S. Cs and K. Jh, “TRAF6 and A20 regulate lysine 63-linked ubiquitination of Beclin-1 to control TLR4-induced autophagy,” *Science signaling*, vol. 3, no. 123, May 2010, doi: 10.1126/scisignal.2000751.
- [37] F. Cg, Z. L, L. Mj, and S. A, “Interferon-inducible immunity-related GTPase Irgm1 regulates IFN gamma-dependent host defense, lymphocyte survival and autophagy,” *Autophagy*, vol. 5, no. 2, Feb. 2009, doi: 10.4161/auto.5.2.7445.
- [38] A.-L. Neehus *et al.*, “Impaired IFN $\gamma$ -Signaling and Mycobacterial Clearance in IFN $\gamma$ R1-Deficient Human iPSC-Derived Macrophages,” *Stem Cell Reports*, vol. 10, no. 1, p. 7, Jan. 2018, doi: 10.1016/j.stemcr.2017.11.011.
- [39] C.-P. Chang, M.-C. Yang, and H.-Y. Lei, “Concanavalin A/IFN-Gamma Triggers Autophagy-Related Necrotic Hepatocyte Death through IRGM1-Mediated Lysosomal Membrane Disruption,” *PLOS ONE*, vol. 6, no. 12, p. e28323, Dec. 2011, doi: 10.1371/journal.pone.0028323.
- [40] T. Matsuzawa, B.-H. Kim, A. R. Shenoy, S. Kamitani, M. Miyake, and J. D. Macmicking, “IFN- $\gamma$  elicits macrophage autophagy via the p38 MAPK signaling pathway,” *J Immunol*, vol. 189, no. 2, pp. 813–818, Jul. 2012, doi: 10.4049/jimmunol.1102041.
- [41] R. K. Dutta, M. Kathania, M. Raje, and S. Majumdar, “IL-6 inhibits IFN- $\gamma$  induced autophagy in Mycobacterium tuberculosis H37Rv infected macrophages,” *The International Journal of Biochemistry & Cell Biology*, vol. 44, no. 6, pp. 942–954, Jun. 2012, doi: 10.1016/j.biocel.2012.02.021.
- [42] G. Sharma *et al.*, “IL-27 inhibits IFN- $\gamma$  induced autophagy by concomitant induction of JAK/PI3 K/Akt/mTOR cascade and up-regulation of Mcl-1 in Mycobacterium tuberculosis H37Rv infected macrophages,” *The International Journal of Biochemistry & Cell Biology*, vol. 55, pp. 335–347, Oct. 2014, doi: 10.1016/j.biocel.2014.08.022.
- [43] K. Assani, M. F. Tazi, A. O. Amer, and B. T. Kopp, “IFN- $\gamma$  Stimulates Autophagy-Mediated Clearance of Burkholderia cenocepacia in Human Cystic Fibrosis Macrophages,” *PLOS ONE*, vol. 9, no. 5, p. e96681, May 2014, doi: 10.1371/journal.pone.0096681.
- [44] J. Kaur and J. Debnath, “Autophagy at the crossroads of catabolism and anabolism,” *Nature Reviews Molecular Cell Biology*, vol. 16, no. 8, Art. no. 8, Aug. 2015, doi: 10.1038/nrm4024.
- [45] S. Fougeray, I. Mami, G. Bertho, P. Beaune, E. Thervet, and N. Pallet, “Tryptophan Depletion and the Kinase GCN2 Mediate IFN- $\gamma$ -Induced Autophagy,” *The Journal of Immunology*, vol. 189, no. 6, pp. 2954–2964, Sep. 2012, doi: 10.4049/jimmunol.1201214.
- [46] Y.-P. Chang *et al.*, “Autophagy Facilitates IFN- $\gamma$ -induced Jak2-STAT1 Activation and Cellular Inflammation\*,” *Journal of Biological Chemistry*, vol. 285, no. 37, pp. 28715–28722, Sep. 2010, doi: 10.1074/jbc.M110.133355.
- [47] E. Liu, J. Van Grol, and C. S. Subauste, “Atg5 but not Atg7 in dendritic cells enhances IL-2 and IFN- $\gamma$  production by Toxoplasma gondii-reactive CD4+ T cells,” *Microbes and Infection*, vol. 17, no. 4, pp. 275–284, Apr. 2015, doi: 10.1016/j.micinf.2014.12.008.

- [48] Y.-D. Chen *et al.*, “S100A10 Regulates ULK1 Localization to ER–Mitochondria Contact Sites in IFN- $\gamma$ -Triggered Autophagy,” *Journal of Molecular Biology*, vol. 429, no. 1, pp. 142–157, Jan. 2017, doi: 10.1016/j.jmb.2016.11.009.
- [49] T. Yu *et al.*, “SENP1 regulates IFN- $\gamma$ -STAT1 signaling through STAT3–SOCS3 negative feedback loop,” *Journal of Molecular Cell Biology*, vol. 9, no. 2, pp. 144–153, Apr. 2017, doi: 10.1093/jmcb/mjw042.
- [50] X. Zhang *et al.*, “MCOLN1 is a ROS sensor in lysosomes that regulates autophagy,” *Nature Communications*, vol. 7, 2016, doi: 10.1038/ncomms12109.
- [51] X. J. Li *et al.*, “Protein-tyrosine Phosphatase Shp2 Positively Regulates Macrophage Oxidative Burst\*,” *Journal of Biological Chemistry*, vol. 290, no. 7, pp. 3894–3909, Feb. 2015, doi: 10.1074/jbc.M114.614057.
- [52] N.-Y. Lin, A. Stefanica, and J. H. W. Distler, “Autophagy,” *Autophagy*, vol. 9, no. 8, pp. 1253–1255, Aug. 2013, doi: 10.4161/auto.25467.
- [53] C. W. Keller *et al.*, “TNF- $\alpha$  Induces Macroautophagy and Regulates MHC Class II Expression in Human Skeletal Muscle Cells\*,” *Journal of Biological Chemistry*, vol. 286, no. 5, pp. 3970–3980, Feb. 2011, doi: 10.1074/jbc.M110.159392.
- [54] M.-X. Wang *et al.*, “TNF compromises lysosome acidification and reduces  $\alpha$ -synuclein degradation via autophagy in dopaminergic cells,” *Experimental Neurology*, vol. 271, pp. 112–121, Sep. 2015, doi: 10.1016/j.expneurol.2015.05.008.
- [55] N.-Y. Lin *et al.*, “Autophagy regulates TNF $\alpha$ -mediated joint destruction in experimental arthritis,” *Annals of the Rheumatic Diseases*, vol. 72, no. 5, pp. 761–768, May 2013, doi: 10.1136/annrheumdis-2012-201671.
- [56] A. Prokesch *et al.*, “Placental DAPK1 and autophagy marker LC3B-II are dysregulated by TNF- $\alpha$  in a gestational age-dependent manner,” *Histochem Cell Biol*, vol. 147, no. 6, pp. 695–705, Jun. 2017, doi: 10.1007/s00418-016-1537-1.
- [57] A. Rodríguez *et al.*, “The ghrelin O-acyltransferase–ghrelin system reduces TNF- $\alpha$ -induced apoptosis and autophagy in human visceral adipocytes,” *Diabetologia*, vol. 55, no. 11, pp. 3038–3050, Nov. 2012, doi: 10.1007/s00125-012-2671-5.
- [58] G. Jia, G. Cheng, D. M. Gangahar, and D. K. Agrawal, “Insulin-like growth factor-1 and TNF- $\alpha$  regulate autophagy through c-jun N-terminal kinase and Akt pathways in human atherosclerotic vascular smooth cells,” *Immunology & Cell Biology*, vol. 84, no. 5, pp. 448–454, 2006, doi: <https://doi.org/10.1111/j.1440-1711.2006.01454.x>.
- [59] N. Baregamian, J. Song, C. E. Bailey, J. Papaconstantinou, B. M. Evers, and D. H. Chung, “Tumor Necrosis Factor- $\alpha$  and Apoptosis Signal-Regulating Kinase 1 Control Reactive Oxygen Species Release, Mitochondrial Autophagy and C-Jun N-Terminal Kinase/P38 Phosphorylation During Necrotizing Enterocolitis,” *Oxidative Medicine and Cellular Longevity*, vol. 2, no. 5, pp. 297–306, 2009, doi: 10.4161/oxim.2.5.9541.
- [60] U. Sivaprasad and A. Basu, “Inhibition of ERK attenuates autophagy and potentiates tumour necrosis factor- $\alpha$ -induced cell death in MCF-7 cells,” *Journal of Cellular and Molecular Medicine*, vol. 12, no. 4, pp. 1265–1271, 2008, doi: <https://doi.org/10.1111/j.1582-4934.2008.00282.x>.
- [61] C. Bell *et al.*, “Quantitative Proteomics Reveals the Induction of Mitophagy in Tumor Necrosis Factor- $\alpha$ -activated (TNF $\alpha$ ) Macrophages\*,” *Molecular & Cellular Proteomics*, vol. 12, no. 9, pp. 2394–2407, Sep. 2013, doi: 10.1074/mcp.M112.025775.
- [62] Y.-C. Y. Takashi Ikejima<sup>1,\*</sup>, “TNF $\alpha$ -Induced Necroptosis and Autophagy via Suppression of the p38–NF- $\kappa$ B Survival Pathway in L929 Cells,” *Journal of Pharmacological Sciences*, vol. 117, no. 3, pp. 160–169, Jan. 2011, doi: 10.1254/jphs.11105FP.

- [63] T. Kuwabara, F. Ishikawa, M. Kondo, and T. Kakiuchi, "The Role of IL-17 and Related Cytokines in Inflammatory Autoimmune Diseases," *Mediators of Inflammation*, vol. 2017, 2017, doi: 10.1155/2017/3908061.
- [64] J. Yuan *et al.*, "Autophagy contributes to IL-17-induced plasma cell differentiation in experimental autoimmune myocarditis," *International Immunopharmacology*, vol. 18, no. 1, pp. 98–105, Jan. 2014, doi: 10.1016/j.intimp.2013.11.008.
- [65] L. Orosz, E. G. Papanicolaou, G. Seprényi, and K. Megyeri, "IL-17A and IL-17F induce autophagy in RAW 264.7 macrophages," *Biomedicine & Pharmacotherapy*, vol. 77, pp. 129–134, Feb. 2016, doi: 10.1016/j.biopha.2015.12.020.
- [66] E. K. Kim *et al.*, "IL-17-mediated mitochondrial dysfunction impairs apoptosis in rheumatoid arthritis synovial fibroblasts through activation of autophagy," *Cell Death and Disease*, vol. 8, no. 1, 2017, doi: 10.1038/cddis.2016.490.
- [67] H. Liu, S. Mi, Z. Li, F. Hua, and Z.-W. Hu, "Interleukin 17A inhibits autophagy through activation of PIK3CA to interrupt the GSK3B-mediated degradation of BCL2 in lung epithelial cells," *Autophagy*, vol. 9, no. 5, pp. 730–742, May 2013, doi: 10.4161/auto.24039.
- [68] Y. Zhou, P.-W. Wu, X.-W. Yuan, J. Li, and X.-L. Shi, "Interleukin-17A inhibits cell autophagy under starvation and promotes cell migration via TAB2/TAB3-p38 mitogen-Activated protein kinase pathways in hepatocellular carcinoma," *European Review for Medical and Pharmacological Sciences*, vol. 20, no. 2, pp. 250–263, 2016.
- [69] A. Said, S. Bock, T. Lajqi, G. Müller, and G. Weindl, "Chloroquine Promotes IL-17 Production by CD4+ T Cells via p38-Dependent IL-23 Release by Monocyte-Derived Langerhans-like Cells," *The Journal of Immunology*, vol. 193, no. 12, pp. 6135–6143, Dec. 2014, doi: 10.4049/jimmunol.1303276.
- [70] M. Reed, S. H. Morris, A. B. Owczarczyk, and N. W. Lukacs, "Deficiency of autophagy protein Map1-LC3b mediates IL-17-dependent lung pathology during respiratory viral infection via ER stress-associated IL-1," *Mucosal Immunology*, vol. 8, no. 5, Art. no. 5, Sep. 2015, doi: 10.1038/mi.2015.3.
- [71] J. E. Sims and D. E. Smith, "The IL-1 family: regulators of immunity," *Nature Reviews Immunology*, vol. 10, no. 2, Art. no. 2, Feb. 2010, doi: 10.1038/nri2691.
- [72] M. Zhang, S. J. Kenny, L. Ge, K. Xu, and R. Schekman, "Translocation of interleukin-1 $\beta$  into a vesicle intermediate in autophagy-mediated secretion," *eLife*, vol. 4, no. NOVEMBER2015, 2015, doi: 10.7554/eLife.11205.001.
- [73] B. Xu *et al.*, "Interleukin-1 $\beta$  induces autophagy by affecting calcium homeostasis and trypsinogen activation in pancreatic acinar cells," *Int J Clin Exp Pathol*, vol. 7, no. 7, pp. 3620–3631, Jun. 2014.
- [74] J. Shen *et al.*, "IL-1 $\beta$  induces apoptosis and autophagy via mitochondria pathway in human degenerative nucleus pulposus cells," *Scientific Reports*, vol. 7, 2017, doi: 10.1038/srep41067.
- [75] L.-J. Wang *et al.*, "The Microtubule-associated Protein EB1 Links AIM2 Inflammasomes with Autophagy-dependent Secretion\*," *Journal of Biological Chemistry*, vol. 289, no. 42, pp. 29322–29333, Oct. 2014, doi: 10.1074/jbc.M114.559153.
- [76] T. Saitoh *et al.*, "Loss of the autophagy protein Atg16L1 enhances endotoxin-induced IL-1 $\beta$  production," *Nature*, vol. 456, no. 7219, Art. no. 7219, Nov. 2008, doi: 10.1038/nature07383.
- [77] J. W. Symington *et al.*, "ATG16L1 deficiency in macrophages drives clearance of uropathogenic E. coli in an IL-1 $\beta$ -dependent manner," *Mucosal Immunology*, vol. 8, no. 6, Art. no. 6, Nov. 2015, doi: 10.1038/mi.2015.7.

- [78] G. Ilyas *et al.*, “Macrophage autophagy limits acute toxic liver injury in mice through down regulation of interleukin-1 $\beta$ ,” *Journal of Hepatology*, vol. 64, no. 1, pp. 118–127, Jan. 2016, doi: 10.1016/j.jhep.2015.08.019.
- [79] G. Petrovski *et al.*, “Phagocytosis of cells dying through autophagy induces inflammasome activation and IL-1 $\beta$  release in human macrophages,” *Autophagy*, vol. 7, no. 3, pp. 321–330, Mar. 2011, doi: 10.4161/auto.7.3.14583.
- [80] A. Brickle, H. T. Tran, R. Lim, S. Liong, and M. Lappas, “Autophagy, which is decreased in labouring fetal membranes, regulates IL-1 $\beta$  production via the inflammasome,” *Placenta*, vol. 36, no. 12, pp. 1393–1404, Dec. 2015, doi: 10.1016/j.placenta.2015.10.015.
- [81] N. Dupont, S. Jiang, M. Pilli, W. Ornatowski, D. Bhattacharya, and V. Deretic, “Autophagy-based unconventional secretory pathway for extracellular delivery of IL-1 $\beta$ ,” *The EMBO Journal*, vol. 30, no. 23, pp. 4701–4711, Nov. 2011, doi: 10.1038/emboj.2011.398.
- [82] J. Lee *et al.*, “Autophagy Suppresses Interleukin-1 $\beta$  (IL-1 $\beta$ ) Signaling by Activation of p62 Degradation via Lysosomal and Proteasomal Pathways\*,” *Journal of Biological Chemistry*, vol. 287, no. 6, pp. 4033–4040, Feb. 2012, doi: 10.1074/jbc.M111.280065.
- [83] C.-S. Shi *et al.*, “Activation of autophagy by inflammatory signals limits IL-1 $\beta$  production by targeting ubiquitinated inflammasomes for destruction,” *Nature Immunology*, vol. 13, no. 3, Art. no. 3, Mar. 2012, doi: 10.1038/ni.2215.
- [84] C. P. de Castro *et al.*, “Autophagy Regulates IL-23 Secretion and Innate T Cell Responses through Effects on IL-1 Secretion,” *The Journal of Immunology*, vol. 189, no. 8, pp. 4144–4153, Oct. 2012, doi: 10.4049/jimmunol.1201946.
- [85] A. de Luca *et al.*, “IL-1 receptor blockade restores autophagy and reduces inflammation in chronic granulomatous disease in mice and in humans,” *PNAS*, vol. 111, no. 9, pp. 3526–3531, Mar. 2014, doi: 10.1073/pnas.1322831111.
- [86] Y. Gao *et al.*, “IL-33 Exerts Neuroprotective Effect in Mice Intracerebral Hemorrhage Model Through Suppressing Inflammation/Apoptotic/Autophagic Pathway,” *Mol Neurobiol*, vol. 54, no. 5, pp. 3879–3892, Jul. 2017, doi: 10.1007/s12035-016-9947-6.
- [87] Y. Gao *et al.*, “IL-33 Provides Neuroprotection through Suppressing Apoptotic, Autophagic and NF- $\kappa$ B-Mediated Inflammatory Pathways in a Rat Model of Recurrent Neonatal Seizure,” *Front. Mol. Neurosci.*, vol. 10, 2017, doi: 10.3389/fnmol.2017.00423.
- [88] C. Gabay and J. E. Towne, “Regulation and function of interleukin-36 cytokines in homeostasis and pathological conditions,” *Journal of Leukocyte Biology*, vol. 97, no. 4, pp. 645–652, 2015, doi: <https://doi.org/10.1189/jlb.3RI1014-495R>.
- [89] C. A. Dinarello, “Overview of the IL-1 family in innate inflammation and acquired immunity,” *Immunol Rev*, vol. 281, no. 1, pp. 8–27, Jan. 2018, doi: 10.1111/imr.12621.
- [90] J. M. Murrieta-Coxca, S. Rodríguez-Martínez, M. E. Cancino-Díaz, U. R. Markert, R. R. Favaro, and D. M. Morales-Prieto, “IL-36 Cytokines: Regulators of Inflammatory Responses and Their Emerging Role in Immunology of Reproduction,” *Int J Mol Sci*, vol. 20, no. 7, p. E1649, Apr. 2019, doi: 10.3390/ijms20071649.
- [91] C. Garlanda, C. A. Dinarello, and A. Mantovani, “The interleukin-1 family: back to the future,” *Immunity*, vol. 39, no. 6, pp. 1003–1018, Dec. 2013, doi: 10.1016/j.immuni.2013.11.010.
- [92] D. E. Smith, B. R. Renshaw, R. R. Ketchem, M. Kubin, K. E. Garka, and J. E. Sims, “Four new members expand the interleukin-1 superfamily,” *J Biol Chem*, vol. 275, no. 2, pp. 1169–1175, Jan. 2000, doi: 10.1074/jbc.275.2.1169.

- [93] D. M. Clancy, C. M. Henry, G. P. Sullivan, and S. J. Martin, "Neutrophil extracellular traps can serve as platforms for processing and activation of IL-1 family cytokines," *FEBS J*, vol. 284, no. 11, pp. 1712–1725, Jun. 2017, doi: 10.1111/febs.14075.
- [94] C. M. Henry, G. P. Sullivan, D. M. Clancy, I. S. Afonina, D. Kulms, and S. J. Martin, "Neutrophil-Derived Proteases Escalate Inflammation through Activation of IL-36 Family Cytokines," *Cell Rep*, vol. 14, no. 4, pp. 708–722, Feb. 2016, doi: 10.1016/j.celrep.2015.12.072.
- [95] L. Zhou and V. Todorovic, "Interleukin-36: Structure, Signaling and Function," *Adv Exp Med Biol*, vol. 21, pp. 191–210, 2021, doi: 10.1007/5584\_2020\_488.
- [96] D. Boraschi, P. Italiani, S. Weil, and M. U. Martin, "The family of the interleukin-1 receptors," *Immunol Rev*, vol. 281, no. 1, pp. 197–232, Jan. 2018, doi: 10.1111/imr.12606.
- [97] G. Yi *et al.*, "Structural and Functional Attributes of the Interleukin-36 Receptor," *J Biol Chem*, vol. 291, no. 32, pp. 16597–16609, Aug. 2016, doi: 10.1074/jbc.M116.723064.
- [98] J. E. Towne, K. E. Garka, B. R. Renshaw, G. D. Virca, and J. E. Sims, "Interleukin (IL)-1F6, IL-1F8, and IL-1F9 signal through IL-1Rrp2 and IL-1RAcP to activate the pathway leading to NF-kappaB and MAPKs," *J Biol Chem*, vol. 279, no. 14, pp. 13677–13688, Apr. 2004, doi: 10.1074/jbc.M400117200.
- [99] C. Bridgewood, M. Stacey, A. Alase, D. Lagos, A. Graham, and M. Wittmann, "IL-36 $\gamma$  has proinflammatory effects on human endothelial cells," *Exp Dermatol*, vol. 26, no. 5, pp. 402–408, May 2017, doi: 10.1111/exd.13228.
- [100] A. M. Foster *et al.*, "IL-36 promotes myeloid cell infiltration, activation, and inflammatory activity in skin," *J Immunol*, vol. 192, no. 12, pp. 6053–6061, Jun. 2014, doi: 10.4049/jimmunol.1301481.
- [101] S. Vigne *et al.*, "IL-36 signaling amplifies Th1 responses by enhancing proliferation and Th1 polarization of naive CD4<sup>+</sup> T cells," *Blood*, vol. 120, no. 17, pp. 3478–3487, Oct. 2012, doi: 10.1182/blood-2012-06-439026.
- [102] A. Johnston *et al.*, "IL-1F5, -F6, -F8, and -F9: a novel IL-1 family signaling system that is active in psoriasis and promotes keratinocyte antimicrobial peptide expression," *J Immunol*, vol. 186, no. 4, pp. 2613–2622, Feb. 2011, doi: 10.4049/jimmunol.1003162.
- [103] Q. Qu, Z. Zhai, J. Xu, S. Li, C. Chen, and B. Lu, "IL36 Cooperates With Anti-CTLA-4 mAbs to Facilitate Antitumor Immune Responses," *Front Immunol*, vol. 11, p. 634, 2020, doi: 10.3389/fimmu.2020.00634.
- [104] A. Harusato *et al.*, "IL-36 $\gamma$  signaling controls the induced regulatory T cell-Th9 cell balance via NF $\kappa$ B activation and STAT transcription factors," *Mucosal Immunol*, vol. 10, no. 6, pp. 1455–1467, Nov. 2017, doi: 10.1038/mi.2017.21.
- [105] V. L. Ngo, M. Kuczma, E. Maxim, and T. L. Denning, "IL-36 cytokines and gut immunity," *Immunology*, vol. 163, no. 2, pp. 145–154, Jun. 2021, doi: 10.1111/imm.13310.
- [106] E. Y. Bassoy, J. E. Towne, and C. Gabay, "Regulation and function of interleukin-36 cytokines," *Immunol Rev*, vol. 281, no. 1, pp. 169–178, Jan. 2018, doi: 10.1111/imr.12610.
- [107] M. S. Gresnigt *et al.*, "The IL-36 receptor pathway regulates *Aspergillus fumigatus*-induced Th1 and Th17 responses," *Eur J Immunol*, vol. 43, no. 2, pp. 416–426, Feb. 2013, doi: 10.1002/eji.201242711.
- [108] N. Mizushima, B. Levine, A. M. Cuervo, and D. J. Klionsky, "Autophagy fights disease through cellular self-digestion," *Nature*, vol. 451, no. 7182, Art. no. 7182, Feb. 2008, doi: 10.1038/nature06639.

- [109] J. D. Rabinowitz and E. White, "Autophagy and Metabolism," *Science*, vol. 330, no. 6009, pp. 1344–1348, Dec. 2010, doi: 10.1126/science.1193497.
- [110] T. Saitoh, N. Fujita, T. Yoshimori, and S. Akira, "[Autophagy and innate immunity]," *Tanpakushitsu Kakusan Koso*, vol. 53, no. 16 Suppl, pp. 2279–2285, Dec. 2008.
- [111] C. Jagannath, D. R. Lindsey, S. Dhandayuthapani, Y. Xu, R. L. Hunter, and N. T. Eissa, "Autophagy enhances the efficacy of BCG vaccine by increasing peptide presentation in mouse dendritic cells," *Nature Medicine*, vol. 15, no. 3, Art. no. 3, Mar. 2009, doi: 10.1038/nm.1928.
- [112] M. A. Al-Zeer, H. M. Al-Younes, P. R. Braun, J. Zerrahn, and T. F. Meyer, "IFN- $\gamma$ -Inducible Irga6 Mediates Host Resistance against *Chlamydia trachomatis* via Autophagy," *PLOS ONE*, vol. 4, no. 2, p. e4588, Feb. 2009, doi: 10.1371/journal.pone.0004588.
- [113] J. Ohshima *et al.*, "Role of Mouse and Human Autophagy Proteins in IFN- $\gamma$ -Induced Cell-Autonomous Responses against *Toxoplasma gondii*," *The Journal of Immunology*, vol. 192, no. 7, pp. 3328–3335, Apr. 2014, doi: 10.4049/jimmunol.1302822.
- [114] P. Kumar, H. Gauba, P. Pratim Roy, and D. Prosad Dogra, "A multimodal framework for sensor based sign language recognition," *Neurocomputing*, vol. 259, pp. 21–38, Oct. 2017, doi: 10.1016/j.neucom.2016.08.132.
- [115] G. Nakos *et al.*, "Immunoparalysis in patients with severe trauma and the effect of inhaled interferon-gamma," *Crit Care Med*, vol. 30, no. 7, pp. 1488–1494, Jul. 2002, doi: 10.1097/00003246-200207000-00015.
- [116] M. Nalos, B. Santner-Nanan, G. Parnell, B. Tang, A. S. McLean, and R. Nanan, "Immune Effects of Interferon Gamma in Persistent Staphylococcal Sepsis," *Am J Respir Crit Care Med*, vol. 185, no. 1, pp. 110–112, Jan. 2012, doi: 10.1164/ajrccm.185.1.110.
- [117] D. Grimaldi, O. Pradier, R. S. Hotchkiss, and J.-L. Vincent, "Nivolumab plus interferon- $\gamma$  in the treatment of intractable mucormycosis," *The Lancet Infectious Diseases*, vol. 17, no. 1, p. 18, Jan. 2017, doi: 10.1016/S1473-3099(16)30541-2.
- [118] L. Mazgaeen and P. Gurung, "Recent Advances in Lipopolysaccharide Recognition Systems," *Int J Mol Sci*, vol. 21, no. 2, p. E379, Jan. 2020, doi: 10.3390/ijms21020379.
- [119] A. Steimle, I. B. Autenrieth, and J.-S. Frick, "Structure and function: Lipid A modifications in commensals and pathogens," *Int J Med Microbiol*, vol. 306, no. 5, pp. 290–301, Aug. 2016, doi: 10.1016/j.ijmm.2016.03.001.
- [120] S. W. Brubaker, K. S. Bonham, I. Zanoni, and J. C. Kagan, "Innate immune pattern recognition: a cell biological perspective," *Annu Rev Immunol*, vol. 33, pp. 257–290, 2015, doi: 10.1146/annurev-immunol-032414-112240.
- [121] K. J. Kieser and J. C. Kagan, "Multi-receptor detection of individual bacterial products by the innate immune system," *Nat Rev Immunol*, vol. 17, no. 6, pp. 376–390, Jun. 2017, doi: 10.1038/nri.2017.25.
- [122] A. Ciesielska, M. Matyjek, and K. Kwiatkowska, "TLR4 and CD14 trafficking and its influence on LPS-induced pro-inflammatory signaling," *Cell Mol Life Sci*, vol. 78, no. 4, pp. 1233–1261, Feb. 2021, doi: 10.1007/s00018-020-03656-y.
- [123] N. J. Gay, M. F. Symmons, M. Gangloff, and C. E. Bryant, "Assembly and localization of Toll-like receptor signalling complexes," *Nat Rev Immunol*, vol. 14, no. 8, pp. 546–558, Aug. 2014, doi: 10.1038/nri3713.
- [124] B. Boonen, Y. A. Alpizar, V. M. Meseguer, and K. Talavera, "TRP Channels as Sensors of Bacterial Endotoxins," *Toxins (Basel)*, vol. 10, no. 8, p. E326, Aug. 2018, doi: 10.3390/toxins10080326.

- [125] M. S. Schappe *et al.*, “Chanzyme TRPM7 Mediates the Ca<sup>2+</sup> Influx Essential for Lipopolysaccharide-Induced Toll-Like Receptor 4 Endocytosis and Macrophage Activation,” *Immunity*, vol. 48, no. 1, pp. 59–74.e5, Jan. 2018, doi: 10.1016/j.immuni.2017.11.026.
- [126] R. G. Scheraga *et al.*, “TRPV4 Mechanosensitive Ion Channel Regulates Lipopolysaccharide-Stimulated Macrophage Phagocytosis,” *J Immunol*, vol. 196, no. 1, pp. 428–436, Jan. 2016, doi: 10.4049/jimmunol.1501688.
- [127] J. Shi *et al.*, “Inflammatory caspases are innate immune receptors for intracellular LPS,” *Nature*, vol. 514, no. 7521, pp. 187–192, Oct. 2014, doi: 10.1038/nature13683.
- [128] Coronaviridae Study Group of the International Committee on Taxonomy of Viruses, “The species Severe acute respiratory syndrome-related coronavirus: classifying 2019-nCoV and naming it SARS-CoV-2,” *Nat Microbiol*, vol. 5, no. 4, pp. 536–544, Apr. 2020, doi: 10.1038/s41564-020-0695-z.
- [129] B. Hu, H. Guo, P. Zhou, and Z.-L. Shi, “Characteristics of SARS-CoV-2 and COVID-19,” *Nat Rev Microbiol*, vol. 19, no. 3, pp. 141–154, Mar. 2021, doi: 10.1038/s41579-020-00459-7.
- [130] M. Z. Tay, C. M. Poh, L. Rénia, P. A. MacAry, and L. F. P. Ng, “The trinity of COVID-19: immunity, inflammation and intervention,” *Nat Rev Immunol*, vol. 20, no. 6, pp. 363–374, Jun. 2020, doi: 10.1038/s41577-020-0311-8.
- [131] N. Vabret *et al.*, “Immunology of COVID-19: Current State of the Science,” *Immunity*, vol. 52, no. 6, pp. 910–941, Jun. 2020, doi: 10.1016/j.immuni.2020.05.002.
- [132] K. Megyeri, Á. Dernovics, Z. I. I. Al-Luhaibi, and A. Rosztóczy, “COVID-19-associated diarrhea,” *WJG*, vol. 27, no. 23, pp. 3208–3222, Jun. 2021, doi: 10.3748/wjg.v27.i23.3208.
- [133] R. Lu *et al.*, “Genomic characterisation and epidemiology of 2019 novel coronavirus: implications for virus origins and receptor binding,” *The Lancet*, vol. 395, no. 10224, pp. 565–574, Feb. 2020, doi: 10.1016/S0140-6736(20)30251-8.
- [134] Y. A. Helmy, M. Fawzy, A. Elaswad, A. Sobieh, S. P. Kenney, and A. A. Shehata, “The COVID-19 Pandemic: A Comprehensive Review of Taxonomy, Genetics, Epidemiology, Diagnosis, Treatment, and Control,” *JCM*, vol. 9, no. 4, p. 1225, Apr. 2020, doi: 10.3390/jcm9041225.
- [135] S. E. Miller and C. S. Goldsmith, “Caution in Identifying Coronaviruses by Electron Microscopy,” *JASN*, vol. 31, no. 9, pp. 2223–2224, Sep. 2020, doi: 10.1681/ASN.2020050755.
- [136] A. A. T. Naqvi *et al.*, “Insights into SARS-CoV-2 genome, structure, evolution, pathogenesis and therapies: Structural genomics approach,” *Biochimica et Biophysica Acta (BBA) - Molecular Basis of Disease*, vol. 1866, no. 10, p. 165878, Oct. 2020, doi: 10.1016/j.bbadis.2020.165878.
- [137] P. Zhou *et al.*, “A pneumonia outbreak associated with a new coronavirus of probable bat origin,” *Nature*, vol. 579, no. 7798, pp. 270–273, Mar. 2020, doi: 10.1038/s41586-020-2012-7.
- [138] M. Hoffmann *et al.*, “SARS-CoV-2 Cell Entry Depends on ACE2 and TMPRSS2 and Is Blocked by a Clinically Proven Protease Inhibitor,” *Cell*, vol. 181, no. 2, pp. 271–280.e8, Apr. 2020, doi: 10.1016/j.cell.2020.02.052.
- [139] B. J. Bosch, R. van der Zee, C. A. M. de Haan, and P. J. M. Rottier, “The Coronavirus Spike Protein Is a Class I Virus Fusion Protein: Structural and Functional Characterization of the Fusion Core Complex,” *J Virol*, vol. 77, no. 16, pp. 8801–8811, Aug. 2003, doi: 10.1128/JVI.77.16.8801-8811.2003.

- [140] M. Letko, A. Marzi, and V. Munster, “Functional assessment of cell entry and receptor usage for SARS-CoV-2 and other lineage B betacoronaviruses,” *Nat Microbiol*, vol. 5, no. 4, pp. 562–569, Apr. 2020, doi: 10.1038/s41564-020-0688-y.
- [141] R. Zang *et al.*, “TMPRSS2 and TMPRSS4 promote SARS-CoV-2 infection of human small intestinal enterocytes,” *Sci. Immunol.*, vol. 5, no. 47, p. eabc3582, May 2020, doi: 10.1126/sciimmunol.abc3582.
- [142] W. Wruck and J. Adjaye, “SARS-CoV-2 receptor ACE2 is co-expressed with genes related to transmembrane serine proteases, viral entry, immunity and cellular stress,” *Sci Rep*, vol. 10, no. 1, p. 21415, Dec. 2020, doi: 10.1038/s41598-020-78402-2.
- [143] M. Hussain *et al.*, “Molecular docking between human TMPRSS2 and SARS-CoV-2 spike protein: conformation and intermolecular interactions,” *AIMS Microbiology*, vol. 6, no. 3, pp. 350–360, 2020, doi: 10.3934/microbiol.2020021.
- [144] A. C. Walls, Y.-J. Park, M. A. Tortorici, A. Wall, A. T. McGuire, and D. Veelsler, “Structure, Function, and Antigenicity of the SARS-CoV-2 Spike Glycoprotein,” *Cell*, vol. 181, no. 2, pp. 281-292.e6, Apr. 2020, doi: 10.1016/j.cell.2020.02.058.
- [145] X. Ou *et al.*, “Characterization of spike glycoprotein of SARS-CoV-2 on virus entry and its immune cross-reactivity with SARS-CoV,” *Nat Commun*, vol. 11, no. 1, p. 1620, Dec. 2020, doi: 10.1038/s41467-020-15562-9.
- [146] L. Du *et al.*, “Cleavage of spike protein of SARS coronavirus by protease factor Xa is associated with viral infectivity,” *Biochemical and Biophysical Research Communications*, vol. 359, no. 1, pp. 174–179, Jul. 2007, doi: 10.1016/j.bbrc.2007.05.092.
- [147] H.-L. Ji, R. Zhao, S. Matalon, and M. A. Matthay, “Elevated Plasmin(ogen) as a Common Risk Factor for COVID-19 Susceptibility,” *Physiological Reviews*, vol. 100, no. 3, pp. 1065–1075, Jul. 2020, doi: 10.1152/physrev.00013.2020.
- [148] S. Belouzard, I. Madu, and G. R. Whittaker, “Elastase-mediated Activation of the Severe Acute Respiratory Syndrome Coronavirus Spike Protein at Discrete Sites within the S2 Domain,” *Journal of Biological Chemistry*, vol. 285, no. 30, pp. 22758–22763, Jul. 2010, doi: 10.1074/jbc.M110.103275.
- [149] L. Mendonça *et al.*, “SARS-CoV-2 Assembly and Egress Pathway Revealed by Correlative Multi-modal Multi-scale Cryo-imaging,” *Microbiology*, preprint, Nov. 2020. doi: 10.1101/2020.11.05.370239.
- [150] S. Klein *et al.*, “SARS-CoV-2 structure and replication characterized by in situ cryo-electron tomography,” *Nat Commun*, vol. 11, no. 1, p. 5885, Dec. 2020, doi: 10.1038/s41467-020-19619-7.
- [151] D. P. Oran and E. J. Topol, “The Proportion of SARS-CoV-2 Infections That Are Asymptomatic: A Systematic Review,” *Ann Intern Med*, vol. 174, no. 5, pp. 655–662, May 2021, doi: 10.7326/M20-6976.
- [152] F. Lauretani *et al.*, “Assessment and treatment of older individuals with COVID 19 multi-system disease: Clinical and ethical implications,” *Acta Bio Medica Atenei Parmensis*, vol. 91, no. 2, pp. 150–168, May 2020, doi: 10.23750/abm.v91i2.9629.
- [153] World Health Organization, “Clinical management of severe acute respiratory infection when novel coronavirus (2019-nCoV) infection is suspected: interim guidance, 28 January 2020,” World Health Organization, WHO/nCoV/Clinical/2020.3, 2020. Accessed: Aug. 08, 2021. [Online]. Available: <https://apps.who.int/iris/handle/10665/330893>
- [154] Y. Zhu *et al.*, “Clinical and CT imaging features of 2019 novel coronavirus disease (COVID-19),” *Journal of Infection*, vol. 81, no. 1, pp. 147–178, Jul. 2020, doi: 10.1016/j.jinf.2020.03.033.

- [155] Z. Wang and X. Xu, “scRNA-seq Profiling of Human Testes Reveals the Presence of the ACE2 Receptor, A Target for SARS-CoV-2 Infection in Spermatogonia, Leydig and Sertoli Cells,” *Cells*, vol. 9, no. 4, p. 920, Apr. 2020, doi: 10.3390/cells9040920.
- [156] G. Grasselli *et al.*, “Baseline Characteristics and Outcomes of 1591 Patients Infected With SARS-CoV-2 Admitted to ICUs of the Lombardy Region, Italy,” *JAMA*, vol. 323, no. 16, pp. 1574–1581, Apr. 2020, doi: 10.1001/jama.2020.5394.
- [157] F. Zhou *et al.*, “Clinical course and risk factors for mortality of adult inpatients with COVID-19 in Wuhan, China: a retrospective cohort study,” *The Lancet*, vol. 395, no. 10229, pp. 1054–1062, Mar. 2020, doi: 10.1016/S0140-6736(20)30566-3.
- [158] J. Villar *et al.*, “Dexamethasone treatment for the acute respiratory distress syndrome: a multicentre, randomised controlled trial,” *The Lancet Respiratory Medicine*, vol. 8, no. 3, pp. 267–276, Mar. 2020, doi: 10.1016/S2213-2600(19)30417-5.
- [159] L. M. Barton, E. J. Duval, E. Stroberg, S. Ghosh, and S. Mukhopadhyay, “COVID-19 Autopsies, Oklahoma, USA,” *Am J Clin Pathol*, vol. 153, no. 6, pp. 725–733, May 2020, doi: 10.1093/ajcp/aqaa062.
- [160] B. Bikdeli *et al.*, “COVID-19 and Thrombotic or Thromboembolic Disease: Implications for Prevention, Antithrombotic Therapy, and Follow-Up: JACC State-of-the-Art Review,” *J Am Coll Cardiol*, vol. 75, no. 23, pp. 2950–2973, Jun. 2020, doi: 10.1016/j.jacc.2020.04.031.
- [161] J. Thachil, “The versatile heparin in COVID-19,” *J Thromb Haemost*, vol. 18, no. 5, pp. 1020–1022, May 2020, doi: 10.1111/jth.14821.
- [162] P. Ramachandran *et al.*, “Gastrointestinal Symptoms and Outcomes in Hospitalized Coronavirus Disease 2019 Patients,” *DDI*, vol. 38, no. 5, pp. 373–379, 2020, doi: 10.1159/000509774.
- [163] L. Li *et al.*, “COVID-19 patients’ clinical characteristics, discharge rate, and fatality rate of meta-analysis,” *Journal of Medical Virology*, vol. 92, no. 6, pp. 577–583, 2020, doi: 10.1002/jmv.25757.
- [164] X. Jin *et al.*, “Epidemiological, clinical and virological characteristics of 74 cases of coronavirus-infected disease 2019 (COVID-19) with gastrointestinal symptoms,” *Gut*, vol. 69, no. 6, pp. 1002–1009, Jun. 2020, doi: 10.1136/gutjnl-2020-320926.
- [165] F. Xiao, M. Tang, X. Zheng, Y. Liu, X. Li, and H. Shan, “Evidence for Gastrointestinal Infection of SARS-CoV-2,” *Gastroenterology*, vol. 158, no. 6, pp. 1831–1833.e3, May 2020, doi: 10.1053/j.gastro.2020.02.055.
- [166] S. Parasa *et al.*, “Prevalence of Gastrointestinal Symptoms and Fecal Viral Shedding in Patients With Coronavirus Disease 2019: A Systematic Review and Meta-analysis,” *JAMA Network Open*, vol. 3, no. 6, p. e2011335, Jun. 2020, doi: 10.1001/jamanetworkopen.2020.11335.
- [167] M. Galanopoulos *et al.*, “COVID-19 pandemic: Pathophysiology and manifestations from the gastrointestinal tract,” *World J Gastroenterol*, vol. 26, no. 31, pp. 4579–4588, Aug. 2020, doi: 10.3748/wjg.v26.i31.4579.
- [168] L. Pan *et al.*, “Clinical Characteristics of COVID-19 Patients With Digestive Symptoms in Hubei, China: A Descriptive, Cross-Sectional, Multicenter Study,” *Official journal of the American College of Gastroenterology | ACG*, vol. 115, no. 5, pp. 766–773, May 2020, doi: 10.14309/ajg.0000000000000620.
- [169] N. Chen *et al.*, “Epidemiological and clinical characteristics of 99 cases of 2019 novel coronavirus pneumonia in Wuhan, China: a descriptive study,” *The Lancet*, vol. 395, no. 10223, pp. 507–513, Feb. 2020, doi: 10.1016/S0140-6736(20)30211-7.

- [170] P. Mo *et al.*, “Clinical Characteristics of Refractory Coronavirus Disease 2019 in Wuhan, China,” *Clinical Infectious Diseases*, no. ciaa270, Mar. 2020, doi: 10.1093/cid/ciaa270.
- [171] W. Guan *et al.*, “Clinical Characteristics of Coronavirus Disease 2019 in China,” *New England Journal of Medicine*, Feb. 2020, doi: 10.1056/NEJMoa2002032.
- [172] W. K. Leung *et al.*, “Enteric involvement of severe acute respiratory syndrome-associated coronavirus infection,” *Gastroenterology*, vol. 125, no. 4, pp. 1011–1017, Oct. 2003, doi: 10.1016/s0016-5085(03)01215-0.
- [173] E. Mahase, “Covid-19: six million doses of hydroxychloroquine donated to US despite lack of evidence,” *BMJ*, vol. 368, p. m1166, Mar. 2020, doi: 10.1136/bmj.m1166.
- [174] B. Cao *et al.*, “A Trial of Lopinavir–Ritonavir in Adults Hospitalized with Severe Covid-19,” *New England Journal of Medicine*, vol. 382, no. 19, pp. 1787–1799, May 2020, doi: 10.1056/NEJMoa2001282.
- [175] Gilead Sciences, “A Phase 3 Randomized Study to Evaluate the Safety and Antiviral Activity of Remdesivir (GS-5734<sup>TM</sup>) in Participants With Moderate COVID-19 Compared to Standard of Care Treatment,” [clinicaltrials.gov](https://clinicaltrials.gov/ct2/show/NCT04292730), Clinical trial registration NCT04292730, Jan. 2021. Accessed: Sep. 08, 2021. [Online]. Available: <https://clinicaltrials.gov/ct2/show/NCT04292730>
- [176] C. Chen *et al.*, “Favipiravir versus Arbidol for COVID-19: A Randomized Clinical Trial,” Apr. 2020. doi: 10.1101/2020.03.17.20037432.
- [177] A. Sayburn, “Covid-19: trials of four potential treatments to generate ‘robust data’ of what works,” *BMJ*, vol. 368, p. m1206, Mar. 2020, doi: 10.1136/bmj.m1206.
- [178] C. A. Schneider, W. S. Rasband, and K. W. Eliceiri, “NIH Image to ImageJ: 25 years of image analysis,” *Nat Methods*, vol. 9, no. 7, pp. 671–675, Jul. 2012, doi: 10.1038/nmeth.2089.
- [179] V. Deretic, “Autophagy: an emerging immunological paradigm,” *J Immunol*, vol. 189, no. 1, pp. 15–20, Jul. 2012, doi: 10.4049/jimmunol.1102108.
- [180] L. C. Gomes and I. Dikic, “Autophagy in antimicrobial immunity,” *Mol Cell*, vol. 54, no. 2, pp. 224–233, Apr. 2014, doi: 10.1016/j.molcel.2014.03.009.
- [181] D. J. Klionsky *et al.*, “Guidelines for the use and interpretation of assays for monitoring autophagy (4th edition)1,” *Autophagy*, vol. 17, no. 1, pp. 1–382, Jan. 2021, doi: 10.1080/15548627.2020.1797280.
- [182] Y. Ge, M. Huang, N. Dong, and Y.-M. Yao, “Effect of Interleukin-36 $\beta$  on Activating Autophagy of CD4<sup>+</sup>CD25<sup>+</sup> Regulatory T cells and Its Immune Regulation in Sepsis,” *J Infect Dis*, vol. 222, no. 9, pp. 1517–1530, Oct. 2020, doi: 10.1093/infdis/jiaa258.
- [183] Y. Gao *et al.*, “IL-36 $\gamma$  Promotes Killing of Mycobacterium tuberculosis by Macrophages via WNT5A-Induced Noncanonical WNT Signaling,” *The Journal of Immunology*, vol. 203, no. 4, pp. 922–935, Aug. 2019, doi: 10.4049/jimmunol.1900169.
- [184] C.-S. Shi and J. H. Kehrl, “MyD88 and Trif Target Beclin 1 to Trigger Autophagy in Macrophages,” *J Biol Chem*, vol. 283, no. 48, pp. 33175–33182, Nov. 2008, doi: 10.1074/jbc.M804478200.
- [185] M. A. Delgado, R. A. Elmaoued, A. S. Davis, G. Kyei, and V. Deretic, “Toll-like receptors control autophagy,” *EMBO J*, vol. 27, no. 7, pp. 1110–1121, Apr. 2008, doi: 10.1038/emboj.2008.31.
- [186] S. Sarkar, “Regulation of autophagy by mTOR-dependent and mTOR-independent pathways: autophagy dysfunction in neurodegenerative diseases and therapeutic

- application of autophagy enhancers,” *Biochem Soc Trans*, vol. 41, no. 5, pp. 1103–1130, Oct. 2013, doi: 10.1042/BST20130134.
- [187] E. B. M. Nascimento and D. M. Ouwens, “PRAS40: target or modulator of mTORC1 signalling and insulin action?,” *Arch Physiol Biochem*, vol. 115, no. 4, pp. 163–175, Oct. 2009, doi: 10.1080/13813450902988580.
- [188] X. Zhao *et al.*, “IL-36 $\beta$  Promotes CD8<sup>+</sup> T Cell Activation and Antitumor Immune Responses by Activating mTORC1,” *Front Immunol*, vol. 10, p. 1803, 2019, doi: 10.3389/fimmu.2019.01803.
- [189] S. Gallolu Kankanamalage *et al.*, “Multistep regulation of autophagy by WNK1,” *Proc Natl Acad Sci U S A*, vol. 113, no. 50, pp. 14342–14347, Dec. 2016, doi: 10.1073/pnas.1617649113.
- [190] L. You *et al.*, “The role of STAT3 in autophagy,” *Autophagy*, vol. 11, no. 5, pp. 729–739, 2015, doi: 10.1080/15548627.2015.1017192.
- [191] K. Hagio-Izaki *et al.*, “Lipopolysaccharide induces bacterial autophagy in epithelial keratinocytes of the gingival sulcus,” *BMC Cell Biol*, vol. 19, no. 1, p. 18, Dec. 2018, doi: 10.1186/s12860-018-0168-x.
- [192] J. Rex *et al.*, “Model-Based Characterization of Inflammatory Gene Expression Patterns of Activated Macrophages,” *PLoS Comput Biol*, vol. 12, no. 7, p. e1005018, Jul. 2016, doi: 10.1371/journal.pcbi.1005018.
- [193] K. Oda and H. Kitano, “A comprehensive map of the toll-like receptor signaling network,” *Mol Syst Biol*, vol. 2, p. 2006.0015, Apr. 2006, doi: 10.1038/msb4100057.
- [194] T. Fukao and S. Koyasu, “PI3K and negative regulation of TLR signaling,” *Trends Immunol*, vol. 24, no. 7, pp. 358–363, Jul. 2003, doi: 10.1016/s1471-4906(03)00139-x.
- [195] E. Aksoy *et al.*, “The p110 $\delta$  isoform of the kinase PI(3)K controls the subcellular compartmentalization of TLR4 signaling and protects from endotoxic shock,” *Nat Immunol*, vol. 13, no. 11, pp. 1045–1054, Nov. 2012, doi: 10.1038/ni.2426.
- [196] M. Bouhaddou *et al.*, “The Global Phosphorylation Landscape of SARS-CoV-2 Infection,” *Cell*, vol. 182, no. 3, pp. 685–712.e19, Aug. 2020, doi: 10.1016/j.cell.2020.06.034.
- [197] P. Fagone *et al.*, “Transcriptional landscape of SARS-CoV-2 infection dismantles pathogenic pathways activated by the virus, proposes unique sex-specific differences and predicts tailored therapeutic strategies,” *Autoimmun Rev*, vol. 19, no. 7, p. 102571, Jul. 2020, doi: 10.1016/j.autrev.2020.102571.
- [198] E. Cavalli *et al.*, “Transcriptomic analysis of COVID-19 lungs and bronchoalveolar lavage fluid samples reveals predominant B cell activation responses to infection,” *Int J Mol Med*, vol. 46, no. 4, pp. 1266–1273, Oct. 2020, doi: 10.3892/ijmm.2020.4702.
- [199] A. Ehrlich and Y. Nahmias, “The SARS-CoV-2 Transcriptional Metabolic Signature in Lung Epithelium,” 2020, Accessed: Sep. 29, 2021. [Online]. Available: <https://pesquisa.bvsalud.org/global-literature-on-novel-coronavirus-2019-ncov/resource/en/ppcovidwho-1648>
- [200] D. E. Gordon *et al.*, “A SARS-CoV-2 protein interaction map reveals targets for drug repurposing,” *Nature*, vol. 583, no. 7816, pp. 459–468, Jul. 2020, doi: 10.1038/s41586-020-2286-9.
- [201] J. Hadjadj *et al.*, “Impaired type I interferon activity and inflammatory responses in severe COVID-19 patients,” *Science*, vol. 369, no. 6504, pp. 718–724, Aug. 2020, doi: 10.1126/science.abc6027.
- [202] J. Wang, M. Jiang, X. Chen, and L. J. Montaner, “Cytokine storm and leukocyte changes in mild versus severe SARS-CoV-2 infection: Review of 3939 COVID-19 patients in China and emerging pathogenesis and therapy concepts,” *J Leukoc Biol*, vol. 108, no. 1, pp. 17–41, Jul. 2020, doi: 10.1002/JLB.3COVR0520-272R.

- [203] G. Chen *et al.*, “Clinical and immunological features of severe and moderate coronavirus disease 2019,” *J Clin Invest*, vol. 130, no. 5, pp. 2620–2629, May 2020, doi: 10.1172/JCI137244.
- [204] C. Huang *et al.*, “Clinical features of patients infected with 2019 novel coronavirus in Wuhan, China,” *Lancet*, vol. 395, no. 10223, pp. 497–506, Feb. 2020, doi: 10.1016/S0140-6736(20)30183-5.
- [205] Y. Xiong *et al.*, “Transcriptomic characteristics of bronchoalveolar lavage fluid and peripheral blood mononuclear cells in COVID-19 patients,” *Emerg Microbes Infect*, vol. 9, no. 1, pp. 761–770, Dec. 2020, doi: 10.1080/22221751.2020.1747363.
- [206] D. Blanco-Melo *et al.*, “Imbalanced Host Response to SARS-CoV-2 Drives Development of COVID-19,” *Cell*, vol. 181, no. 5, pp. 1036-1045.e9, May 2020, doi: 10.1016/j.cell.2020.04.026.
- [207] I.-E. Galani *et al.*, “Untuned antiviral immunity in COVID-19 revealed by temporal type I/III interferon patterns and flu comparison,” *Nat Immunol*, vol. 22, no. 1, pp. 32–40, Jan. 2021, doi: 10.1038/s41590-020-00840-x.
- [208] S. J. Theobald *et al.*, “The SARS-CoV-2 spike protein primes inflammasome-mediated interleukin-1- beta secretion in COVID-19 patient-derived macrophages.” Sep. 14, 2021. doi: 10.21203/rs.3.rs-30407/v1.
- [209] N. Zhu *et al.*, “Morphogenesis and cytopathic effect of SARS-CoV-2 infection in human airway epithelial cells,” *Nat Commun*, vol. 11, no. 1, p. 3910, Aug. 2020, doi: 10.1038/s41467-020-17796-z.
- [210] H. Xu *et al.*, “SARS-CoV-2 viroporin triggers the NLRP3 inflammatory pathway,” Oct. 2020. doi: 10.1101/2020.10.27.357731.
- [211] S. Li *et al.*, “SARS-CoV-2 triggers inflammatory responses and cell death through caspase-8 activation,” *Signal Transduct Target Ther*, vol. 5, no. 1, p. 235, Oct. 2020, doi: 10.1038/s41392-020-00334-0.
- [212] Y. Qu *et al.*, “ORF3a mediated-incomplete autophagy facilitates SARS-CoV-2 replication,” Nov. 2020. doi: 10.1101/2020.11.12.380709.
- [213] F. Hikmet, L. Méar, Å. Edvinsson, P. Micke, M. Uhlén, and C. Lindskog, “The protein expression profile of ACE2 in human tissues,” *Mol Syst Biol*, vol. 16, no. 7, p. e9610, Jul. 2020, doi: 10.15252/msb.20209610.
- [214] X. Zou, K. Chen, J. Zou, P. Han, J. Hao, and Z. Han, “Single-cell RNA-seq data analysis on the receptor ACE2 expression reveals the potential risk of different human organs vulnerable to 2019-nCoV infection,” *Front Med*, vol. 14, no. 2, pp. 185–192, Apr. 2020, doi: 10.1007/s11684-020-0754-0.
- [215] H. Zhang *et al.*, “Digestive system is a potential route of COVID-19: an analysis of single-cell coexpression pattern of key proteins in viral entry process,” *Gut*, vol. 69, no. 6, pp. 1010–1018, Jun. 2020, doi: 10.1136/gutjnl-2020-320953.

## **10. Annexes**

**I.**



## Article

# IL-36 $\alpha$ and Lipopolysaccharide Cooperatively Induce Autophagy by Triggering Pro-Autophagic Biased Signaling

Zaid I. I. Al-Luhaibi <sup>1</sup>, Áron Dernovics <sup>1</sup>, György Seprényi <sup>2</sup>, Ferhan Ayaydin <sup>3,4</sup>, Zsolt Boldogkői <sup>5</sup>, Zoltán Veréb <sup>6</sup> and Klára Megyeri <sup>1,\*</sup>

- <sup>1</sup> Department of Medical Microbiology, Albert Szent-Györgyi Medical School, University of Szeged, Dóm tér 10, H-6720 Szeged, Hungary; alluhaibi.zaid@med.u-szeged.hu (Z.I.I.A.-L.); dernovics.aron@med.u-szeged.hu (Á.D.)
- <sup>2</sup> Department of Anatomy, Histology and Embryology, Albert Szent-Györgyi Medical School, University of Szeged, Kossuth L. sgt. 40, H-6724 Szeged, Hungary; seprenyi.gyorgy@med.u-szeged.hu
- <sup>3</sup> Hungarian Centre of Excellence for Molecular Medicine (HCEMM) Nonprofit Ltd., Római krt. 21, H-6723 Szeged, Hungary; ferhan.ayaydin@hceimm.eu
- <sup>4</sup> Biological Research Centre, Laboratory of Cellular Imaging, Eötvös Loránd Research Network, Temesvári krt. 62, H-6726 Szeged, Hungary
- <sup>5</sup> Department of Medical Biology, Albert Szent-Györgyi Medical School, University of Szeged, Somogyi Béla u. 4, H-6720 Szeged, Hungary; boldogkoi.zsolt@med.u-szeged.hu
- <sup>6</sup> Regenerative Medicine and Cellular Pharmacology Laboratory, Albert Szent-Györgyi Medical School, University of Szeged, Korányi fasor 6, H-6720 Szeged, Hungary; vereb.zoltan@med.u-szeged.hu
- \* Correspondence: megyeri.klara@med.u-szeged.hu; Tel.: +36-62-545115



**Citation:** Al-Luhaibi, Z.I.I.; Dernovics, Á.; Seprényi, G.; Ayaydin, F.; Boldogkői, Z.; Veréb, Z.; Megyeri, K. IL-36 $\alpha$  and Lipopolysaccharide Cooperatively Induce Autophagy by Triggering Pro-Autophagic Biased Signaling. *Biomedicines* **2021**, *9*, 1541. <https://doi.org/10.3390/biomedicines9111541>

**Academic Editors:** Alessandro Rimessi and Simone Patergnani

Received: 24 September 2021  
Accepted: 20 October 2021  
Published: 26 October 2021

**Publisher's Note:** MDPI stays neutral with regard to jurisdictional claims in published maps and institutional affiliations.



**Copyright:** © 2021 by the authors. Licensee MDPI, Basel, Switzerland. This article is an open access article distributed under the terms and conditions of the Creative Commons Attribution (CC BY) license (<https://creativecommons.org/licenses/by/4.0/>).

**Abstract:** Autophagy is an intracellular catabolic process that controls infections both directly and indirectly via its multifaceted effects on the innate and adaptive immune responses. It has been reported that LPS stimulates this cellular process, whereas the effect of IL-36 $\alpha$  on autophagy remains largely unknown. We therefore investigated how IL-36 $\alpha$  modulates the endogenous and LPS-induced autophagy in THP-1 cells. The levels of LC3B-II and autophagic flux were determined by Western blotting. The intracellular localization of LC3B was measured by immunofluorescence assay. The activation levels of signaling pathways implicated in autophagy regulation were evaluated by using a phosphokinase array. Our results showed that combined IL-36 $\alpha$  and LPS treatment cooperatively increased the levels of LC3B-II and Beclin-1, stimulated the autophagic flux, facilitated intracellular redistribution of LC3B, and increased the average number of autophagosomes per cell. The IL36 $\alpha$ /LPS combined treatment increased phosphorylation of STAT5a/b, had minimal effect on the Akt/PRAS40/mTOR pathway, and reduced the levels of phospho-Yes, phospho-FAK, and phospho-WNK1. Thus, this cytokine/PAMP combination triggers pro-autophagic biased signaling by several mechanisms and thus cooperatively stimulates the autophagic cascade. An increased autophagic activity of innate immune cells simultaneously exposed to IL-36 $\alpha$  and LPS may play an important role in the pathogenesis of Gram-negative bacterial infections.

**Keywords:** IL-36 $\alpha$ ; LPS; autophagy; LC3B; Beclin-1

## 1. Introduction

Interleukin-36 $\alpha$  (IL-36 $\alpha$ ), IL-36 $\beta$ , IL-36 $\gamma$ , and IL-36 receptor antagonist (IL-36Ra) belong to the IL-36 subfamily of the IL-1 cytokine family [1–3]. The IL-36 subfamily includes three agonist cytokines (IL-36 $\alpha$ / $\beta$ / $\gamma$ ) as well as the natural antagonist of IL-36 (IL-36Ra). Expression of IL-36 $\alpha$  can be observed at low levels in many different tissues, most notably in the skin, esophagus, tonsil, lung, gut, and brain. IL-36 $\alpha$  can also be secreted by the immune cells including monocytes/macrophages and T cells [4]. IL-36 $\alpha$ / $\beta$ / $\gamma$  are highly induced in response to several stimuli including cytokines, Toll-like receptor agonists, bacteria, viruses, and various pathological conditions. The IL-36 subtypes are synthesized as precursor proteins. Cleavage of the precursor form of IL-36 $\alpha$  at a specific site located at

nine amino acids N-terminal to a conserved A-X-Asp motif highly increases the affinity of the truncated cytokine to the receptor and enhances its biological activity [5–7]. The truncated IL-36 $\alpha$ / $\beta$ / $\gamma$  bind to the same heterodimeric receptor complex. Ligand binding leads to the sequential formation of a signaling complex containing some adaptors, kinases, and the E3 ubiquitin ligase, tumor necrosis factor receptor-associated kinase 6 (TRAF-6). This platform triggers a signaling cascade involving mitogen-activated protein kinases (MAPKs) and the activation of several transcription factors (Figure 1A) [3,7–10].

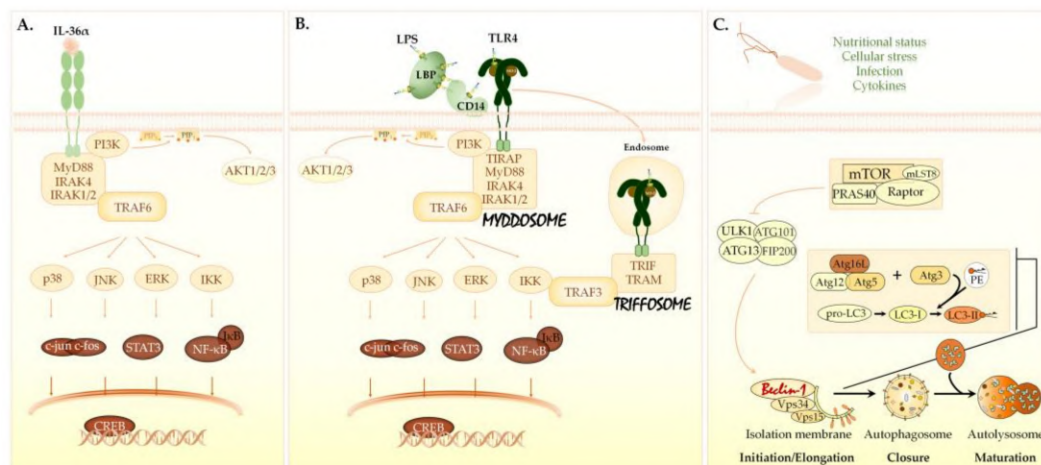


**Figure 1.** Signaling pathways triggered by IL-36 $\alpha$ , LPS, and autophagy inducers. (A) The IL-36 $\alpha$  signaling pathway. IL-36 $\alpha$ / $\beta$ / $\gamma$  bind to the IL-36R (IL-1Rrp2) and use the IL-1 receptor accessory protein (IL-1RAcP) as a co-receptor. Following ligand binding, the TIR domain—located in the intracellular portion of the IL-36R:IL-1RAcP heterodimer—recruits MyD88 adaptor protein, which in turn interacts with IRAKs and TRAF-6. The MyD88/IRAK/TRAF6 platform activates AP-1, CREB and NF- $\kappa$ B transcription factors via IKK, ERKs, JNKs, and p38. (B) The LPS/TLR4 signaling pathway. LBP and CD14 bind and transfer LPS monomers to the TLR4/MD-2 heterodimer. The dimerized TIR domain in the cytoplasmic portion of TLR4 consecutively recruits TIRAP, MyD88, and IRAK proteins, thus leading to the assembly of a supramolecular complex termed the myddosome. The LPS-TLR4/MD2 complexes can also be internalized into endosomes. The TIR domain of endosomal TLR4 binds TRAM, which attracts TRIF resulting in the formation of another complex called the trifosome. Myddosomes and trifosomes recruit TRAF6 or TRAF3 and activate AP-1, NF- $\kappa$ B, CREB, and IRF-3 via MAPKs, IKK, and PI3K. (C) The autophagy-related signaling pathway. The major element in the regulation of autophagy is the mTORC1. Besides mTOR, mTORC1 is comprised of the Raptor and mLST8 molecules. The non-core components associated with mTORC1 include PRAS40 and DEPTOR. Autophagy inducers inhibit mTORC1, and thereby activate the autophagic cascade. Inhibition of mTORC1 results in the consecutive activation of the ULK1 and PI3KC3 complexes. The PI3KC3 complex contains Beclin-1 protein. The activated PI3KC3 induces local production of PI3P at the endoplasmic reticulum membrane and thereby promotes the generation of an omegasome from which the isolation membrane is generated. PI3P recruits two ubiquitin-like conjugation systems, the ATG12–ATG5–ATG16L1 and ATG7/ATG3 complexes, to the omegasome. ATG3 forms a covalent bond between the membrane-resident phosphatidylethanolamine and the microtubule-associated protein 1 light chain 3B-I (LC3B-I) protein. The ATG12–ATG5–ATG16L1 complex enhances the ATG3-mediated conjugation of LC3B-I. The lipidated LC3B protein is termed LC3B-II. LC3B-II is essential for the elongation and closure of the phagophore membrane, trafficking of the autophagosomes, and their fusion with lysosomes. AP-1, activator protein 1; CREB, cAMP response element-binding protein; DEPTOR, DEP-domain containing mTOR-interacting protein; ERKs, extracellular signal-regulated kinases; IKK, I $\kappa$ B kinase; IRAKs, IL-1 receptor-associated kinases; IRF-3, interferon regulatory factor 3; JNKs, c-Jun N-terminal kinases; LBP, LPS-binding protein; MD-2, myeloid differentiation factor 2; mLST8, mammalian lethal with sec-13 protein 8; mTOR, mechanistic target of rapamycin; mTORC1, mTOR complex 1; MyD88, myeloid differentiation primary response 88; NF- $\kappa$ B, nuclear factor- $\kappa$ B; PE, phosphatidylethanolamine; PI3K, class I phosphatidylinositol 3-kinase; PI3KC3, class III phosphatidylinositol 3-kinase; PI3P, phosphatidylinositol-3-phosphate; PRAS40, proline-rich Akt substrate of 40 kDa; Raptor, regulatory-associated protein of mTOR; TIR, Toll/IL-1 receptor domain; TLR4, Toll-like receptor 4; TRAF-6, tumor necrosis factor receptor-associated kinase 6; TRAM, TRIF-related adaptor molecule; TRIF; TIR domain-containing adaptor-inducing interferon- $\beta$ ; ULK1, Unc-51-like kinase 1; WIPI, WD repeat domain phosphoinositide-interacting proteins.

IL-36 subtypes stimulate the production of several cytokines (IL-1 $\alpha$ , IL-1 $\beta$ , IL-2, IL-4, IL-6, IL-8, IL-10, IL-12, IL-17, IL-18, IL-22, IL-23, TNF $\alpha$ , HB-EGF, and IFN- $\gamma$ ), colony-stimulating factors (GM-CSF and G-CSF), chemokines (CCL1-3, CCL20, CXCL1-3, CXCL5, CXCL10, CXCL12), and cell adhesion molecules (VCAM-1, ICAM-1) in various cell types [11–13]. Furthermore, IL-36 cytokines increase the intracellular level of antimicrobial peptides (beta-defensins 2 and 3, LL37, and protein S100-A7) and elevate the expression of major histocompatibility complex class 2 and clusters of differentiation 14 (CD14), CD40, CD80/CD86, and CD83 [12–14]. IL-36 $\alpha/\beta/\gamma$  thereby activate innate immune cells and induce inflammation. The pro-inflammatory IL-36 subfamily members also modulate the adaptive immune responses by stimulating TH-cell proliferation and promoting CD4+ T lymphocyte differentiation toward TH1, TH17, and TH9 phenotypes. IL-36 $\gamma$  was shown to activate natural regulatory T-cells (Tregs) [15] and inhibit the generation of induced Tregs [16]. In acute resolving inflammation, IL-36  $\alpha/\beta/\gamma$  has been suggested to facilitate the elimination of pathogenic microorganisms, the resolution of tissue injury, and the restoration of tissue integrity. However, in chronic inflammatory processes, these IL-36 subtypes can exert a pathogenic effect by amplifying inflammatory processes [17–19].

Lipopolysaccharide (LPS) is a powerful immunomodulatory molecule that contributes to the pathogenesis and clinical symptoms of infections caused by Gram-negative bacteria. LPS is the major structural component of the outer bacterial membrane and is composed of O antigen, poly/oligosaccharide core, and lipid A, termed endotoxin [20,21]. LPS is a pathogen-associated molecular pattern (PAMP) detected by sensor molecules located in the cytoplasmic and endosomal membranes as well as in the cytoplasm of cells [22–24]. Extracellular LPS is sensed and extracted from the bacterial outer membrane by the LPS-binding protein (LBP) and CD14 [22–24]. CD14 transfers monomeric LPS molecules to the Toll-like receptor 4 (TLR4) leading to the assembly of a supramolecular complex termed the myddosome. The LPS-TLR4 complexes can also be internalized into endosomes resulting in the formation of another complex called the triffosome. These platforms trigger a signaling cascade involving MAPKs and the activation of several transcription factors (Figure 1B) [20,22–25]. The activated transcription factors turn on the expression of various cellular genes encoding inflammatory mediators including cytokines [20,22,23]. In addition to TLR4, another group of cytoplasmic membrane receptors—the transient receptor potential (TRP) cationic channels—can bind LPS [20,26]. TRP cation channel subfamily V members 2 and 4 (TRPV2 and TRPV4) and TRPM7 also contribute to the LPS-mediated activation of innate immune cells by triggering intracellular Ca<sup>2+</sup> mobilization and secretion of nitric oxide [27,28]. Additionally, intracellular LPS within the cytoplasm of cells directly binds to the caspase activation and recruitment domains of caspase-4/5 in humans and caspase-11 in mice, which in turn leads to activation of inflammatory caspases, secretion of IL-1 $\beta$  and IL-18, as well as induction of pyroptosis [29]. In localized infections caused by Gram-negative bacteria, LPS-mediated activation of the immune response is protective by restricting bacterial invasion whereas the exaggerated inflammation seen in systemic infections is of pivotal pathogenetic and prognostic importance.

Autophagy is an intracellular metabolic process in which cytoplasmic target molecules are transferred to the lysosome for degradation and recycling [30–32]. Depending on the type of cargo delivery, three different forms of autophagy can be distinguished: (1) macroautophagy, (2) microautophagy, and (3) chaperon-mediated autophagy [32]. The difference among these types is how the constituents to be degraded are transported to the lysosome. Macroautophagy (hereafter referred to as autophagy) occurs under basal conditions and can be stimulated by environmental cues, nutrient starvation, growth factor depletion, various pathological conditions, infections, hypoxia, or pharmacological treatment [33]. The major element in the regulation of autophagy is the mechanistic target of rapamycin complex 1 (mTORC1) [34,35]. Autophagy inducers inhibit mTORC1, and thereby activate the autophagic cascade. Inhibition of mTORC1 results in the activation of the class III phosphatidylinositol 3-kinase (PI3KC3) complex. The PI3KC3 complex contains Beclin-1 protein [36,37]. The activated PI3KC3 induces local production of phosphatidylinositol-

3-phosphate (PI3P) at the endoplasmic reticulum membrane and thereby promotes the generation of an omegasome from which the isolation membrane is generated [37–39]. PI3P recruits two ubiquitin-like conjugation systems to the omegasome, which form a covalent bond between the membrane-resident phosphatidylethanolamine (PE) and the microtubule-associated protein 1 light chain 3B-I (LC3B-I) protein [38,39]. The lipidated LC3B, termed LC3B-II, is essential for the elongation and closure of the phagophore membrane, trafficking of the autophagosomes, and their fusion with lysosomes [40–42]. The level of LC3B-II reflects the cellular autophagic activity and it is used as a marker to measure autophagy. Upon autophagy induction, LC3B translocates from the cytoplasm to autophagic membranes, and can be detected as fluorescent puncta (Figure 1C) [41].

The autophagosomes eventually fuse with lysosomes, and the content of the autophagic cargo is thus degraded and made available for reuse [43,44]. Autophagy is essential for the maintenance of cellular homeostasis and plays a substantial role in pathological processes including bacterial infections [33,45]. Autophagic capture and delivery of bacteria to lysosomes functions as a protective cellular antimicrobial defense mechanism known as xenophagy [46]. Autophagy also controls bacterial infections indirectly via its multifaceted effects on the innate and adaptive immune responses [47,48]. mTORC1 signaling affects the maturation, metabolic activity, activation, and differentiation of innate immune cells [49,50]. The mTORC1 pathway can also stimulate the production of type I interferons (IFN), IL-10, and transforming growth factor- $\beta$ , and downregulates the expression of IL-6, IL-12, IL-23, and TNF- $\alpha$  in monocytes, macrophages, and dendritic cells [51]. The autophagic machinery promotes the secretion of IL-1 $\beta$ , IL-18, and high-mobility group protein B1 and also facilitates antigen presentation to CD4<sup>+</sup> and CD8<sup>+</sup> T-cells. Conversely, immune processes may profoundly alter the cellular autophagic activity [47]. Ample evidence indicates that LPS induces autophagy via some mTOR-independent mechanisms. In response to binding of LPS to TLR4, the myddosomes and triffosomes recruit, whereas TRAF6 ubiquitinates Beclin-1, leading to the more efficient assembly of PI3KC3 with subsequent activation of the autophagic cascade [52,53].

Besides the signaling events elicited by pathogen-recognition receptors, cytokines may also modulate autophagy. IL-1 $\alpha$ , IL-1 $\beta$ , IL-2, IL-6, IL-17, TNF- $\alpha$ , TWEAK (tumor necrosis factor-like weak inducer of apoptosis), and IFN- $\gamma$  act as inducers whereas IL-4, IL-10, and IL-13 function as inhibitors of autophagy [54,55]. Recent data demonstrate the pro-autophagic effect of IL-36 $\beta$  and IL-36 $\gamma$  [56,57]. IL-36 $\beta$  enhanced the expression of key autophagy markers, LC3-II, Beclin-1, and p62, as well as elevated autophagic flux in CD4<sup>+</sup>CD25<sup>+</sup> Treg cells [57]. This IL-36 subtype played protective role in sepsis by diminishing the immunosuppressive activity of CD4<sup>+</sup>CD25<sup>+</sup> Tregs [57]. The signal transduction mechanisms involved in IL-36 $\beta$ -mediated induction of autophagy, however, have not been identified. IL-36 $\gamma$  triggered autophagy via WNT5A-induced noncanonical WNT signaling in macrophages infected with *Mycobacterium tuberculosis* [56]. Moreover, IL-36 $\gamma$ -induced autophagy promoted the killing of intracellular bacteria [56]. In contrast, the effect of IL-36 $\alpha$  on the autophagic process has not yet been elucidated. Infections involve a variety of pathogen-related molecular pattern (PAMP)—cytokine recognition events that can profoundly affect the antimicrobial response of immune cells. Thus, we investigated the effect of IL-36 $\alpha$  upon endogenous and LPS-induced autophagy. We report that IL-36 $\alpha$  can synergize with LPS for the induction of the autophagic process in the THP-1 cell line by triggering pro-autophagic biased signaling.

## 2. Materials and Methods

### 2.1. Chemical Compounds

Human recombinant IL-36 $\alpha$  (Biomol GmbH, Hamburg, Germany) was prepared in sterile distilled water and used at 10 ng/mL concentration in all experiments. Human recombinant IL-36Ra (Sigma–Aldrich, St. Louis, MO, USA) was prepared in sterile distilled water and used at 20-fold molar excess.

A stock solution of autophagy inhibitor bafilomycin A1 BFLA (Santa Cruz Biotechnology, Dallas, TX, USA) was prepared in dimethyl sulfoxide. BFLA was used at a concentration of 100 nM in all experiments.

## 2.2. Cell Culture

The THP-1 human pro-monocytic cell line was grown in Dulbecco's modified Eagle's minimal essential medium (Sigma–Aldrich) supplemented with 10% fetal calf serum (Lonza, Verviers, Belgium) and 1% of an antibiotic/antimycotic (AB/AM) solution (Lonza) at 37 °C in a 5% CO<sub>2</sub> atmosphere.

## 2.3. Immunofluorescence Assay

Cytospin cell preparations were fixed in methanol acetone (1:1) for 10 min at –20 °C. The cells were treated with 1% bovine serum albumin in PBS for 30 min at 37 °C to block non-specific binding of the antibodies. To detect LC3B, the slides were stained with a 1:150 dilution of rabbit polyclonal antibody to LC3B (Sigma-Aldrich) for 1 h at 37 °C. To detect Beclin-1, the slides were stained with a 1:100 dilution of rabbit polyclonal antibody to Beclin-1 (Sigma-Aldrich) for 1 h at 37 °C. After washing with PBS, the samples were reacted with a 1:300 dilution of CF488A-conjugated anti-rabbit antibody (Sigma-Aldrich) for 1 h at 37 °C. The cells were visualized by confocal microscopy using an Olympus FV1000 confocal laser scanning microscope using UPLSAPO 60X (N.A. 1.35) oil immersion objective and 488 nm laser excitation with 500–600 nm detection range. LC3B-positive vacuoles were automatically quantified for each field after subtraction of the background level and establishment of an intensity threshold using Image J software (U.S. National Institutes of Health, Bethesda, MD, USA). The numbers of the LC3B-positive puncta were normalized by the numbers of cells in each field. An average of 500 cells was analyzed for each condition. The fluorescence intensity of LC3B was determined using the surface plot functions of the Image J software. The mean fluorescence intensity (MFI) method was used to quantify the fluorescent signal intensities of cells. ImageJ software was used to draw an outline around each cell, and the MFI was measured. The corrected total cell fluorescence (CTCF) was calculated via the following formula: CTCF = integrated density—(area of selected cell × mean fluorescence of background readings).

## 2.4. Western Blot Assays

The cells were homogenized in CytoBuster lysis buffer (Merck KGaA, Darmstadt, Germany), and the mixture was then centrifuged at 10,000 g for 10 min to remove cell debris. Protein concentrations of cell lysates were determined using the Bio-Rad protein assay (Bio-Rad Laboratories Inc., Hercules, CA, USA). Supernatants were mixed with Laemmli sample buffer and boiled for 3 min. Aliquots of the supernatants were resolved by SDS-PAGE and electrotransferred onto Immun-Blot polyvinylidene difluoride (PVDF) membranes (Bio-Rad Laboratories Inc.). The membranes were blocked in PBS containing 0.05% Tween 20, and 5% dried non-fat milk (Difco Laboratories Inc., Detroit, MI, USA). The pre-blocked blots were probed with the appropriate antibodies for 4 h in PBS containing 0.05% Tween 20, 1% dried non-fat milk and 1% bovine serum albumin (Sigma-Aldrich). Rabbit anti-LC3B (Sigma-Aldrich) and rabbit anti-β-actin (Sigma-Aldrich) primary antibodies were used at a 1:1000 dilution. Blots were then incubated for 2 h with peroxidase-conjugated anti-rabbit antibody (Sigma-Aldrich). Membranes were developed using a chemiluminescence detection system (GE Healthcare, Chicago, IL, USA). The blots were scanned and the relative band intensities were quantified using ImageJ software (U.S. National Institutes of Health, Bethesda, MD, USA) [58].

## 2.5. Phospho-Kinase Array Analysis

A human phospho-kinase array (R & D Systems Inc., Minneapolis, MN, USA) was used to measure the relative phosphorylation levels of 43 signaling molecules. Control cells and cultures treated with IL-36α and LPS alone or in combination for 30 min were homoge-

nized in a lysis buffer and centrifuged for five min at  $14,000 \times g$ . Protein concentrations of the supernatants were determined using a Bio-Rad protein assay (Bio-Rad Laboratories Inc.). From each treatment group, three individual samples containing 100–100  $\mu\text{g}$  protein were combined. After blocking, 300  $\mu\text{g}$  of protein was incubated overnight at  $4^\circ\text{C}$  with each array comprising two technical replicates. After washing, the arrays were reacted with a cocktail of phospho-site-specific biotinylated antibodies for two hours at room temperature, carefully washed again, and incubated with streptavidin–peroxidase for 30 min at room temperature. Signals were developed using a chemiluminescence detection system. The arrays were scanned, spot densities of phospho-proteins were quantified using ImageJ software (U.S. National Institutes of Health, Bethesda, MD, USA) [58] and normalized to those of positive controls on the same membrane after subtraction of background values.

### 2.6. Statistical Analysis

Statistical significance was analyzed by one-way ANOVA followed by Tukey's or Sidak's multiple comparison post-hoc tests. All statistical analyses were performed using GraphPad Prism 6 software (GraphPad Software Inc., San Diego, CA, USA), and  $p$  values less than 0.05 were considered statistically significant.

## 3. Results

### 3.1. The Effects of IL-36 $\alpha$ and LPS on the Subcellular Localization of LC3B in the THP-1 Cell Line

To elucidate how IL-36 $\alpha$  and LPS affect the basal autophagy, we treated THP-1 cells with IL-36 $\alpha$  and LPS alone or in combination and measured the subcellular localization of LC3B.

Immunofluorescence assays could determine the intracellular localization of LC3B at the 6-h time point and demonstrated that the control cells and the cultures treated with LPS have faint cytoplasmic LC3B staining (Figure 2A). Accordingly, the 3D surface plots revealed a few peaks of low height (Figure 2A). Cells treated with IL-36 $\alpha$  displayed staining patterns characterized by faint, punctate LC3B staining (Figure 2A). In contrast, the cells treated with the combination of IL-36 $\alpha$  and LPS displayed very bright LC3B staining, and the 3D surface plot consisted of numerous robust peaks (Figure 2A). This result indicates that IL-36 $\alpha$  and LPS cooperatively increased the accumulation of LC3B-positive vacuoles.

IL-36 receptor antagonist (IL-36Ra) was used to investigate the role of IL-36 $\alpha$  in the synergistic activation of autophagy elicited by the combined treatment with IL-36 $\alpha$  and LPS. The cultures were pre-treated with IL-36Ra for 30 min, and then IL-36 $\alpha$  or a double combination of IL-36 $\alpha$  and LPS were added. The cultures treated either with IL-36Ra alone or in combination with IL-36 $\alpha$  displayed a faint cytoplasmic LC3B staining (Figure 2A). Cells treated with the triple combination of IL-36 $\alpha$ -IL-36Ra-LPS likewise displayed staining patterns characterized by faint, punctate LC3B staining (Figure 2A). Accordingly, the 3D surface plots revealed a few peaks of low height (Figure 2A).

To investigate the effects of IL-36 $\alpha$  and LPS on autophagosome formation, the abundances of LC3B-positive vacuoles were determined at the 6-h time point. The average numbers of LC3B-positive vacuoles per cell in the control, IL-36 $\alpha$ -, or LPS-treated cultures were 4.72, 6.73, and 2.8, respectively (Figure 2B). Thus, the cells treated with IL-36 $\alpha$  alone displayed increased abundances of autophagic vesicles, this difference, however, was not statistically significant. The average numbers of LC3B-positive vacuoles per cell in cultures treated with a combination of IL-36 $\alpha$  and LPS were significantly higher than that observed in the control cultures (the average number of autophagosomes in the cultures treated with IL-36 $\alpha$ -LPS was 10.97 versus 4.72 in the control,  $p < 0.0001$ ) (Figure 2B). Moreover, the cells treated with the triple combination of IL-36 $\alpha$ -IL-36Ra-LPS exhibited significantly lower numbers of LC3B-positive vacuoles per cell than in the cultures treated with the IL-36 $\alpha$ -LPS combination: The average number of autophagosomes in the cultures treated with IL-36 $\alpha$ -IL-36Ra-LPS was 7.58 vs. 10.97 in cells treated with IL-36 $\alpha$ -LPS,  $p < 0.05$  (Figure 2B). Thus, although IL-36 $\alpha$  and LPS alone do not cause a significant alteration in the

number of LC3B-positive vacuoles, the combination of IL-36 $\alpha$  and LPS does significantly stimulate the accumulation of autophagosomes.

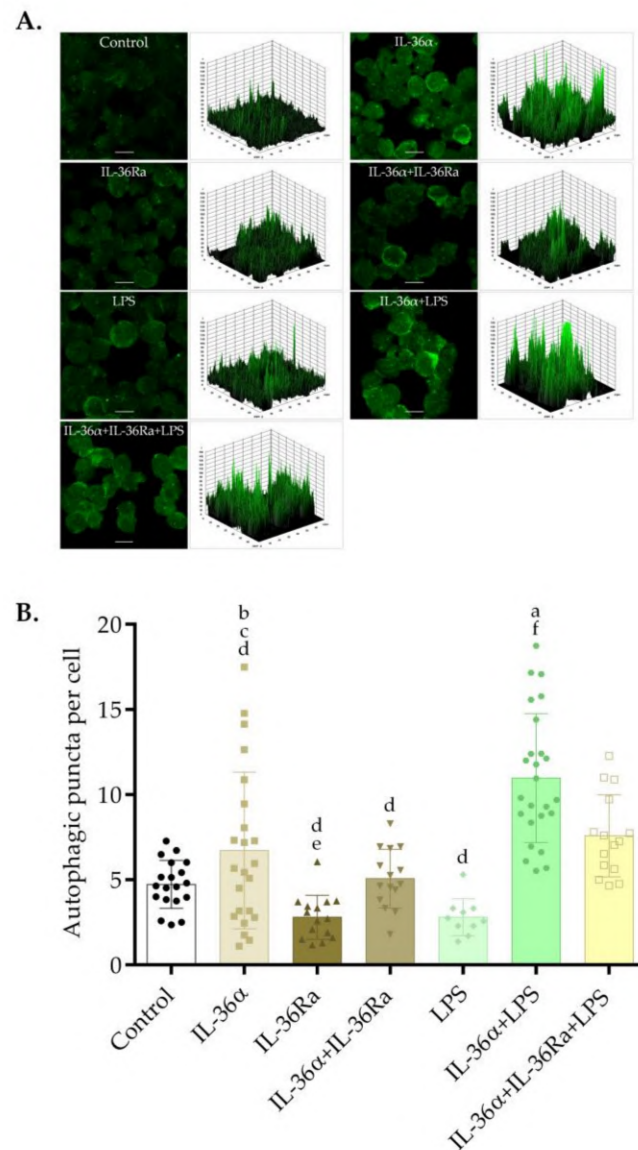


**Figure 2.** IL-36 $\alpha$  and LPS cooperatively increase the accumulation of LC3B-positive vacuoles. THP-1 cells were treated with 10 ng/mL IL-36 $\alpha$ , IL-36Ra, and LPS alone or in combination for 6 h, and the intracellular localization of LC3B was analyzed. Control cultures incubated in parallel were left untreated. (A) Immunofluorescence assays showing the fluorescence intensities of LC3B-positive vacuoles. The samples were stained for endogenous LC3B protein, and images were obtained by confocal microscopy. The images were subjected to fluorescence intensity analysis by using the Image J software. The 3D surface plots represent the intensity values of the whole image. The results are representative of two independent experiments. Scale bar, 10  $\mu$ m. (B) The average numbers of LC3B-positive autophagic vacuoles. The LC3B-positive autophagic vacuoles were automatically quantified with Image J software. The values on the bar graphs denote the means  $\pm$  SD of the results of two independent experiments. *p* values were calculated by the ANOVA test with the Tukey post-test. <sup>a</sup> *p* < 0.0001 vs. Control; <sup>b</sup> *p* < 0.01 vs. IL-36Ra; <sup>c</sup> *p* < 0.05 vs. LPS; <sup>d</sup> *p* < 0.001 vs. IL-36 $\alpha$ -LPS combination; <sup>e</sup> *p* < 0.05 vs. IL-36 $\alpha$ -IL-36Ra-LPS combination; <sup>f</sup> *p* < 0.001 vs. IL-36 $\alpha$ -IL-36Ra-LPS combination.

### 3.2. The Effects of IL-36 $\alpha$ and LPS on the Levels of LC3B-I and LC3B-II

The effects of IL-36 $\alpha$  and LPS on the levels of LC3B-I and LC3B-II were determined by Western blot analysis (Figures 3 and S1). The control THP-1 cells displayed endogenous expression of both the lipidated and the non-lipidated forms of LC3B at each time point (Figure 3A, lanes 1–4). IL-36 $\alpha$ -treated cells exhibited slightly higher LC3B-II levels at the 0.5-, 2-, and 6-h time points than controls (Figure 3A, lanes 5–7). However, these alterations were not statistically significant (Figure 3B). Likewise, there were no significant alterations in LPS-treated cells versus controls (Figure 3). In contrast, the simultaneous treatment of cells with IL-36 $\alpha$  and LPS triggered a significant increase in the level of LC3B-II as compared with the controls (at the 0.5-, 6-, and 24-h time points the fold increases of LC3B-II levels in cells treated with IL-36 $\alpha$ -LPS combination were 3.52,  $p < 0.01$ , 3.0, and 3.02,  $p < 0.05$  for both, respectively) (Figure 3A, lanes 13, 15 and 16, and Figure 3B). The LC3B-II level at the 2-h time point dropped compared to the values measured at 0.5, 6, and 24 h after the IL-36 $\alpha$  and LPS combined treatment (Figure 3). These data suggest that IL-36 $\alpha$  and LPS alone do not increase the level of LC3B-II, whereas combined IL-36 $\alpha$  and LPS treatment cooperatively stimulates the lipidation of LC3B with characteristic kinetics.

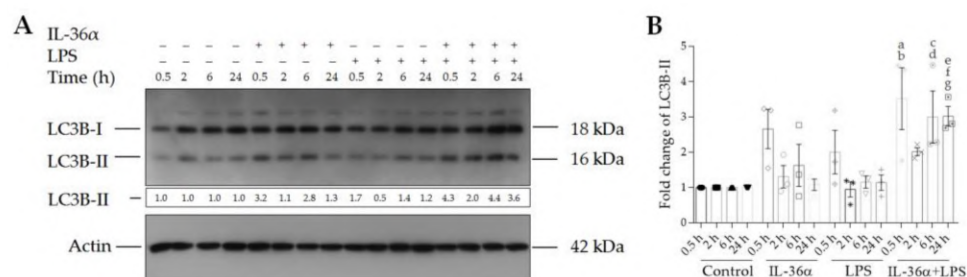


**Figure 3.** IL-36 $\alpha$  and LPS cooperatively increase the level of LC3B-II. **(A)** Western blot analysis showing the kinetics of endogenous LC3B-II expression. Total protein was isolated from controls (lanes 1–4), IL-36 $\alpha$ -treated cells (lanes 5–8), LPS-treated cells (lanes 9–12), and cells treated with IL-36 $\alpha$ -LPS combination (lanes 13–16) at the indicated time points. Samples were resolved on SDS-PAGE and transferred to PVDF filters. After incubation with the corresponding antibody, the levels of LC3B-I and LC3B-II were determined with a chemiluminescence detection system. Band intensities were quantified with ImageJ software. The ratios of the protein levels measured at 0.5, 2, 6, and 24 h were compared to the corresponding time point controls and expressed as fold change (shown below each lane). The results are representative of three independent experiments. **(B)** The values on the bar graph denote the means  $\pm$  SD of the results of three independent experiments.  $p$  values were calculated by the ANOVA test with the Sidak post-test. <sup>a</sup>  $p < 0.01$  vs. the 0.5-h time point control, <sup>b</sup>  $p < 0.05$  vs. the 0.5-h time point LPS, <sup>c</sup>  $p < 0.05$  vs. the 6-h time point control, <sup>d</sup>  $p < 0.01$  vs. the 6-h time point LPS, <sup>e</sup>  $p < 0.05$  vs. the 24-h time point control, <sup>f</sup>  $p < 0.01$  vs. the 24-h time point IL-36 $\alpha$ , and <sup>g</sup>  $p < 0.01$  vs. the 24-h time point LPS.

### 3.3. The Effects of IL-36 $\alpha$ and LPS on the Autophagic Flux

Bafilomycin A1 (BFLA) is an inhibitor of autophagosome-lysosome fusion and lysosomal hydrolase activity and was used to investigate the autophagic flux (Figures 4 and S2). The cultures were incubated with IL-36 $\alpha$  and LPS alone or in combination for 2 h and then treated with BFLA for another 4-h period just before the preparation of cell lysates. Compared with the control, BFLA increased the level of LC3B-II (Figure 4A, lanes 1 and 2, respectively). The elevated LC3B-II level of the BFLA-treated cells indicates that this drug efficiently blocked the autophagic flux under the experimental conditions used. In the presence of BFLA, IL-36 $\alpha$  triggered a higher increase in the level of LC3B-II than in the corresponding drug control (Figure 4A, lanes 4 and 2, respectively). However, this alteration was not statistically significant (Figure 4B). In contrast, compared with the BFLA control, LPS—acting singly or in combination with IL-36 $\alpha$ —elicited a significant increase in the levels of LC3B-II of cells incubated in the presence of BFLA (the fold increases of LC3B-II levels in cells treated either with LPS alone or the IL-36 $\alpha$ -LPS combination in the presence of BFLA were 6.22, and 6.47,  $p < 0.05$  for both) (Figure 4B). In the presence of BFLA, the cells treated with the IL-36 $\alpha$ -LPS combination exhibited higher increases in the level of LC3B-II than cultures

stimulated only with LPS. These data indicate that combined IL-36 $\alpha$  and LPS treatment cooperatively stimulates the autophagic flux.

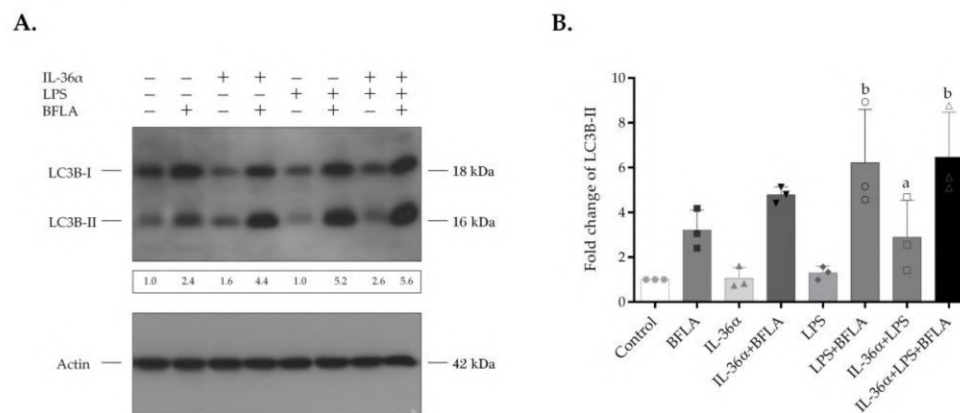


**Figure 4.** IL-36 $\alpha$  and LPS cooperatively stimulate the autophagic flux. THP-1 cells were treated with IL-36 $\alpha$ , and LPS alone or in combination for 2 h and then exposed to 100 nM bafilomycin A1 for another 4-h period. The total protein extracted was analyzed for LC3B expression by Western blot analysis. (A) Western blot analysis showing increased autophagic flux in cells treated with IL-36 $\alpha$ , and LPS alone, or in combination. The ratios of the protein levels were calculated, and expressed as fold change, shown below each lane. Results are representative of three independent experiments. (B) The values on the bar graph denote the means  $\pm$  SD of the results of three independent experiments.  $p$  values were calculated by the ANOVA test with the Sidak post-test. <sup>a</sup>  $p < 0.05$  vs. control, <sup>b</sup>  $p < 0.05$  vs. BFLA control. BFLA, bafilomycin A1.

### 3.4. The Effects of IL-36 $\alpha$ and LPS on the Level of Beclin-1

The effects of IL-36 $\alpha$  and LPS on the level and intracellular localization of Beclin-1 were determined by immunofluorescence assay at the 6-h time point. The control cells showed a faint cytoplasmic Beclin-1 staining (Figure 5A). Accordingly, the 3D surface plots revealed a few peaks of low height (Figure 5A). In contrast, the cells treated with IL-36 $\alpha$  and LPS alone or in combination displayed very bright Beclin-1 staining, and the 3D surface plots consisted of numerous robust peaks (Figure 5A). Measurement of the staining intensities showed that IL-36 $\alpha$  and LPS acting singly or in combination elicited significant increases as compared with the control (the CTCF values in cells treated with IL-36 $\alpha$ , LPS, or IL-36 $\alpha$ -LPS combination were 1.35, 1.66, or 1.8 vs. 1.0 in the control,  $p < 0.0001$  for all, respectively) (Figure 5B). Measurement of the abundances of Beclin-1-positive vacuoles likewise revealed that IL-36 $\alpha$  and LPS acting singly or in combination triggered significant increases as compared with the control (the average numbers of Beclin-1-positive puncta in cells treated with IL-36 $\alpha$ , LPS or IL-36 $\alpha$ -LPS combination were 5.86, 8.18, or 13.55 vs. 2.72 in the control,  $p < 0.01$ ,  $p < 0.0001$  and  $p < 0.0001$ , respectively) (Figure 5C). These data indicate that IL-36 $\alpha$  and LPS cooperatively elevate the level of Beclin-1.

### 3.5. The Effects of IL-36 $\alpha$ and LPS on Cellular Signaling in the THP-1 Cell Line

A phospho-kinase array that detects the phosphorylation levels of 43 major protein kinases (Table S1) was used to investigate the effect of IL-36 $\alpha$  and LPS on the activation level of signaling pathways implicated in autophagy regulation. IL-36 $\alpha$  led to the activation of a subset of kinases (Figures 6 and S3). Compared with the control, the most significant effect was an increase in Akt strain transforming factor 1/2/3 (Akt1/2/3) (S473) phosphorylation. The phosphorylation levels of the proline-rich Akt substrate of 40 kDa (PRAS40) (T246) and mechanistic target of rapamycin (mTOR) (S2448)—two signaling molecules downstream of Akt1/2/3—were also increased (Figures 6 and S3). IL-36 $\alpha$  triggered phosphorylation of with no lysine kinase 1 (WNK1) (T60), some steroid receptor coactivator (Src) family kinases including Src (Y419) and Lyn (Y397), and signal transducer and activator of transcription (STAT) family members such as STAT2 (Y689), STAT3 (S727) and STAT5a/b (Y694/Y699). Compared with the control, LPS increased the levels of phospho-Akt1/2/3

(S473), phospho-Src (Y419), and STAT5a/b (Y694/Y699); it decreased phosphorylation of adenosine monophosphate-activated protein kinase  $\alpha$ 1 (AMPK $\alpha$ 1) (Figure 6). Compared with the control, IL-36 $\alpha$  and LPS combined treatment increased phosphorylation of STAT5a/b, whereas the levels of phospho-Yes (Y426), phospho-focal adhesion kinase (FAK) (Y397), and phospho-WNK1 (T60) were decreased (Figures 6 and S3). Thus, IL-36 $\alpha$ , LPS, and the combined treatment elicit distinct phosphorylation patterns of signaling molecules.

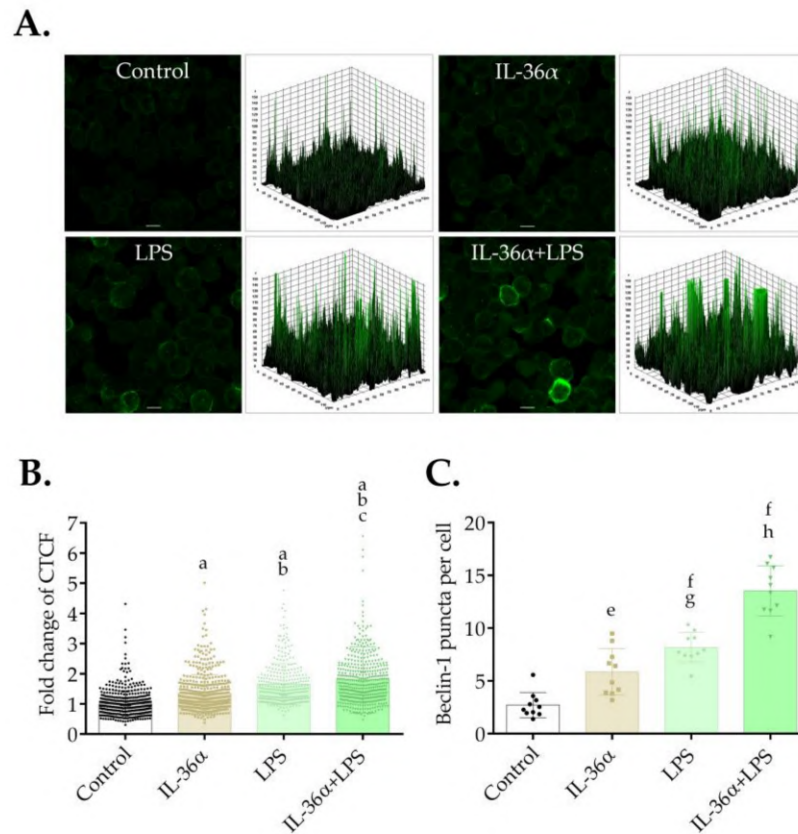


**Figure 5.** IL-36 $\alpha$  and LPS cooperatively increase Beclin-1 levels. THP-1 cells were treated with 10 ng/mL IL-36 $\alpha$ , IL-36Ra, and LPS alone or in combination for 6 h, and the level of Beclin-1 fluorescence was analyzed. Control cultures incubated in parallel were left untreated. (A) Immunofluorescence assay showing the fluorescence intensities of Beclin-1. The samples were stained for the endogenous Beclin-1 protein, and images were obtained by confocal microscopy. The images were subjected to fluorescence intensity analysis with Image J. The 3D surface plots represent the intensity values of the entire image. The results are representative of two independent experiments. Scale bar, 10  $\mu$ m. (B) Quantification of Beclin-1 fluorescence intensities. The fold changes of CTCF values were calculated as the CTCF of cells treated with 10 ng/mL IL-36 $\alpha$ , and LPS alone or in combination/CTCF of control cultures. The values on the bar graphs denote the means  $\pm$  SD of the results of two independent experiments. *p* values were calculated by the ANOVA test with the Tukey post-test. <sup>a</sup> *p* < 0.0001 vs. Control; <sup>b</sup> *p* < 0.0001 vs. IL-36 $\alpha$ ; <sup>c</sup> *p* < 0.05 vs. LPS. (C) Quantification of the intracellular abundances of Beclin-1 puncta. The Beclin-1-positive puncta were quantified with Image J software. The values on the bar graphs denote the means  $\pm$  SD of the results of two independent experiments. *p* values were calculated by the ANOVA test with Tukey post-test. <sup>e</sup> *p* < 0.01 vs. Control; <sup>f</sup> *p* < 0.0001 vs. Control; <sup>g</sup> *p* < 0.05 vs. IL-36 $\alpha$ ; <sup>h</sup> *p* < 0.0001 vs. IL-36 $\alpha$  and LPS.

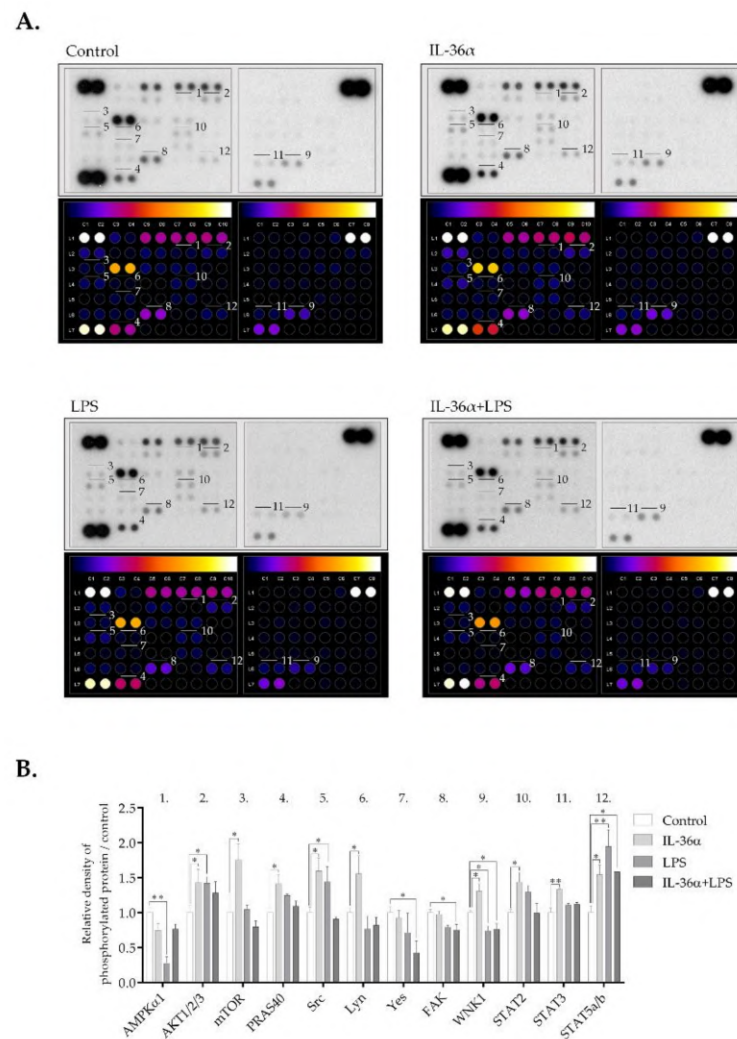


**Figure 6.** Differential phospho-kinase array profiles of cells treated with IL-36 $\alpha$  and LPS. **(A)** Phospho-kinase array analysis. Total protein was isolated from THP-1 cells treated with IL-36 $\alpha$ , and LPS alone or in combination for 30 min. Control cells were left untreated. The samples were hybridized with a phospho-kinase array kit. The labeled spots correspond to the phospho-proteins modulated by IL-36 $\alpha$  and LPS. **(B)** Quantification of phosphoproteins from the proteomic array (average of duplicate spots). Spot densities of phosphoproteins were quantified using Image J analysis software and normalized to positive controls on the same membrane. *p* values were calculated by the ANOVA test with the Sidak post-test. \* *p* < 0.05; \*\* *p* < 0.01.

#### 4. Discussion

Compelling evidence indicates that cellular autophagic and immune processes are highly intertwined and that their coordinated functioning is essential for the efficient protection of the human body against pathogenic Gram-negative bacteria [33,45–47,59]. During infections, cytokines and molecules defined as PAMP act simultaneously to activate partially overlapping signaling pathways. The combined effect may differentially regulate cellular autophagic activity. Thus, this study investigated the impact of IL-36 $\alpha$  upon endogenous and LPS-induced autophagy.

To study the autophagic activity of THP-1 cells treated with IL-36 $\alpha$  and LPS alone or in combination, we determined the intracellular distribution of LC3B and measured LC3B lipidation as well as the autophagic flux [60]. These experiments demonstrated that the cells treated with IL-36 $\alpha$  alone displayed increased abundances of autophagic vesicles, elevated endogenous LC3B-II levels, and stimulated autophagic flux; these differences, however, were not statistically significant (Figures 2–4). Recent observations indicated that IL-36 $\beta$

and IL-36 $\gamma$  activate the autophagic process in primary murine CD4<sup>+</sup>CD25<sup>+</sup> Treg cells [57] and human macrophages [56], respectively. There may be several explanations for the weaker pro-autophagic effect of IL-36 $\alpha$  revealed in our present study such as differences between IL-36 subtypes and different sensitivities of various cell types to this cytokine. Consistent with previous findings [52,53,61], our results demonstrated that LPS significantly increased autophagosome synthesis (Figure 3). The combination of IL-36 $\alpha$  and LPS raised the intensity level of LC3B staining and cooperatively stimulated the translocation of this protein into autophagic vesicles (Figure 2). Supporting this observation, we found that IL-36Ra significantly inhibited the pro-autophagic effect of the IL-36 $\alpha$ /LPS combined treatment (Figure 2). The IL-36 $\alpha$ -LPS combination elevated LC3B-II and decreased LC3B-I levels indicating that the lipidation of LC3B is highly stimulated (Figure 3). Finally, our experiments showed that in cultures treated with the combination of IL-36 $\alpha$  and LPS, the autophagic flux is increased considerably by this cytokine/PAMP combination (Figure 4). These results suggest that IL-36 $\alpha$  and LPS cooperatively stimulate autophagy.

To investigate the effect of IL-36 $\alpha$  and LPS on the activation of some signaling pathways, we determined the phosphorylation levels of protein kinases implicated in autophagy regulation (Figure 6). Our studies have shown that IL-36 $\alpha$  increased the phosphorylation of Akt1/2/3 (S473), PRAS40 (T246), mTOR (S2448), WNK1 (T60), and some Src as well as STAT family kinases such as Src, Lyn, STAT2, STAT3, and STAT5a/b. PRAS40 is a negative regulator of mTORC1 [34,62]. Akt- and mTORC1-mediated phosphorylation of PRAS40 results in its dissociation from mTORC1 that in turn alleviates inhibition of mTORC1 and blocks induction of the autophagic cascade [34,62]. An interesting recent study revealed that IL-36 $\beta$  stimulates mTORC1 via the PI3K/Akt, I $\kappa$ B kinase and MyD88 pathways [63]. Our experiments demonstrate that, like IL-36 $\beta$ , IL36 $\alpha$  activates mTORC1 via the PIK/Akt pathway. Moreover, we suggest that the Akt-mediated activation of mTOR involves PRAS40. Other previous studies indicated that WNK1 acts as an autophagy inhibitor by interfering with the activation of AMPK and PI3KC3 [64]. STAT3 has been shown to regulate autophagy in localization- and context-dependent manners and can elicit both pro-autophagic and anti-autophagic effects [65]. In light of these observations, our data suggest that in the early phase of IL-36 $\alpha$  signaling, both anti- and pro-autophagic pathways are activated. Our observations show that LPS increases phosphorylation of Akt1/2/3, Src as well as STAT5a/b and decreases the level of phospho-AMPK $\alpha$ 1 in THP-1 cells; this is fully consistent with previous reports [66,67]. Interestingly, the phosphorylation pattern of cells incubated with IL36 $\alpha$  and LPS differed from the signatures detected either in IL36 $\alpha$ - or LPS-treated cells. We found that the IL36 $\alpha$ /LPS combined treatment increased phosphorylation of STAT5a/b, had minimal effect on the Akt/PRAS40/mTOR pathway, and reduced the levels of phospho-Yes, phospho-FAK, and phospho-WNK1. Thus, the combined treatment of IL-36 $\alpha$  and LPS appears to dampen PI3K/Akt/mTOR, FAK and WNK1 signaling. The TLR4 signal transduction network is known to be kept under strict control by multiple mechanisms including positive and negative crosstalk regulations that maintain the integrity of immune cells by preventing excessive inflammation [68]. The negative regulators acting through the activation of transcription play a primary role in the late phase of TLR and IL-36 signaling; their role in the early stage thus can be excluded. Important studies, however, revealed that PI3K has an essential role in the safety mechanism controlling the early-stage of TLR4-mediated signaling [69]. PI3K can suppress TLR4 signaling by altering the availability of phosphatidylinositol-(4,5)bisphosphate (PIP<sub>2</sub>) at the cytoplasmic membrane and hence can modulate the intracellular localization of adaptors, the magnitude of activation, and signal output [70]. Based on these observations, we suggest that the combinatorial effect of IL-36 $\alpha$ /LPS may exert an excessive PI3K activation, which—while not suspending the inhibition of downstream events of autophagy—can significantly reduce it by decreasing the Akt-mediated activation of mTORC1.

Previous studies have demonstrated that Beclin-1 plays a pivotal role in the autophagic process. Beclin-1 was shown to interact with Bcl-2 and Bcl-X<sub>L</sub>, which suppresses autophagosome biogenesis. The release of Beclin-1 is a prerequisite for the formation of a functional

PI3KC3 complex. Phosphorylation events and TRAF6-mediated ubiquitination of Beclin-1 may destabilize Beclin-1-Bcl-2/Bcl-X<sub>L</sub> association and abrogate BECN1-BCL2/Bcl-X<sub>L</sub> interaction. Some IL-36 $\alpha$  and LPS signaling intermediates have the potential to regulate the functional activity of Beclin-1 [71,72]. Thus, we investigated the effect of IL-36 $\alpha$  and LPS on Beclin-1 protein. Our results showed that IL-36 $\alpha$  and LPS acting singly or in combination elevated the staining intensities and increased the abundances of Beclin-1-positive vacuoles (Figure 5). The IL-36 $\alpha$ /LPS treatment was again more efficient than IL-36 $\alpha$  or LPS alone. These data further support the notion that IL-36 $\alpha$  and LPS cooperatively promote the autophagic process because increased Beclin-1 levels were shown to correlate with enhanced autophagy [60].

Our results suggest a hypothetical model for the mechanism of the enhanced pro-autophagic effect observed in cells treated with IL-36 $\alpha$  and LPS simultaneously. The IL-36 $\alpha$ /LPS combination reduces the activation level of the PI3K/Akt/mTORC1 axis by triggering rapid depletion of PIP<sub>2</sub> at the cytoplasmic membrane. As a result, mTOR-mediated inhibition of autophagy is alleviated. Some components of the IL-36 $\alpha$  and LPS signaling networks are known to induce autophagy. MyD88 binds directly whereas TRAF3 and TRAF6 ubiquitinate the Beclin-1 protein, thus disrupting the interaction between Beclin-1 and Bcl-2 [52,53]. This results in increased oligomerization of Beclin-1, activation of the PI3KC3 complex, and initiation of autophagosome formation [52,53]. The IL-36 $\alpha$ /LPS combination increases the activation level of PI3KC3 complex directly and subsequently stimulates autophagy. Thus, this cytokine/PAMP combination triggers pro-autophagic biased signaling by several mechanisms and thereby cooperatively stimulates the autophagic cascade (Figure S4). Previous studies have shown that bacteria affect the autophagic cascade and, conversely, autophagy influences the infection process. The bacteria studied so far all interact with the autophagic machinery but in different ways. The structural components, PAMPs, and exotoxins of several bacteria induce autophagy. However, some bacteria can effectively prevent autophagic recognition, inhibit autophagy initiation and maturation of autophagosomes or block the fusion of lysosomes with autophagosomes, while others hijack the autophagic compartment to support their intracellular survival. Our data indicate that cytokines may modify the pro-autophagic effect of bacterial PAMPs. An increased xenophagic activity of innate immune cells exposed to IL-36 $\alpha$  and LPS—functioning as part of the cell-autonomous defense system—may play a protective role in the pathogenesis of infections caused by Gram-negative bacteria [73,74]. Our data indicate that cytokines may modify the pro-autophagic effect of bacterial PAMPs. An increased xenophagic activity of innate immune cells exposed to IL-36 $\alpha$  and LPS—functioning as part of the cell-autonomous defense system—may play an important role in the pathogenesis of infections caused by Gram-negative bacteria.

In conclusion, our results demonstrate that the IL-36 $\alpha$ /LPS triggers pro-autophagic biased signaling by several mechanisms and thereby stimulates the autophagic cascade cooperatively in the THP-1 cell line. However, some limitations of this investigation, such as the need for additional experimental evidence that can corroborate the synergistic effect of this cytokine/PAMP combination in other cell types, have yet to be addressed. Moreover, further studies are needed to investigate the effect of increased autophagic activity on the functions of innate immune cells treated with IL-36 $\alpha$  and LPS simultaneously.

**Supplementary Materials:** The following are available online at <https://www.mdpi.com/article/10.3390/biomedicines9111541/s1>, Figure S1: IL-36 $\alpha$  and LPS cooperatively increase the level of LC3B-II, Figure S2: IL-36 $\alpha$  and LPS cooperatively stimulate the autophagic flux. Figure S3: Differential phospho-kinase array profiles of cells treated with IL-36 $\alpha$  and LPS. Figure S4: IL36 $\alpha$  and LPS cooperatively induced autophagy by multiple mechanisms. Table S1: List of the detected phospho-proteins by using the Proteome Profiler™ human phospho-kinase array kit.

**Author Contributions:** Conceptualization, K.M., Z.V. and Z.B.; methodology, Z.I.I.A.-L., K.M., G.S., Á.D. and F.A.; software, Z.I.I.A.-L., G.S., Á.D.; validation, K.M., Z.I.I.A.-L., F.A., G.S. and Á.D.; formal analysis, K.M., Z.I.I.A.-L., and Á.D.; investigation, K.M., Z.V., F.A. and Z.B.; resources, K.M., and Z.I.I.A.-L.; data curation, K.M., Z.I.I.A.-L., and Á.D.; writing—original draft preparation,

K.M.; writing—review and editing, K.M., Z.V., Z.B., F.A., Z.I.I.A.-L., Á.D. and G.S.; visualization, Z.I.I.A.-L., K.M., G.S., Á.D.; supervision, K.M. and Z.V.; project administration, K.M. and Z.I.I.A.-L.; funding acquisition, K.M. and Z.I.I.A.-L. All authors have read and agreed to the published version of the manuscript.

**Funding:** This research was funded by the Tempus Közalapítvány (Stipendium Hungaricum scholarship) SHE-03673-007/2016, grant number 109162, and by the EFOP-3.6.1-16-2016-00008 project co-financed by the European Union and the European Regional Development Fund. The APC was funded by the University of Szeged Open Access Fund, grant number 5514, and the EFOP-3.6.1-16-2016-00008 project co-financed by the European Union and the European Regional Development Fund. Z.I.I.A. was funded by Tempus Közalapítvány (Stipendium Hungaricum scholarship) SHE-03673-007/2016, grant number 109162. F.A. was funded by EU's Horizon 2020, grant number 739593.

**Institutional Review Board Statement:** Not applicable.

**Informed Consent Statement:** Not applicable.

**Data Availability Statement:** Data presented in this study are available on request from the corresponding author.

**Conflicts of Interest:** The authors declare no conflict of interest. The funders had no role in the design of the study; in the collection, analyses, or interpretation of data; in the writing of the manuscript, or in the decision to publish the results.

## References

- Dinarello, C.A. Overview of the IL-1 Family in Innate Inflammation and Acquired Immunity. *Immunol. Rev.* **2018**, *281*, 8–27. [[CrossRef](#)] [[PubMed](#)]
- Garlanda, C.; Dinarello, C.A.; Mantovani, A. The Interleukin-1 Family: Back to the Future. *Immunity* **2013**, *39*, 1003–1018. [[CrossRef](#)] [[PubMed](#)]
- Murrieta-Coxca, J.M.; Rodríguez-Martínez, S.; Cancino-Díaz, M.E.; Markert, U.R.; Favaro, R.R.; Morales-Prieto, D.M. IL-36 Cytokines: Regulators of Inflammatory Responses and Their Emerging Role in Immunology of Reproduction. *Int. J. Mol. Sci.* **2019**, *20*, 1649. [[CrossRef](#)] [[PubMed](#)]
- Smith, D.E.; Renshaw, B.R.; Ketchum, R.R.; Kubin, M.; Garka, K.E.; Sims, J.E. Four New Members Expand the Interleukin-1 Superfamily. *J. Biol. Chem.* **2000**, *275*, 1169–1175. [[CrossRef](#)] [[PubMed](#)]
- Clancy, D.M.; Henry, C.M.; Sullivan, G.P.; Martin, S.J. Neutrophil Extracellular Traps Can Serve as Platforms for Processing and Activation of IL-1 Family Cytokines. *FEBS J.* **2017**, *284*, 1712–1725. [[CrossRef](#)] [[PubMed](#)]
- Henry, C.M.; Sullivan, G.P.; Clancy, D.M.; Afonina, I.S.; Kulms, D.; Martin, S.J. Neutrophil-Derived Proteases Escalate Inflammation through Activation of IL-36 Family Cytokines. *Cell Rep.* **2016**, *14*, 708–722. [[CrossRef](#)] [[PubMed](#)]
- Zhou, L.; Todorovic, V. Interleukin-36: Structure, Signaling and Function. In *Protein Reviews: Volume 21*; Atassi, M.Z., Ed.; Advances in Experimental Medicine and Biology; Springer International Publishing: Cham, Switzerland, 2021; pp. 191–210. ISBN 978-3-030-67814-2.
- Towne, J.E.; Garka, K.E.; Renshaw, B.R.; Virca, G.D.; Sims, J.E. Interleukin (IL)-1F6, IL-1F8, and IL-1F9 Signal through IL-1Rrp2 and IL-1RAcP to Activate the Pathway Leading to NF-KappaB and MAPKs. *J. Biol. Chem.* **2004**, *279*, 13677–13688. [[CrossRef](#)]
- Boraschi, D.; Tagliabue, A. The Interleukin-1 Receptor Family. *Semin. Immunol.* **2013**, *25*, 394–407. [[CrossRef](#)]
- Yi, G.; Ybe, J.A.; Saha, S.S.; Caviness, G.; Raymond, E.; Ganesan, R.; Mbow, M.L.; Kao, C.C. Structural and Functional Attributes of the Interleukin-36 Receptor. *J. Biol. Chem.* **2016**, *291*, 16597–16609. [[CrossRef](#)]
- Bridgewood, C.; Stacey, M.; Alase, A.; Lagos, D.; Graham, A.; Wittmann, M. IL-36 $\gamma$  Has Proinflammatory Effects on Human Endothelial Cells. *Exp. Dermatol.* **2017**, *26*, 402–408. [[CrossRef](#)] [[PubMed](#)]
- Foster, A.M.; Baliwag, J.; Chen, C.S.; Guzman, A.M.; Stoll, S.W.; Gudjonsson, J.E.; Ward, N.L.; Johnston, A. IL-36 Promotes Myeloid Cell Infiltration, Activation, and Inflammatory Activity in Skin. *J. Immunol.* **2014**, *192*, 6053–6061. [[CrossRef](#)]
- Vigne, S.; Palmer, G.; Martin, P.; Lamacchia, C.; Strebler, D.; Rodriguez, E.; Olleros, M.L.; Vesin, D.; Garcia, I.; Ronchi, F.; et al. IL-36 Signaling Amplifies Th1 Responses by Enhancing Proliferation and Th1 Polarization of Naive CD4<sup>+</sup> T Cells. *Blood* **2012**, *120*, 3478–3487. [[CrossRef](#)] [[PubMed](#)]
- Johnston, A.; Xing, X.; Guzman, A.M.; Riblett, M.; Loyd, C.M.; Ward, N.L.; Wohn, C.; Prens, E.P.; Wang, F.; Maier, L.E.; et al. IL-1F5, -F6, -F8, and -F9: A Novel IL-1 Family Signaling System That Is Active in Psoriasis and Promotes Keratinocyte Antimicrobial Peptide Expression. *J. Immunol.* **2011**, *186*, 2613–2622. [[CrossRef](#)]
- Qu, Q.; Zhai, Z.; Xu, J.; Li, S.; Chen, C.; Lu, B. IL36 Cooperates with Anti-CTLA-4 MAbs to Facilitate Antitumor Immune Responses. *Front. Immunol.* **2020**, *11*, 634. [[CrossRef](#)]
- Harusato, A.; Abo, H.; Ngo, V.L.; Yi, S.W.; Mitsutake, K.; Osuka, S.; Kohlmeier, J.E.; Li, J.D.; Gewirtz, A.T.; Nusrat, A.; et al. IL-36 $\gamma$  Signaling Controls the Induced Regulatory T Cell–Th9 Cell Balance via NF $\kappa$ B Activation and STAT Transcription Factors. *Mucosal. Immunol.* **2017**, *10*, 1455–1467. [[CrossRef](#)] [[PubMed](#)]

17. Ngo, V.L.; Kuczma, M.; Maxim, E.; Denning, T.L. IL-36 Cytokines and Gut Immunity. *Immunology* **2021**, *163*, 145–154. [[CrossRef](#)] [[PubMed](#)]
18. Bassoy, E.Y.; Towne, J.E.; Gabay, C. Regulation and Function of Interleukin-36 Cytokines. *Immunol. Rev.* **2018**, *281*, 169–178. [[CrossRef](#)] [[PubMed](#)]
19. Gresnigt, M.S.; Rösler, B.; Jacobs, C.W.M.; Becker, K.L.; Joosten, L.A.B.; van der Meer, J.W.M.; Netea, M.G.; Dinarello, C.A.; van de Veerdonk, F.L. The IL-36 Receptor Pathway Regulates Aspergillus Fumigatus-Induced Th1 and Th17 Responses. *Eur. J. Immunol.* **2013**, *43*, 416–426. [[CrossRef](#)] [[PubMed](#)]
20. Mazgaen, L.; Gurung, P. Recent Advances in Lipopolysaccharide Recognition Systems. *IJMS* **2020**, *21*, 379. [[CrossRef](#)] [[PubMed](#)]
21. Steimle, A.; Autenrieth, I.B.; Frick, J.-S. Structure and Function: Lipid A Modifications in Commensals and Pathogens. *Int. J. Med. Microbiol.* **2016**, *306*, 290–301. [[CrossRef](#)]
22. Brubaker, S.W.; Bonham, K.S.; Zanoni, I.; Kagan, J.C. Innate Immune Pattern Recognition: A Cell Biological Perspective. *Annu. Rev. Immunol.* **2015**, *33*, 257–290. [[CrossRef](#)] [[PubMed](#)]
23. Kieser, K.J.; Kagan, J.C. Multi-Receptor Detection of Individual Bacterial Products by the Innate Immune System. *Nat. Rev. Immunol.* **2017**, *17*, 376–390. [[CrossRef](#)] [[PubMed](#)]
24. Ciesielska, A.; Matyjek, M.; Kwiatkowska, K. TLR4 and CD14 Trafficking and Its Influence on LPS-Induced pro-Inflammatory Signaling. *Cell. Mol. Life Sci.* **2021**, *78*, 1233–1261. [[CrossRef](#)] [[PubMed](#)]
25. Gay, N.J.; Symmons, M.F.; Gangloff, M.; Bryant, C.E. Assembly and Localization of Toll-like Receptor Signalling Complexes. *Nat. Rev. Immunol.* **2014**, *14*, 546–558. [[CrossRef](#)] [[PubMed](#)]
26. Boonen, B.; Alpizar, Y.A.; Meseguer, V.M.; Talavera, K. TRP Channels as Sensors of Bacterial Endotoxins. *Toxins* **2018**, *10*, 326. [[CrossRef](#)]
27. Schappe, M.S.; Sztejn, K.; Stremiska, M.E.; Mendu, S.K.; Downs, T.K.; Seegren, P.V.; Mahoney, M.A.; Dixit, S.; Krupa, J.K.; Stipes, E.J.; et al. Chanzyme TRPM7 Mediates the Ca<sup>2+</sup> Influx Essential for Lipopolysaccharide-Induced Toll-Like Receptor 4 Endocytosis and Macrophage Activation. *Immunity* **2018**, *48*, 59–74.e5. [[CrossRef](#)] [[PubMed](#)]
28. Scheraga, R.G.; Abraham, S.; Niese, K.A.; Southern, B.D.; Grove, L.M.; Hite, R.D.; McDonald, C.; Hamilton, T.A.; Olman, M.A. TRPV4 Mechanosensitive Ion Channel Regulates Lipopolysaccharide-Stimulated Macrophage Phagocytosis. *J. Immunol.* **2016**, *196*, 428–436. [[CrossRef](#)] [[PubMed](#)]
29. Shi, J.; Zhao, Y.; Wang, Y.; Gao, W.; Ding, J.; Li, P.; Hu, L.; Shao, F. Inflammatory Caspases Are Innate Immune Receptors for Intracellular LPS. *Nature* **2014**, *514*, 187–192. [[CrossRef](#)] [[PubMed](#)]
30. Dikic, I.; Elazar, Z. Mechanism and Medical Implications of Mammalian Autophagy. *Nat. Rev. Mol. Cell. Biol.* **2018**, *19*, 349–364. [[CrossRef](#)]
31. Yang, Z.; Klionsky, D.J. Mammalian Autophagy: Core Molecular Machinery and Signaling Regulation. *Curr. Opin. Cell. Biol.* **2010**, *22*, 124–131. [[CrossRef](#)] [[PubMed](#)]
32. Parzych, K.R.; Klionsky, D.J. An Overview of Autophagy: Morphology, Mechanism, and Regulation. *Antioxid. Redox Signal.* **2014**, *20*, 460–473. [[CrossRef](#)] [[PubMed](#)]
33. Khandia, R.; Dadar, M.; Munjal, A.; Dhama, K.; Karthik, K.; Tiwari, R.; Yattoo, M.I.; Iqbal, H.M.N.; Singh, K.P.; Joshi, S.K.; et al. A Comprehensive Review of Autophagy and Its Various Roles in Infectious, Non-Infectious, and Lifestyle Diseases: Current Knowledge and Prospects for Disease Prevention, Novel Drug Design, and Therapy. *Cells* **2019**, *8*, 674. [[CrossRef](#)] [[PubMed](#)]
34. Sarkar, S. Regulation of Autophagy by MTOR-Dependent and MTOR-Independent Pathways: Autophagy Dysfunction in Neurodegenerative Diseases and Therapeutic Application of Autophagy Enhancers. *Biochem. Soc. Trans.* **2013**, *41*, 1103–1130. [[CrossRef](#)]
35. Kim, Y.C.; Guan, K.-L. MTOR: A Pharmacologic Target for Autophagy Regulation. *J. Clin. Invest.* **2015**, *125*, 25–32. [[CrossRef](#)] [[PubMed](#)]
36. Kim, J.; Guan, K.-L. MTOR as a Central Hub of Nutrient Signalling and Cell Growth. *Nat. Cell Biol.* **2019**, *21*, 63–71. [[CrossRef](#)]
37. Yang, J.; Carra, S.; Zhu, W.-G.; Kampinga, H.H. The Regulation of the Autophagic Network and Its Implications for Human Disease. *Int. J. Biol. Sci.* **2013**, *9*, 1121–1133. [[CrossRef](#)]
38. Carlsson, S.R.; Simonsen, A. Membrane Dynamics in Autophagosome Biogenesis. *J. Cell Sci.* **2015**, *128*, 193–205. [[CrossRef](#)]
39. Lamb, C.A.; Yoshimori, T.; Tooze, S.A. The Autophagosome: Origins Unknown, Biogenesis Complex. *Nat. Rev. Mol. Cell Biol.* **2013**, *14*, 759–774. [[CrossRef](#)] [[PubMed](#)]
40. Ichimura, Y.; Kirisako, T.; Takao, T.; Satomi, Y.; Shimonishi, Y.; Ishihara, N.; Mizushima, N.; Tanida, I.; Kominami, E.; Ohsumi, M.; et al. A Ubiquitin-like System Mediates Protein Lipidation. *Nature* **2000**, *408*, 488–492. [[CrossRef](#)] [[PubMed](#)]
41. Mizushima, N. The ATG Conjugation Systems in Autophagy. *Curr. Opin. Cell Biol.* **2020**, *63*, 1–10. [[CrossRef](#)]
42. Mizushima, N.; Noda, T.; Yoshimori, T.; Tanaka, Y.; Ishii, T.; George, M.D.; Klionsky, D.J.; Ohsumi, M.; Ohsumi, Y. A Protein Conjugation System Essential for Autophagy. *Nature* **1998**, *395*, 395–398. [[CrossRef](#)]
43. Klionsky, D.J.; Schulman, B.A. Dynamic Regulation of Macroautophagy by Distinctive Ubiquitin-like Proteins. *Nat. Struct. Mol. Biol.* **2014**, *21*, 336–345. [[CrossRef](#)] [[PubMed](#)]
44. Nakamura, S.; Yoshimori, T. New Insights into Autophagosome–Lysosome Fusion. *J. Cell Sci.* **2017**, *130*, 1209–1216. [[CrossRef](#)]
45. Levine, B.; Mizushima, N.; Virgin, H.W. Autophagy in Immunity and Inflammation. *Nature* **2011**, *469*, 323–335. [[CrossRef](#)]
46. Sharma, V.; Verma, S.; Seranova, E.; Sarkar, S.; Kumar, D. Selective Autophagy and Xenophagy in Infection and Disease. *Front. Cell Dev. Biol.* **2018**, *6*, 147. [[CrossRef](#)] [[PubMed](#)]

47. Deretic, V. Autophagy: An Emerging Immunological Paradigm. *J. Immunol.* **2012**, *189*, 15–20. [[CrossRef](#)] [[PubMed](#)]
48. Qian, M.; Fang, X.; Wang, X. Autophagy and Inflammation. *Clin. Transl. Med.* **2017**, *6*, 1–11. [[CrossRef](#)]
49. Ge, Y.; Huang, M.; Yao, Y. Autophagy and Proinflammatory Cytokines: Interactions and Clinical Implications. *Cytokine Growth Factor Rev.* **2018**, *43*, 38–46. [[CrossRef](#)] [[PubMed](#)]
50. Weichhart, T.; Hengstschläger, M.; Linke, M. Regulation of Innate Immune Cell Function by MTOR. *Nat. Rev. Immunol.* **2015**, *15*, 599–614. [[CrossRef](#)] [[PubMed](#)]
51. Katholnig, K.; Linke, M.; Pham, H.; Hengstschläger, M.; Weichhart, T. Immune Responses of Macrophages and Dendritic Cells Regulated by MTOR Signalling. *Biochem. Soc. Trans.* **2013**, *41*, 927–933. [[CrossRef](#)] [[PubMed](#)]
52. Shi, C.-S.; Kehrl, J.H. MyD88 and Trif Target Beclin 1 to Trigger Autophagy in Macrophages. *J. Biol. Chem.* **2008**, *283*, 33175–33182. [[CrossRef](#)]
53. Shi, C.S.; Kehrl, J.H. TRAF6 and A20 Regulate Lysine 63-Linked Ubiquitination of Beclin-1 to Control TLR4-Induced Autophagy. *Sci. Signal.* **2010**, *3*, ra42. [[CrossRef](#)]
54. Harris, J. Autophagy and Cytokines. *Cytokine* **2011**, *56*, 140–144. [[CrossRef](#)]
55. Orosz, L.; Papanicolaou, E.G.; Seprényi, G.; Megyeri, K. IL-17A and IL-17F Induce Autophagy in RAW 264.7 Macrophages. *Biomed. Pharmacother.* **2016**, *77*, 129–134. [[CrossRef](#)]
56. Gao, Y.; Wen, Q.; Hu, S.; Zhou, X.; Xiong, W.; Du, X.; Zhang, L.; Fu, Y.; Yang, J.; Zhou, C.; et al. IL-36 $\gamma$  Promotes Killing of Mycobacterium Tuberculosis by Macrophages via WNT5A-Induced Noncanonical WNT Signaling. *J. Immunol.* **2019**, *203*, 922–935. [[CrossRef](#)]
57. Ge, Y.; Huang, M.; Dong, N.; Yao, Y.-M. Effect of Interleukin-36 $\beta$  on Activating Autophagy of CD4+CD25+ Regulatory T Cells and Its Immune Regulation in Sepsis. *J. Infect. Dis.* **2020**, *222*, 1517–1530. [[CrossRef](#)]
58. Schneider, C.A.; Rasband, W.S.; Eliceiri, K.W. NIH Image to ImageJ: 25 Years of Image Analysis. *Nat. Methods.* **2012**, *9*, 671–675. [[CrossRef](#)] [[PubMed](#)]
59. Gomes, L.C.; Dikic, I. Autophagy in Antimicrobial Immunity. *Mol. Cell.* **2014**, *54*, 224–233. [[CrossRef](#)] [[PubMed](#)]
60. Klionsky, D.J.; Abdel-Aziz, A.K.; Abdelfatah, S.; Abdellatif, M.; Abdoli, A.; Abel, S.; Abeliovich, H.; Abildgaard, M.H.; Abudu, Y.P.; Acevedo-Arozena, A.; et al. Guidelines for the Use and Interpretation of Assays for Monitoring Autophagy (4th Edition)<sup>1</sup>. *Autophagy* **2021**, *17*, 1–382. [[CrossRef](#)] [[PubMed](#)]
61. Delgado, M.A.; Elmaoued, R.A.; Davis, A.S.; Kyei, G.; Deretic, V. Toll-like Receptors Control Autophagy. *EMBO J.* **2008**, *27*, 1110–1121. [[CrossRef](#)] [[PubMed](#)]
62. Nascimento, E.B.M.; Ouwens, D.M. PRAS40: Target or Modulator of MTORC1 Signalling and Insulin Action? *Arch. Physiol. Biochem.* **2009**, *115*, 163–175. [[CrossRef](#)] [[PubMed](#)]
63. Zhao, X.; Chen, X.; Shen, X.; Tang, P.; Chen, C.; Zhu, Q.; Li, M.; Xia, R.; Yang, X.; Feng, C.; et al. IL-36 $\beta$  Promotes CD8+ T Cell Activation and Antitumor Immune Responses by Activating MTORC1. *Front. Immunol.* **2019**, *10*, 1803. [[CrossRef](#)] [[PubMed](#)]
64. Gallolu Kankanamalage, S.; Lee, A.-Y.; Wichaidit, C.; Lorente-Rodriguez, A.; Shah, A.M.; Stippec, S.; Whitehurst, A.W.; Cobb, M.H. Multistep Regulation of Autophagy by WNK1. *Proc. Natl. Acad. Sci. USA* **2016**, *113*, 14342–14347. [[CrossRef](#)]
65. You, L.; Wang, Z.; Li, H.; Shou, J.; Jing, Z.; Xie, J.; Sui, X.; Pan, H.; Han, W. The Role of STAT3 in Autophagy. *Autophagy* **2015**, *11*, 729–739. [[CrossRef](#)] [[PubMed](#)]
66. Fan, K.; Lin, L.; Ai, Q.; Wan, J.; Dai, J.; Liu, G.; Tang, L.; Yang, Y.; Ge, P.; Jiang, R.; et al. Lipopolysaccharide-Induced Dephosphorylation of AMPK-Activated Protein Kinase Potentiates Inflammatory Injury via Repression of ULK1-Dependent Autophagy. *Front. Immunol.* **2018**, *9*, 1464. [[CrossRef](#)]
67. Rex, J.; Albrecht, U.; Ehrling, C.; Thomas, M.; Zanger, U.M.; Sawodny, O.; Häussinger, D.; Ederer, M.; Feuer, R.; Bode, J.G. Model-Based Characterization of Inflammatory Gene Expression Patterns of Activated Macrophages. *PLoS Comput. Biol.* **2016**, *12*, e1005018. [[CrossRef](#)] [[PubMed](#)]
68. Oda, K.; Kitano, H. A Comprehensive Map of the Toll-like Receptor Signaling Network. *Mol. Syst. Biol.* **2006**, *2*, 2006.0015. [[CrossRef](#)]
69. Fukao, T.; Koyasu, S. PI3K and Negative Regulation of TLR Signaling. *Trends Immunol.* **2003**, *24*, 358–363. [[CrossRef](#)]
70. Aksoy, E.; Taboubi, S.; Torres, D.; Delbauve, S.; Hachani, A.; Whitehead, M.A.; Pearce, W.P.; Berenjeno, I.M.; Nock, G.; Filloux, A.; et al. The P110 $\delta$  Isoform of the Kinase PI(3)K Controls the Subcellular Compartmentalization of TLR4 Signaling and Protects from Endotoxic Shock. *Nat. Immunol.* **2012**, *13*, 1045–1054. [[CrossRef](#)] [[PubMed](#)]
71. Boutouja, F.; Brinkmeier, R.; Mastalski, T.; El Magraoui, F.; Platta, H.W. Regulation of the Tumor-Suppressor BECLIN 1 by Distinct Ubiquitination Cascades. *Int. J. Mol. Sci.* **2017**, *18*, 2541. [[CrossRef](#)]
72. Xu, H.-D.; Qin, Z.-H. Beclin 1, Bcl-2 and Autophagy. In *Autophagy: Biology and Diseases*; Qin, Z.-H., Ed.; Advances in Experimental Medicine and Biology; Springer: Singapore, 2019; Volume 1206, pp. 109–126. ISBN 9789811506017.
73. Huang, J.; Brumell, J.H. Bacteria-Autophagy Interplay: A Battle for Survival. *Nat. Rev. Microbiol.* **2014**, *12*, 101–114. [[CrossRef](#)] [[PubMed](#)]
74. Wu, Y.-W.; Li, F. Bacterial Interaction with Host Autophagy. *Virulence* **2019**, *10*, 352–362. [[CrossRef](#)] [[PubMed](#)]

**II.**

## COVID-19-associated diarrhea

Klara Megyeri, Áron Dernovics, Zaid I I Al-Luhaibi, András Rosztóczy

**ORCID number:** Klara Megyeri 0000-0002-8255-8272; Áron Dernovics 0000-0003-3759-2524; Zaid I I Al-Luhaibi 0000-0001-6840-1749; András Rosztóczy 0000-0002-8597-8934.

**Author contributions:** Megyeri K and Rosztóczy A made contributions to the concept and were involved in writing of the manuscript; Dernovics Á was involved in writing of the manuscript and creating the image; Al-Luhaibi ZII was involved in writing of the manuscript; all authors approved the final version of the article.

**Supported by** Stipendium Hungaricum Program, No. 109162 (to Al-Luhaibi ZII).

**Conflict-of-interest statement:** Authors declare no conflict of interests for this article.

**Open-Access:** This article is an open-access article that was selected by an in-house editor and fully peer-reviewed by external reviewers. It is distributed in accordance with the Creative Commons Attribution NonCommercial (CC BY-NC 4.0) license, which permits others to distribute, remix, adapt, build upon this work non-commercially, and license their derivative works on different terms, provided the original work is properly cited and the use is non-commercial. See: [http](http://creativecommons.org/licenses/by-nc/4.0/)

**Klara Megyeri, Áron Dernovics, Zaid I I Al-Luhaibi,** Department of Medical Microbiology and Immunobiology, University of Szeged, Szeged 6720, Csongrad, Hungary

**András Rosztóczy,** Division of Gastroenterology, Department of Internal Medicine, University of Szeged, Szeged 6720, Csongrad, Hungary

**Corresponding author:** Klara Megyeri, MD, PhD, Associate Professor, Department of Medical Microbiology and Immunobiology, University of Szeged, Dóm tér 10, Szeged 6720, Csongrad, Hungary. [megyeri.klara@med.u-szeged.hu](mailto:megyeri.klara@med.u-szeged.hu)

### Abstract

Severe acute respiratory syndrome coronavirus 2 (SARS-CoV-2) recently emerged as a highly virulent respiratory pathogen that is known as the causative agent of coronavirus disease 2019 (COVID-19). Diarrhea is a common early symptom in a significant proportion of patients with SARS-CoV-2 infection. SARS-CoV-2 can infect and replicate in esophageal cells and enterocytes, leading to direct damage to the intestinal epithelium. The infection decreases the level of angiotensin-converting enzyme 2 receptors, thereby altering the composition of the gut microbiota. SARS-CoV-2 elicits a cytokine storm, which contributes to gastrointestinal inflammation. The direct cytopathic effects of SARS-CoV-2, gut dysbiosis, and aberrant immune response result in increased intestinal permeability, which may exacerbate existing symptoms and worsen the prognosis. By exploring the elements of pathogenesis, several therapeutic options have emerged for the treatment of COVID-19 patients, such as biologics and biotherapeutic agents. However, the presence of SARS-CoV-2 in the feces may facilitate the spread of COVID-19 through fecal-oral transmission and contaminate the environment. Thus gastrointestinal SARS-CoV-2 infection has important epidemiological significance. The development of new therapeutic and preventive options is necessary to treat and restrict the spread of this severe and widespread infection more effectively. Therefore, we summarize the key elements involved in the pathogenesis and the epidemiology of COVID-19-associated diarrhea.

**Key Words:** COVID-19; Diarrhea; Ionic imbalance; Viroporin; Angiotensin-converting enzyme type 2; Leaky gut

©The Author(s) 2021. Published by Baishideng Publishing Group Inc. All rights reserved.

[p://creativecommons.org/licenses/by-nc/4.0/](https://creativecommons.org/licenses/by-nc/4.0/)

**Manuscript source:** Invited manuscript

**Specialty type:** Gastroenterology and hepatology

**Country/Territory of origin:** Hungary

**Peer-review report's scientific quality classification**

Grade A (Excellent): 0  
Grade B (Very good): B, B  
Grade C (Good): 0  
Grade D (Fair): 0  
Grade E (Poor): 0

**Received:** January 28, 2021

**Peer-review started:** January 29, 2021

**First decision:** March 6, 2021

**Revised:** March 19, 2021

**Accepted:** May 20, 2021

**Article in press:** May 20, 2021

**Published online:** June 21, 2021

**P-Reviewer:** Ding X

**S-Editor:** Gao CC

**L-Editor:** A

**P-Editor:** Liu JH



**Core Tip:** Severe acute respiratory syndrome coronavirus 2 (SARS-CoV-2) replicates in enterocytes, triggers ionic imbalances, activates the NLRP3 inflammasome pathway, induces apoptosis, and exerts a dual effect on the autophagic process. These effects of SARS-CoV-2 lead to the development of leaky gut. Increased permeability triggers the absorption of lipopolysaccharide into the circulation, further exacerbating inflammation induced by viral infection. In addition to drugs that affect the inflammatory response and viral replication, agents targeting autophagy and apoptosis appear to be potentially suitable for the treatment of coronavirus disease 2019 (COVID-19). The fecal-oral route of SARS-CoV-2 transmission calls for strict and more consistent adherence to hygiene rules to prevent the spread of COVID-19.

**Citation:** Megyeri K, Dernovics Á, Al-Luhaibi ZII, Rosztóczy A. COVID-19-associated diarrhea. *World J Gastroenterol* 2021; 27(23): 3208-3222

**URL:** <https://www.wjgnet.com/1007-9327/full/v27/i23/3208.htm>

**DOI:** <https://dx.doi.org/10.3748/wjg.v27.i23.3208>

## INTRODUCTION

Severe acute respiratory syndrome coronavirus 2 (SARS-CoV-2) recently emerged as a highly virulent respiratory pathogen that is known as the causative agent of coronavirus disease 2019 (COVID-19)[1]. SARS-CoV-2 enters the human body through the airways and multiplies in the lungs. This novel coronavirus causes mild, severe, and critical respiratory disease in 81%, 14%, and 5% of cases, respectively[2]. It may also enter the bloodstream, which results in viremia and systemic spread throughout the body.

In addition to the airways, the virus can multiply in the gastrointestinal (GI) tract (GIT), urinary tract, and central nervous system. The infection elicits an intemperate immune response characterized by a life-threatening cytokine storm and a corrupted interferon (IFN) system, which is unable to eliminate the pathogen effectively. As a result, a systemic inflammatory response syndrome occurs[3,4]. In the severe and critical clinical manifestations of COVID-19, atypical pneumonia leading to progressive respiratory failure develops[2].

As of the 13<sup>th</sup> of January 2021, about 90 million people have been infected, and nearly 2 million people have died during the COVID-19 pandemic[5]. Although the leading COVID-19 symptoms are due to involvement of the respiratory system, it often causes GI symptoms as well. Thus, we examined the current state of knowledge on the pathogenesis, occurrence rate, clinical significance, and epidemiological consequences of COVID-19-associated diarrhea.

## TAXONOMIC CLASSIFICATION, STRUCTURE, AND REPLICATION OF SARS-COV-2

SARS-CoV-2 belongs to the genus *Betacoronavirus* of the family *Coronaviridae*, which comprises enveloped viruses with positive-sense single-stranded RNA genomes[1,6,7]. The spherical or elliptical virions are pleomorphic with diameters of 80-160 nm[8,9]. The capsid has helical symmetry, which is built up by the nucleocapsid (N) protein. The spike (S), membrane (M), and envelope (E) proteins are located in the virion envelope[10]. The S protein forms protrusions of 20 nm in length that provide a characteristic crown-like appearance, which is reflected in the name of the viral family. The S-protein is responsible for binding to the cell surface receptor[10].

Besides the S, E, M, and N structural protein genes, the genome of SARS-CoV-2 contains open reading frames (Orfs) that encode nine accessory proteins (3a, 3b, 6, 7a, 7b, 8, 9b, 9c, and 10) and two polyproteins (pp1a and pp1ab)[10-15]. Polyproteins pp1a and pp1ab are cleaved by viral proteases to form unique non-structural proteins (Nsp), which play an important role in viral replication[10]. Although the accessory proteins of SARS-CoV-2 are not essential for viral multiplication, they are implicated in the pathogenesis[10].

As the first step in infection, the S protein of SARS-CoV-2 binds to its corresponding cell-surface receptor, angiotensin-converting enzyme type 2 (ACE2)[16,17]. The S protein has two subunits: S1 and S2. The S1 subunit has a receptor-binding domain and is responsible for receptor engagement, whereas the S2 subunit is involved in the fusion process[17-19]. Following ACE2 binding, cellular proteases such as transmembrane protease/serine subfamily member 2 (TMPRSS2), TMPRSS4, and cathepsin L cleave S protein into S1 and S2 subunits, and the virus enters the host cell by receptor-mediated endocytosis[17,19-23]. Other proteases have also been shown to be able to cleave S protein, including furin, trypsin-like proteases, elastase, plasmin, and factor Xa. This suggests that these enzymes may also facilitate entry or expand the tissue tropism of SARS-CoV-2[23-27].

Within the endosome, cathepsin-mediated activation of the S protein continues, eventually causing the S2 subunit to gain a fusogenic effect that triggers the fusion of the viral envelope and the endosomal membrane[25]. The nucleocapsid is then released into the cytoplasm, where the translation of Orf1a and Orf1b results in the formation of pp1a and pp1ab, from which Nsp1-16 are generated by proteolysis. Nsp12 functions as an RNA-dependent RNA polymerase and associates with Nsp7 and Nsp8 to form the core of the replication and transcription complex (RTC) of SARS-CoV-2[28,29]. The cofactors Nsp7 and Nsp8 form a hexadecameric ring structure that has a primase function and generates RNA primers for the synthesis of the negative-sense RNA[28,29].

RTC synthesizes the genomic RNA and a set of SARS-CoV-2 mRNAs through full-length and subgenomic negative-sense RNA intermediates[28,29]. The replication of the viral genome and transcription of viral genes takes place in double-membraned vesicles[30,31]. The SARS-CoV-2 replication compartment provides a protected environment which inhibits the antiviral effects of IFN and other cellular antiviral defense mechanisms by hiding the viral genome, transcripts, and replicative intermediates from cellular nucleic acid sensors.

The viral mRNAs are translated in the rough endoplasmic reticulum, leading to the formation of accessory proteins and structural proteins (N, M, E, and S). The M, E, and S proteins then become embedded in the endoplasmic reticulum, whereas the N proteins assemble with the newly synthesized full-length positive-sense RNA to form the nucleocapsid[30,31]. After being transported to the ERGIC (endoplasmic reticulum-Golgi intermediate compartment), the nucleocapsids bud through the ERGIC membrane into its lumen[30,31]. The mature virions reach the cytoplasm membrane *via* vesicular transport and are released from the cell[30,31].

---

## THE MAIN CELLULAR EFFECTS OF SARS-COV-2

---

During multiplication, SARS-CoV-2 modulates several cellular aspects, including signaling, transcription, translation, cell division, the IFN system, autophagy, and apoptosis, as well as the biogenesis, function, and morphology of mitochondria and intracellular vesicles. Phosphoproteomic profiling has revealed that SARS-CoV-2 infection affects the activity of 97 kinases. The activities of several members of the p38 pathway and the guanosine monophosphate-dependent protein kinases are upregulated, while cell cycle kinases (CDK1/2/5), cell growth-related signaling pathway kinases (AKT1/2), and regulators of the cytoskeleton are down-regulated[32]. The functional changes in the signal transduction pathways have been shown to play an important role in SARS-CoV-2-induced cytoskeletal damage, cytokine production, and slow-down in cell proliferation at the S/G2 transition phase[32].

Transcriptomic profiles of SARS-CoV-2-infected primary human bronchial epithelial cells, lung biopsy, and bronchoalveolar lavage fluid samples of COVID-19 patients have demonstrated upregulated expression of genes implicated in metabolism, immunity, and the stress responses of the endoplasmic reticulum and mitochondria[33-35]. It has been shown that the M protein, Nsp7, and ORF9c stimulate lipogenesis, while Nsp7, Nsp12, and ORF8 trigger endoplasmic stress response, and Nsp7 induces mitochondrial dysfunction[34]. Moreover, the M and E proteins, along with Nsp3a, Nsp6, Nsp8, Nsp10, and Nsp13, were shown to be able to modify the structure and function of the endomembrane system and vesicle trafficking, thereby facilitating several steps of viral multiplication[36].

Interestingly, the expression of genes involved in the humoral immune response and innate immune response-activating signal transduction are increased, whereas genes implicated in cytokine-mediated signaling pathways are down-regulated[33]. A multiplex gene expression analysis showed that the genes involved in type I IFN

signaling were highly up-regulated, whereas the expression of IFN-stimulated genes (*ISGs*) was decreased in severe COVID-19 patients[37]. The levels of pro-inflammatory cytokines measured in sera of COVID-19 patients were highly increased in a pattern corresponding to a cytokine storm[38-40].

Consistent with this observation, transcriptional activation of pro-inflammatory cytokine genes was also detected in peripheral blood mononuclear cells and bronchoalveolar lavage fluid[41]. The sera and lung tissue samples of patients have shown interleukin (IL)-1 $\beta$ , IL-6, IL-10, IL-18, IL-33, transforming growth factor- $\beta$ , IFN- $\gamma$ , CSF2/GM-CSF (colony-stimulating factor 2/granulocyte-macrophage colony-stimulating factor), CSF3/G-CSF, CC chemokines [CCL2/MCP-1, CCL3/MIP-1A, CCL4/MIP-1B, CCL5/RANTES, CCL8, CCL3L1] and CXC chemokines [CXCL1, CXCL2 and CXCL10/IP10][38,39,41,42]. However, during SARS-CoV-2 infection, the production of type I and III IFNs is decreased[37,43]. Thus, these data clearly demonstrate that SARS-CoV-2 infection alters both the transcriptional and translational patterns in cells profoundly[32-43].

Other observations indicate that SARS-CoV-2 could trigger several cell-death processes, including apoptosis, necrosis, pyroptosis, and anoikis, depending on the type of cell[44-47]. The death of infected cells may contribute to tissue damage and induce an inflammatory reaction[44-47]. It has also been revealed that SARS-CoV-2 Orf 3a stimulates the formation of the autophagic Beclin-1-Vps34-Atg14 complex while simultaneously inhibiting the Beclin-1 complex containing the UVRAG adaptor protein[48]. Orf 3a thereby exerts a dual effect on the autophagic process manifesting in the induction of the initial steps and a block in the fusion of the autophagosomes with lysosomes[48].

---

## DIARRHEA IN COVID-19

---

GIT involvement is frequent in COVID-19 patients and includes anorexia, nausea, vomiting, diarrhea, and abdominal pain[49-62]. Among the specific GI symptoms, diarrhea is the most common. Based on different studies, the prevalence of diarrhea might range from 2% to 49.5%[50,61,63]. COVID-19-associated diarrhea is characterized by loose or watery stools and is usually mild, self-limiting, and can even be the only symptom of the infection[49,52,58,59,63]. The average frequency of bowel movements is in the range of 3.3-4.3 times per day[53,58], and the average duration of diarrhea is 3-5.4 d[52,53,58,59,63]. In some cases, however, diarrhea is more severe, with patients experiencing more frequent bowel movements of up to 18-30 times per day[58,63].

Rare cases with more severe GI symptoms have also been reported, such as acute hemorrhagic colitis and GI bleeding[53,54,64]. Furthermore, the relationship between GI symptoms and the severity of the disease has been investigated. Statistically significant differences were not observed between COVID-19 patients with and without GI symptoms in clinical severity, length of hospital stay, and mortality rate[49, 59,60]. SARS-CoV-2 mRNA could be detected in the stool of COVID-19 patients in 22%-54.5% of cases, and occasionally, the virus is detectable in the stool even after the airway samples become negative[54,57,58,65-69]. Positive results have been obtained from real-time reverse transcriptase-polymerase chain reaction (Rrt-PCR) tests of stool even in patients without GI symptoms[58]. In patients with GI symptoms, the total time between the onset of symptoms and viral clearance is significantly longer than in those with only respiratory manifestations[58,70].

The reason why GI symptoms occur in only a subset of COVID-19 patients is currently unknown. There are no significant differences between the two patient groups in terms of demographics and certain coexisting conditions, such as pregnancy, cancer, chronic renal disease, chronic obstructive pulmonary disease, or immunosuppression. A study conducted by Jin *et al*[52] revealed that the rate of chronic liver disease in COVID-19 patients with GI symptoms is much higher than among those without GI symptoms. Moreover, the incidence of COVID-19 with GI symptoms displays familial clustering[52]. Based on these interesting observations, it is reasonable to infer that genetic, immunological, and epidemiological factors are involved in the development of COVID-19-associated diarrhea.

## PATHOGENESIS OF COVID-19-ASSOCIATED DIARRHEA

ACE2, the cellular receptor of SARS-CoV-2, is widely expressed in many types of cells and tissues of the GIT, including the esophagus, stomach, small intestine, colon, rectum, pancreatic exocrine glands and islets, and gallbladder[71]. The expression level of ACE2 in the GIT is highest in the ileum epithelial cells, especially in the absorptive enterocytes[72]. It has also been demonstrated that ACE2 is co-expressed with TMPRSS2/4 proteases in the GIT, with the highest level in the ileum[73]. These observations indicate that several cell types in the GIT are potentially susceptible to SARS-CoV-2 infection[71-73].

Studies demonstrating that viral RNA can be detected in the stool samples of COVID-19 patients indicate that SARS-CoV-2 can indeed infect the GIT[54,57-59,66-68]. It is estimated that feces and GI tissues contain  $10^4$ - $10^8$  and  $10^0$ - $10^4$  RNAs per gram, respectively[74,75]. Further studies revealed that SARS-CoV-2 establishes a productive infection in intestinal epithelial cells and human small intestinal organoids, leading to the production of new infectious progeny virions[20,76]. Viral particles within intracytoplasmic vesicles and aggregates of SARS-CoV-2 virions attached to the surface of enterocytes have been detected in intestinal organoids and post-mortem GIT samples from COVID-19 patients by electron microscopy[76,77]. These observations indicate that the GIT can be an entry site and an extra-pulmonary target organ of SARS-CoV-2[20,71-73,76,77].

Further analyses were performed to determine whether infectious viruses are present in the GIT or feces. In most cases, efforts to cultivate infectious SARS-CoV-2 from feces have failed, although Xiao *et al*[78] recently reported the successful isolation of the virus from stool samples by using the Vero E6 cell line. Simulated large intestinal fluid was shown to reduce the infectivity of the virus significantly[20]. Thus, it is possible that most of the virus that multiplies in the enterocytes may be inactivated in the lumen of intestines within a short time after release.

*In vitro* cultivation of SARS-CoV-2 has demonstrated that this virus elicits a cytopathic effect (CPE) on some cell lines, whereas in other cell types, no cytomorphological abnormalities could be observed despite efficient viral replication[79]. In human airway epithelial cells, SARS-CoV-2 causes CPE characterized by the formation of multinucleated syncytia and cilium shrinking, and cell death largely occurs by way of apoptosis[45]. In contrast, the colorectal adenocarcinoma Caco-2 cell line proved to be susceptible to infection, but the multiplication of SARS-CoV-2 was not accompanied by a visible CPE[79]. Likewise, intense tissue damage was not observed in the GIT of COVID-19 patients[80].

SARS-CoV-2 can establish a persistent infection in human C2BBel1 intestinal cells expressing a brush border[81]. Moreover, SARS-CoV-2 was shown to be more effective in inducing the production of IFN- $\alpha$ , IFN- $\beta$ , IFN- $\lambda$ 1, IFN- $\lambda$ 2, and IFN- $\lambda$ 3 in human intestinal tissues *ex vivo* than in lung tissue[80]. Therefore, it is also conceivable that a specific immuno-inflammatory environment develops in the lungs and GIT as a result of infection, which affects the rate of viral replication and cell demise in different ways.

Although SARS-CoV-2 causes no extensive tissue damage in the intestines, the infection seems to harm the enterocytes in a much more sophisticated way. E protein was shown to bind to the tight junction-associated PALS1 (Proteins Associated with Lin Seven 1)[82]. PALS1 interacts with PATJ (PALS1-Associated Tight Junction protein) and CRB3 (Crumbs 3), and the PALS1/PATJ/CRB3 complex that forms is essential for the maintenance of tight junctions connecting epithelial cells[83]. E protein causes functional impairment of PALS1 and interferes with the formation of tight junctions, leading to the disruption of intestinal barrier integrity[82]. By using a biomimetic gut-on-chip system, Guo *et. al.* elegantly demonstrated that SARS-CoV-2 infection destroys tight junctions and adherent junctions in both the endothelium and intestinal epithelium, which in turn may lead to leaky gut syndrome, local and systemic invasion of normal microbiota members, and immune activation[84] (Figure 1).

The E protein of SARS-CoV-2 is a single-spanning membrane protein that forms a homopentameric ion channel, which displays selective permeability for monovalent ions (Na<sup>+</sup>, K<sup>+</sup>, and Cl<sup>-</sup>) and Ca<sup>2+</sup>[85]. E protein accumulates in the endoplasmic reticulum and ERGIC/Golgi membranes and transports Ca<sup>2+</sup> from these compartments to the cytoplasm. Elevated cytoplasmic Ca<sup>2+</sup> concentration can increase the rate of apical Cl<sup>-</sup> exit across the Ca<sup>2+</sup>-activated Cl<sup>-</sup> channels and cyclic-nucleotide-activated cystic fibrosis transmembrane conductance regulator[86].

SARS-CoV-2 also has another ion-channel protein, Orf3a, which is a K<sup>+</sup> ion channel viroporin that exhibits plasma membrane and endomembrane localization[46,87]. Orf3a in the cytoplasmic membrane may cause leakage of K<sup>+</sup> ions from enterocytes.

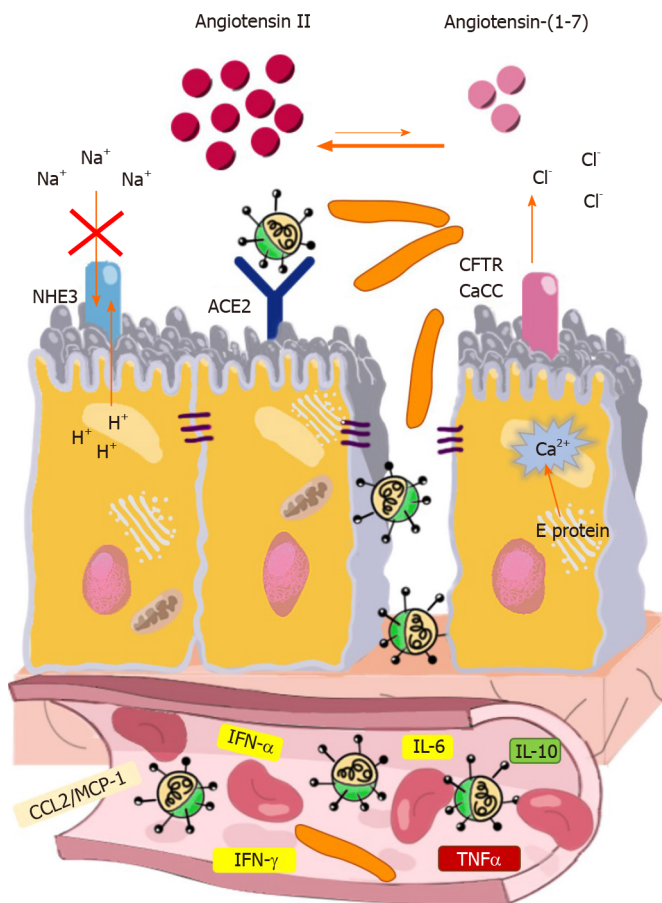


**Figure 1 Mechanism involved in coronavirus disease 2019-associated diarrhea.** Severe acute respiratory syndrome coronavirus 2 (SARS-CoV-2) binds to its corresponding cell-surface receptor, angiotensin-converting enzyme type 2. In the intestines, SARS-CoV-2 viroporins, E protein, dysregulation of the renin-angiotensin-aldosterone system triggering ionic imbalance, disruption of barrier integrity and inflammation play important roles in the development of coronavirus disease 2019-associated secretory diarrhea and leaky gut. ACE: Angiotensin-converting enzyme; IFN: Interferon; IL: Interleukin; TNF $\alpha$ : tumor necrosis factor alpha; CFTR: CF transmembrane conductance regulator; CaCC: Ca<sup>2+</sup>-activated Cl<sup>-</sup> channel; NHE3: Na<sup>+</sup>-H<sup>+</sup> exchanger 3.

Moreover, intracellular ionic imbalances triggered by SARS-CoV-2 viroporins (E protein and Orf3a) can lead to the activation of the NLRP3 inflammasome (NOD-, LRR-, and Pyrin domain-containing 3). This results in the secretion of IL-1 $\beta$  and cell death in a process called pyroptosis[44,46]. By activating innate immune cells, IL-1 $\beta$  contributes to the development of a local inflammatory environment and a systemic cytokine storm. The direct action of viroporins and the indirect effects of cytokines together can trigger an ionic imbalance of enterocytes, which may contribute to the development of diarrhea (Figure 1).

During its multiplication, SARS-CoV-2 disturbs the function of the renin-angiotensin-aldosterone system (RAAS). The main components of this system are ACE, angiotensin II, and AT1R. Angiotensin II is known to elicit vasoconstriction, oxidative stress, and inflammation following binding to AT1R[88]. The ACE2/angiotensin (1-7)/Mas pathway is an important physiological negative regulator of the ACE/angiotensin II/AT1R axis and exerts anti-inflammatory effects[88]. SARS-CoV-2 uses ACE2 for entry as a receptor, which becomes degraded in the endolysosomal compartment after being internalized along with the virion particles[17,19,20].

The viral infection has been shown to increase the expression of ADAM (A Disintegrin and Metalloprotease) metallopeptidase domain 17 enzyme, which is endowed with sheddase activity[89]. ADAM17 functions in the ectodomain shedding of tumor necrosis factor alpha (TNF- $\alpha$ ), EGFR ligands, and ACE2[90,91]. ADAM17-mediated cleavage decreases ACE2 Levels on the cytoplasm membrane and thereby shifts the delicate balance towards the ACE/angiotensin II/AT1R pathway. In turn, this can lead to pro-inflammatory predominance. It has also been demonstrated recently that ACE2 forms dimer-of-heterodimer complexes with the neutral amino acid transporter B<sup>0</sup>AT1 (Broad neutral Amino acid Transporter 1)[91]. B<sup>0</sup>AT1 is involved in the Na<sup>+</sup>-coupled transportation of tryptophan, phenylalanine, glutamine, and leucine[91].

The ADAM17-mediated cleavage of ACE2 ectodomain and attachment of SARS-CoV-2 to the ACE2:B<sup>0</sup>AT1 complex may potentially compromise the transport of Na<sup>+</sup> and neutral amino acids[88]. Impairment of the ACE2:B<sup>0</sup>AT1 complex and the consequential amino acid starvation can decrease Na<sup>+</sup> uptake and affect the activation state of the mechanistic target of rapamycin (mTOR) complex, which is an important regulator of autophagy, xenophagy, metabolism, and various immune processes[88,92-95]. Dysregulated RAAS may aggravate ionic imbalance and inflammation, which may affect the metabolic state of cells, the composition of the microbiota, and cell viability, leading to increasingly severe intestinal dysfunction[88,90,91,94,95] (Figure 1).

## VIRUS-INDEPENDENT CAUSES OF COVID-19-ASSOCIATED DIARRHEA

If diarrhea is not included in the presenting symptoms and develops after admission, it becomes challenging to ascertain the cause of diarrhea. Several confounding variables, such as the hyperinflammatory response, altered gut flora, secondary bacterial infections, antiviral agents, antibiotics, enteral feeding, and the use of proton pump inhibitors can potentially cause diarrhea in hospitalized COVID-19 patients.

In approximately 20% of COVID-19 patients, the infection progresses to severe and critical phases in which an extrapulmonary hyperinflammatory state develops due to cytokine release syndrome[96]. Several cytokines may affect the course and clinical manifestations of SARS-CoV-2 infection by increasing the intestinal and vascular permeability as well as triggering the formation of thrombi in the small blood vessels and the alteration of intestinal microbiota, leading to bacterial translocation towards the bloodstream and the mesenteric lymph node[3,4]. The cytokine-mediated GI damage may thereby further intensify the systemic immunological response and contribute to the deterioration of the patient's condition. A study conducted by Zhang *et al*[97] revealed that the pro-inflammatory cytokine patterns are different in COVID-19 patients with and without diarrhea. Moreover, diarrhea patients were more likely to develop cytokine release syndrome and multi-organ damage[97]. Interestingly, the levels of TNF- $\alpha$ , IL-6, and IL-10 were significantly higher in the sera of diarrhea patients than in the non-diarrhea group[97]. TNF- $\alpha$  is known to increase the expression of adhesion molecules on the surface of endothelial cells, platelets, and leukocytes, thereby facilitating the adhesion of thrombocytes to the vessels and initiating the formation of thrombi in the microcirculation of the GIT and other organs. These effects increase vascular permeability and can lead to inflammation and disseminated intravascular coagulation. Furthermore, TNF- $\alpha$  has the ability to disrupt the intestinal tight junction barrier, which in turn contributes to the development of leaky gut[98]. IL-6 exerts dual effects on the intestinal epithelium. It increases gut permeability to small molecules with a radius < 4Å (< 0.4 nm) *via* activating claudin-2 gene expression[99]. However, by stimulating epithelial proliferation and regeneration, IL-6 plays a beneficial role in the maintenance of intestinal epithelial integrity during acute injury[100]. IL-10 is an anti-inflammatory cytokine that restricts uncontrolled immune responses to the intestinal microbiota and defends gut barrier integrity[101,102]. In light of these data, it is reasonable to infer that TNF- $\alpha$  may be an important factor in COVID-19-associated diarrhea, whereas without IL-10, the cytokine storm and intestinal injury would be even more devastating. However, further studies are needed to identify the precise role of each cytokine in the development of COVID-19-associated diarrhea. Such studies could also contribute to a better understanding of the potential adverse effects of anti-cytokine therapies on the GIT.

Interesting observations revealed that the composition of intestinal microbiota is profoundly altered in COVID-19 patients: The diversity is highly reduced, the proportion of beneficial commensal bacteria is decreased and the opportunistic pathogens are enriched compared with that found in healthy controls[103,104]. It has also been demonstrated that some *Bacteroides spp.*, capable of decreasing ACE2 expression in mice, displayed inverse correlation with the fecal SARS-CoV-2 load [104]. The immune system and the intestinal microbiota are in a continuous dialog. The presence of commensal microorganisms shapes host immunity, and alterations in microbiota composition may lead to increased susceptibility to various pathological conditions, including infections, inflammation, and metabolic and autoimmune disorders. Thus, the altered microbiota observed in COVID-19 patients may be an additional factor contributing to the development of diarrhea by weakening colonization resistance, decreasing the production of beneficial bacterial metabolites, and triggering a local immune recalibration.

For clinical improvement and treatment of secondary bacterial infections, COVID-19 patients are treated with antiviral agents, antibiotics, and corticosteroids. Antiviral agents such as the RNA polymerase inhibitors favipiravir and remdesivir may cause diarrhea[105]. Diarrhea is also a common adverse drug reaction to antibiotics such as cephalosporins, macrolides and fluoroquinolones, largely due to destruction of the normal intestinal microbiota. Moreover, treatment of COVID-19 patients with broad-spectrum antibiotics has the potential to increase the risk of *Clostridioides difficile* (*C. difficile*) infection, including in survivors even long after recovery. In co-infections with SARS-CoV-2 and *C. difficile*, intestinal damage is more extensive and diarrhea symptoms are more severe[106]. To counteract the detrimental effects of various proinflammatory cytokines, biological therapy is used in selected patient groups. IL-6 and IL-6 receptor inhibitors, such as tocilizumab, sarilumab and siltuximab, represent another class of drugs that often cause diarrhea[107]. Although enteral feeding has well-established, clear advantages over parenteral nutrition[108], adverse events, like diarrhea, may develop. Tube feeding-related diarrhea can occur for several reasons, mostly related to the circumstances of feeding (adaptation time, perfusion speed, temperature) or the composition of the used enteral formula (osmolality, fat content, nutrient intolerance), and can be managed easily with careful observation of the patients[109]. Not only is the use of PPIs during the course of COVID-19 infection controversial[110], such drugs may induce diarrhea in general through the alteration of GI microbiota by different mechanisms, including the direct consequences of increased gastric pH itself. This safety issue was evaluated by a number of meta-analyses based on retrospective observational or case-control studies, which suggested an increased risk for enteral infections, especially *C. difficile* infections, in PPI-treated patients[111-113]. In contrast, a recent long-term prospective study (COMPASS) failed to show an increased risk of *C. difficile* infection in PPI users and only a slight increase of enteral infections in general[114].

## POTENTIAL CONSEQUENCES OF COVID-19-ASSOCIATED DIARRHEA

A great body of experimental and clinical evidence demonstrates that SARS-CoV-2 infects and replicates in the GIT, and the stool contains high copies of viral RNA, although the amount of infectious virus in the stool appears to be low. The presence of SARS-CoV-2 in the feces may potentially facilitate the spread of COVID-19 through fecal-oral transmission among humans and contaminate the environment[115-117]. Thus, SARS-CoV-2 infection of the GIT has important epidemiological significance.

The feces of COVID-19 patients pose a serious epidemiological risk, which justifies the use of all available methods of prevention, including protective equipment, disinfection procedures, and vaccination. However, further studies are needed to establish the efficiency of the fecal-oral spread of SARS-CoV-2 precisely. It would be very useful if the concentration of infectious virion particles in the stool were determined in asymptomatic individuals and different patient groups under standardized parameters when discharge frequencies and the grade on the Bristol stool scale are precisely recorded. It is possible that the rate of virus inactivation in the intestinal lumen may significantly differ in COVID-19 patients.

SARS-CoV-2 can extensively contaminate the environment, and viral RNA can be detected in sewage and solid waste[118,119]. Measurement of SARS-CoV-2 RNA in wastewater is used for local monitoring of the epidemic situation, which facilitates the implementation of preventive measures. Wastewater epidemiology involves using Rrt-PCR to determine SARS-CoV-2 RNA in sewage, but how long the virus survives in this environment has not been measured[118,119]. It would be essential to determine the concentration of infectious virion particles to elucidate the risk of SARS-CoV-2 transmission *via* wastewater contamination.

## CONCLUSION

Among the specific GI symptoms, diarrhea is the most common in COVID-19 patients. The ACE2 receptor and other elements required for the attachment of this virus to the various cell types are extensively expressed throughout the GIT. SARS-CoV-2 can establish a productive infection in the enterocytes, leading to mild cellular damage. The infection evokes an inflammatory response in the intestines, which is characterized by the production of various pro-inflammatory cytokines and chemokines, many of which are known to increase intestinal permeability. Direct effects of SARS-

CoV-2 viroporins and dysregulation of the intestinal RAAS triggering ionic imbalance and inflammation in the intestines seem to play important roles in the development of COVID-19-associated secretory diarrhea and leaky gut.

Infection in the lungs and GIT also seems to display some different tissue-specific features. The production of type I and III IFNs is more efficient in the GIT than in the lungs. The antiviral IFNs may restrict viral replication in the GIT to some extent, which may allow the development of a less cytopathogenic or persistent form of infection in this anatomical region. SARS-CoV-2-mediated dysregulation of the ACE2:B<sup>0</sup>AT1 complex may modify the biological response of cells to the infection, and in enterocytes, it may contribute to the development of diarrhea by inducing amino acid starvation, which can decrease Na<sup>+</sup> uptake. These effects are not seen in the lungs, however, as ACE2 does not form a complex with B<sup>0</sup>AT1 in this organ. SARS-CoV-2 infection of the GIT is of pivotal epidemiological significance, but further studies are needed to assess the extent of this risk.

## REFERENCES

- 1 **Coronaviridae Study Group of the International Committee on Taxonomy of Viruses.** The species Severe acute respiratory syndrome-related coronavirus: classifying 2019-nCoV and naming it SARS-CoV-2. *Nat Microbiol* 2020; **5**: 536-544 [PMID: [32123347](#) DOI: [10.1038/s41564-020-0695-z](#)]
- 2 **Hu B, Guo H, Zhou P, Shi ZL.** Characteristics of SARS-CoV-2 and COVID-19. *Nat Rev Microbiol* 2021; **19**: 141-154 [PMID: [33024307](#) DOI: [10.1038/s41579-020-00459-7](#)]
- 3 **Tay MZ, Poh CM, Rénia L, MacAry PA, Ng LFP.** The trinity of COVID-19: immunity, inflammation and intervention. *Nat Rev Immunol* 2020; **20**: 363-374 [PMID: [32346093](#) DOI: [10.1038/s41577-020-0311-8](#)]
- 4 **Vabret N, Britton GJ, Gruber C, Hegde S, Kim J, Kuksin M, Levantovsky R, Malle L, Moreira A, Park MD, Pia L, Risson E, Saffern M, Salomé B, Esai Selvan M, Spindler MP, Tan J, van der Heide V, Gregory JK, Alexandropoulos K, Bhardwaj N, Brown BD, Greenbaum B, Gümüş ZH, Homann D, Horowitz A, Kamphorst AO, Curotto de Lafaille MA, Mehndru S, Merad M, Samstein RM; Sinai Immunology Review Project.** Immunology of COVID-19: Current State of the Science. *Immunity* 2020; **52**: 910-941 [PMID: [32505227](#) DOI: [10.1016/j.immuni.2020.05.002](#)]
- 5 **World Health Organization.** WHO Coronavirus Disease (COVID-19) Dashboard. [cited 13 January 2021]. In: World Health Organization [Internet]. Available from: <https://covid19.who.int>
- 6 **Helmy YA, Fawzy M, Elasad A, Sobieh A, Kenney SP, Shehata AA.** The COVID-19 Pandemic: A Comprehensive Review of Taxonomy, Genetics, Epidemiology, Diagnosis, Treatment, and Control. *J Clin Med* 2020; **9** [PMID: [32344679](#) DOI: [10.3390/jcm9041225](#)]
- 7 **Lu R, Zhao X, Li J, Niu P, Yang B, Wu H, Wang W, Song H, Huang B, Zhu N, Bi Y, Ma X, Zhan F, Wang L, Hu T, Zhou H, Hu Z, Zhou W, Zhao L, Chen J, Meng Y, Wang J, Lin Y, Yuan J, Xie Z, Ma J, Liu WJ, Wang D, Xu W, Holmes EC, Gao GF, Wu G, Chen W, Shi W, Tan W.** Genomic characterisation and epidemiology of 2019 novel coronavirus: implications for virus origins and receptor binding. *Lancet* 2020; **395**: 565-574 [PMID: [32007145](#) DOI: [10.1016/S0140-6736\(20\)30251-8](#)]
- 8 **Miller SE, Goldsmith CS.** Caution in Identifying Coronaviruses by Electron Microscopy. *J Am Soc Nephrol* 2020; **31**: 2223-2224 [PMID: [32651224](#) DOI: [10.1681/ASN.2020050755](#)]
- 9 **Caldas LA, Carneiro FA, Higa LM, Monteiro FL, da Silva GP, da Costa LJ, Durigon EL, Tanuri A, de Souza W.** Ultrastructural analysis of SARS-CoV-2 interactions with the host cell *via* high resolution scanning electron microscopy. *Sci Rep* 2020; **10**: 16099 [PMID: [32999356](#) DOI: [10.1038/s41598-020-73162-5](#)]
- 10 **Naqvi AAT, Fatima K, Mohammad T, Fatima U, Singh IK, Singh A, Atif SM, Hariprasad G, Hasan GM, Hassan MI.** Insights into SARS-CoV-2 genome, structure, evolution, pathogenesis and therapies: Structural genomics approach. *Biochim Biophys Acta Mol Basis Dis* 2020; **1866**: 165878 [PMID: [32544429](#) DOI: [10.1016/j.bbadis.2020.165878](#)]
- 11 **Khailany RA, Safdar M, Ozaslan M.** Genomic characterization of a novel SARS-CoV-2. *Gene Rep* 2020; **19**: 100682 [PMID: [32300673](#) DOI: [10.1016/j.genrep.2020.100682](#)]
- 12 **Michel CJ, Mayer C, Poch O, Thompson JD.** Characterization of accessory genes in coronavirus genomes. *Viral J* 2020; **17**: 131 [PMID: [32854725](#) DOI: [10.1186/s12985-020-01402-1](#)]
- 13 **Finkel Y, Mizrahi O, Nachshon A, Weingarten-Gabbay S, Morgenstern D, Yahalom-Ronen Y, Tamir H, Achdout H, Stein D, Israeli O, Beth-Din A, Melamed S, Weiss S, Israely T, Paran N, Schwartz M, Stern-Ginossar N.** The coding capacity of SARS-CoV-2. *Nature* 2021; **589**: 125-130 [PMID: [32906143](#) DOI: [10.1038/s41586-020-2739-1](#)]
- 14 **Wu F, Zhao S, Yu B, Chen YM, Wang W, Song ZG, Hu Y, Tao ZW, Tian JH, Pei YY, Yuan ML, Zhang YL, Dai FH, Liu Y, Wang QM, Zheng JJ, Xu L, Holmes EC, Zhang YZ.** A new coronavirus associated with human respiratory disease in China. *Nature* 2020; **579**: 265-269 [PMID: [32015508](#) DOI: [10.1038/s41586-020-2008-3](#)]
- 15 **Srinivasan S, Cui H, Gao Z, Liu M, Lu S, Mkwandire W, Narykov O, Sun M, Korkin D.** Structural Genomics of SARS-CoV-2 Indicates Evolutionary Conserved Functional Regions of Viral Proteins.

- Viruses* 2020; **12** [PMID: [32218151](#) DOI: [10.3390/v12040360](#)]
- 16 **Zhou P**, Yang XL, Wang XG, Hu B, Zhang L, Zhang W, Si HR, Zhu Y, Li B, Huang CL, Chen HD, Chen J, Luo Y, Guo H, Jiang RD, Liu MQ, Chen Y, Shen XR, Wang X, Zheng XS, Zhao K, Chen QJ, Deng F, Liu LL, Yan B, Zhan FX, Wang YY, Xiao GF, Shi ZL. A pneumonia outbreak associated with a new coronavirus of probable bat origin. *Nature* 2020; **579**: 270-273 [PMID: [32015507](#) DOI: [10.1038/s41586-020-2012-7](#)]
  - 17 **Hoffmann M**, Kleine-Weber H, Schroeder S, Krüger N, Herrler T, Erichsen S, Schiergens TS, Herrler G, Wu NH, Nitsche A, Müller MA, Drosten C, Pöhlmann S. SARS-CoV-2 Cell Entry Depends on ACE2 and TMPRSS2 and Is Blocked by a Clinically Proven Protease Inhibitor. *Cell* 2020; **181**: 271-280. e8 [PMID: [32142651](#) DOI: [10.1016/j.cell.2020.02.052](#)]
  - 18 **Bosch BJ**, van der Zee R, de Haan CA, Rottier PJ. The coronavirus spike protein is a class I virus fusion protein: structural and functional characterization of the fusion core complex. *J Virol* 2003; **77**: 8801-8811 [PMID: [12885899](#) DOI: [10.1128/JVI.77.16.8801-8811.2003](#)]
  - 19 **Letko M**, Marzi A, Munster V. Functional assessment of cell entry and receptor usage for SARS-CoV-2 and other lineage B betacoronaviruses. *Nat Microbiol* 2020; **5**: 562-569 [PMID: [32094589](#) DOI: [10.1038/s41564-020-0688-y](#)]
  - 20 **Zang R**, Gomez Castro MF, McCune BT, Zeng Q, Rothlauf PW, Sonnek NM, Liu Z, Brulois KF, Wang X, Greenberg HB, Diamond MS, Ciorba MA, Whelan SPJ, Ding S. TMPRSS2 and TMPRSS4 promote SARS-CoV-2 infection of human small intestinal enterocytes. *Sci Immunol* 2020; **5** [PMID: [32404436](#) DOI: [10.1126/sciimmunol.abc3582](#)]
  - 21 **Wruck W**, Adjaye J. SARS-CoV-2 receptor ACE2 is co-expressed with genes related to transmembrane serine proteases, viral entry, immunity and cellular stress. *Sci Rep* 2020; **10**: 21415 [PMID: [33293627](#) DOI: [10.1038/s41598-020-78402-2](#)]
  - 22 **Hussain M**, Jabeen N, Amanullah A, Baig AA, Aziz B, Shabbir S, Raza F, Uddin N. Molecular docking between human TMPRSS2 and SARS-CoV-2 spike protein: conformation and intermolecular interactions. *AIMS Microbiol* 2020; **6**: 350-360 [PMID: [33029570](#) DOI: [10.3934/microbiol.2020021](#)]
  - 23 **Walls AC**, Park YJ, Tortorici MA, Wall A, McGuire AT, Veasley D. Structure, Function, and Antigenicity of the SARS-CoV-2 Spike Glycoprotein. *Cell* 2020; **181**: 281-292. e6 [PMID: [32155444](#) DOI: [10.1016/j.cell.2020.02.058](#)]
  - 24 **Belouzard S**, Madu I, Whittaker GR. Elastase-mediated activation of the severe acute respiratory syndrome coronavirus spike protein at discrete sites within the S2 domain. *J Biol Chem* 2010; **285**: 22758-22763 [PMID: [20507992](#) DOI: [10.1074/jbc.M110.103275](#)]
  - 25 **Ou X**, Liu Y, Lei X, Li P, Mi D, Ren L, Guo L, Guo R, Chen T, Hu J, Xiang Z, Mu Z, Chen X, Chen J, Hu K, Jin Q, Wang J, Qian Z. Characterization of spike glycoprotein of SARS-CoV-2 on virus entry and its immune cross-reactivity with SARS-CoV. *Nat Commun* 2020; **11**: 1620 [PMID: [32221306](#) DOI: [10.1038/s41467-020-15562-9](#)]
  - 26 **Du L**, Kao RY, Zhou Y, He Y, Zhao G, Wong C, Jiang S, Yuen KY, Jin DY, Zheng BJ. Cleavage of spike protein of SARS coronavirus by protease factor Xa is associated with viral infectivity. *Biochem Biophys Res Commun* 2007; **359**: 174-179 [PMID: [17533109](#) DOI: [10.1016/j.bbrc.2007.05.092](#)]
  - 27 **Ji HL**, Zhao R, Matalon S, Matthay MA. Elevated Plasmin(ogen) as a Common Risk Factor for COVID-19 Susceptibility. *Physiol Rev* 2020; **100**: 1065-1075 [PMID: [32216698](#) DOI: [10.1152/physrev.00013.2020](#)]
  - 28 **Gao Y**, Yan L, Huang Y, Liu F, Zhao Y, Cao L, Wang T, Sun Q, Ming Z, Zhang L, Ge J, Zheng L, Zhang Y, Wang H, Zhu Y, Zhu C, Hu T, Hua T, Zhang B, Yang X, Li J, Yang H, Liu Z, Xu W, Guddat LW, Wang Q, Lou Z, Rao Z. Structure of the RNA-dependent RNA polymerase from COVID-19 virus. *Science* 2020; **368**: 779-782 [PMID: [32277040](#) DOI: [10.1126/science.abb7498](#)]
  - 29 **Wang Q**, Wu J, Wang H, Gao Y, Liu Q, Mu A, Ji W, Yan L, Zhu Y, Zhu C, Fang X, Yang X, Huang Y, Gao H, Liu F, Ge J, Sun Q, Xu W, Liu Z, Yang H, Lou Z, Jiang B, Guddat LW, Gong P, Rao Z. Structural Basis for RNA Replication by the SARS-CoV-2 Polymerase. *Cell* 2020; **182**: 417-428. e13 [PMID: [32526208](#) DOI: [10.1016/j.cell.2020.05.034](#)]
  - 30 **Mendonça L**, Howe A, Gilchrist JB, Sun D, Knight ML, Zanetti-Domingues LC, Bateman B, Krebs AS, Chen L, Radecke J, Sheng Y, Li VD, Ni T, Kounatidis I, Koronfel MA, Szykiewicz M, Harkiolaki M, Martin-Fernandez ML, James W, Zhang P. SARS-CoV-2 Assembly and Egress Pathway Revealed by Correlative Multi-modal Multi-scale Cryo-imaging. *bioRxiv* 2020 [PMID: [33173874](#) DOI: [10.1101/2020.11.05.370239](#)]
  - 31 **Klein S**, Cortese M, Winter SL, Wachsmuth-Melm M, Neufeldt CJ, Cerikan B, Stanifer ML, Boulant S, Bartenschlager R, Chlanda P. SARS-CoV-2 structure and replication characterized by in situ cryo-electron tomography. *Nat Commun* 2020; **11**: 5885 [PMID: [33208793](#) DOI: [10.1038/s41467-020-19619-7](#)]
  - 32 **Bouhaddou M**, Memon D, Meyer B, White KM, Rezelj VV, Correa Marrero M, Polacco BJ, Melnyk JE, Ulferts S, Kaake RM, Batra J, Richards AL, Stevenson E, Gordon DE, Rojic A, Obernier K, Fabius JM, Soucheray M, Miorin L, Moreno E, Koh C, Tran QD, Hardy A, Robinot R, Vallet T, Nilsson-Payant BE, Hernandez-Armenta C, Dunham A, Weigang S, Knerr J, Modak M, Quintero D, Zhou Y, Dugourd A, Valdeolivas A, Patil T, Li Q, Hüttenhain R, Cakir M, Muralidharan M, Kim M, Jang G, Tutuncuoglu B, Hiatt J, Guo JZ, Xu J, Bouhaddou S, Mathy CJP, Gaulton A, Manners EJ, Félix E, Shi Y, Goff M, Lim JK, McBride T, O'Neal MC, Cai Y, Chang JCI, Broadhurst DJ, Klippsten S, De Wit E, Leach AR, Kortemme T, Shoichet B, Ott M, Saez-Rodriguez J, tenOever

- BR, Mullins RD, Fischer ER, Kochs G, Grosse R, García-Sastre A, Vignuzzi M, Johnson JR, Shokat KM, Swaney DL, Beltrao P, Krogan NJ. The Global Phosphorylation Landscape of SARS-CoV-2 Infection. *Cell* 2020; **182**: 685-712. e19 [PMID: 32645325 DOI: 10.1016/j.cell.2020.06.034]
- 33 **Cavalli E**, Petralia MC, Basile MS, Bramanti A, Bramanti P, Nicoletti F, Spandidos DA, Shoenfeld Y, Fagone P. Transcriptomic analysis of COVID19 Lungs and bronchoalveolar lavage fluid samples reveals predominant B cell activation responses to infection. *Int J Mol Med* 2020; **46**: 1266-1273 [PMID: 32945352 DOI: 10.3892/ijmm.2020.4702]
- 34 **Ehrlich A**, Uhl S, Ioannidis K, Hofree M. The SARS-CoV-2 transcriptional metabolic signature in lung epithelium. *SSRN* 2020 [DOI: 10.2139/ssrn.3650499]
- 35 **Fagone P**, Ciurleo R, Lombardo SD, Iacobello C, Palermo CI, Shoenfeld Y, Bendtzen K, Bramanti P, Nicoletti F. Transcriptional landscape of SARS-CoV-2 infection dismantles pathogenic pathways activated by the virus, proposes unique sex-specific differences and predicts tailored therapeutic strategies. *Autoimmun Rev* 2020; **19**: 102571 [PMID: 32376402 DOI: 10.1016/j.autrev.2020.102571]
- 36 **Gordon DE**, Jang GM, Bouhaddou M, Xu J, Obernier K, White KM, O'Meara MJ, Rezelj VV, Guo JZ, Swaney DL, Tummino TA, Hüttenhain R, Kaake RM, Richards AL, Tutuncuoglu B, Foussard H, Batra J, Haas K, Modak M, Kim M, Haas P, Polacco BJ, Braberg H, Fabius JM, Eckhardt M, Soucheray M, Bennett MJ, Cakir M, McGregor MJ, Li Q, Meyer B, Roesch F, Vallet T, Mac Kain A, Miorin L, Moreno E, Naing ZZC, Zhou Y, Peng S, Shi Y, Zhang Z, Shen W, Kirby IT, Melnyk JE, Chorba JS, Lou K, Dai SA, Barrio-Hernandez I, Memon D, Hernandez-Armenta C, Lyu J, Mathy CJP, Perica T, Pilla KB, Ganesan SJ, Saltzberg DJ, Rakesh R, Liu X, Rosenthal SB, Calviello L, Venkataramanan S, Liboy-Lugo J, Lin Y, Huang XP, Liu Y, Huang XP, Wankowicz SA, Bohn M, Safari M, Ugur FS, Koh C, Savar NS, Tran QD, Shengjuler D, Fletcher SJ, O'Neal MC, Cai Y, Chang JCI, Broadhurst DJ, Klippsten S, Sharp PP, Wenzell NA, Kuzuoglu-Ozturk D, Wang HY, Trenker R, Young JM, Cavero DA, Hiatt J, Roth TL, Rathore U, Subramanian A, Noack J, Hubert M, Stroud RM, Frankel AD, Rosenberg OS, Verba KA, Agard DA, Ott M, Emerman M, Jura N, von Zastrow M, Verdin E, Ashworth A, Schwartz O, d'Enfert C, Mukherjee S, Jacobson M, Malik HS, Fujimori DG, Ideker T, Craik CS, Floor SN, Fraser JS, Gross JD, Sali A, Roth BL, Ruggero D, Taunton J, Kortemme T, Beltrao P, Vignuzzi M, García-Sastre A, Shokat KM, Shoichet BK, Krogan NJ. A SARS-CoV-2 protein interaction map reveals targets for drug repurposing. *Nature* 2020; **583**: 459-468 [PMID: 32353859 DOI: 10.1038/s41586-020-2286-9]
- 37 **Hadjadj J**, Yatim N, Barnabei L, Corneau A, Boussier J, Smith N, Péré H, Charbit B, Bondet V, Chenevier-Gobeaux C, Breillat P, Carlier N, Gauzit R, Morbieu C, Pène F, Marin N, Roche N, Szwebel TA, Merklings SH, Treluyer JM, Veyer D, Mouthon L, Blanc C, Tharaux PL, Rozenberg F, Fischer A, Duffy D, Rieux-Laucat F, Kernéis S, Terrier B. Impaired type I interferon activity and inflammatory responses in severe COVID-19 patients. *Science* 2020; **369**: 718-724 [PMID: 32661059 DOI: 10.1126/science.abc6027]
- 38 **Wang J**, Jiang M, Chen X, Montaner LJ. Cytokine storm and leukocyte changes in mild vs severe SARS-CoV-2 infection: Review of 3939 COVID-19 patients in China and emerging pathogenesis and therapy concepts. *J Leukoc Biol* 2020; **108**: 17-41 [PMID: 32534467 DOI: 10.1002/JLB.3COVR0520-272R]
- 39 **Huang C**, Wang Y, Li X, Ren L, Zhao J, Hu Y, Zhang L, Fan G, Xu J, Gu X, Cheng Z, Yu T, Xia J, Wei Y, Wu W, Xie X, Yin W, Li H, Liu M, Xiao Y, Gao H, Guo L, Xie J, Wang G, Jiang R, Gao Z, Jin Q, Wang J, Cao B. Clinical features of patients infected with 2019 novel coronavirus in Wuhan, China. *Lancet* 2020; **395**: 497-506 [PMID: 31986264 DOI: 10.1016/S0140-6736(20)30183-5]
- 40 **Chen G**, Wu D, Guo W, Cao Y, Huang D, Wang H, Wang T, Zhang X, Chen H, Yu H, Zhang M, Wu S, Song J, Chen T, Han M, Li S, Luo X, Zhao J, Ning Q. Clinical and immunological features of severe and moderate coronavirus disease 2019. *J Clin Invest* 2020; **130**: 2620-2629 [PMID: 32217835 DOI: 10.1172/JCI137244]
- 41 **Xiong Y**, Liu Y, Cao L, Wang D, Guo M, Jiang A, Guo D, Hu W, Yang J, Tang Z, Wu H, Lin Y, Zhang M, Zhang Q, Shi M, Zhou Y, Lan K, Chen Y. Transcriptomic characteristics of bronchoalveolar lavage fluid and peripheral blood mononuclear cells in COVID-19 patients. *Emerg Microbes Infect* 2020; **9**: 761-770 [PMID: 32228226 DOI: 10.1080/22221751.2020.1747363]
- 42 **Blanco-Melo D**, Nilsson-Payant BE, Liu WC, Uhl S, Hoagland D, Möller R, Jordan TX, Oishi K, Panis M, Sachs D, Wang TT, Schwartz RE, Lim JK, Albrecht RA, tenOever BR. Imbalanced Host Response to SARS-CoV-2 Drives Development of COVID-19. *Cell* 2020; **181**: 1036-1045. e9 [PMID: 32416070 DOI: 10.1016/j.cell.2020.04.026]
- 43 **Galani IE**, Rovina N, Lampropoulou V, Triantafyllia V, Manioudaki M, Pavlos E, Koukaki E, Fragkou PC, Panou V, Rapti V, Koltsida O, Mentis A, Koulouris N, Tsiodras S, Koutsoukou A, Andreaskos E. Untuned antiviral immunity in COVID-19 revealed by temporal type I/III interferon patterns and flu comparison. *Nat Immunol* 2021; **22**: 32-40 [PMID: 33277638 DOI: 10.1038/s41590-020-00840-x]
- 44 **Theobald SJ**, Simonis A, Kreer C, Zehner M, Fischer J, Albert M-C, Malin JJ, Gräß J, Winter S, Silva US de, Böll B, Köhler P, Gruell H, Suárez I, Hallek M, Fätkenheuer G, Jung N, Cornely O, Lehmann C, Kashkar H, Klein F, Rybniker J. The SARS-CoV-2 spike protein primes inflammasome-mediated interleukin-1-beta secretion in COVID-19 patient-derived macrophages. *Res Sq* 2020 [DOI: 10.21203/rs.3.rs-30407/v1]
- 45 **Zhu N**, Wang W, Liu Z, Liang C, Ye F, Huang B, Zhao L, Wang H, Zhou W, Deng Y, Mao L, Su C, Qiang G, Jiang T, Zhao J, Wu G, Song J, Tan W. Morphogenesis and cytopathic effect of SARS-CoV-2 infection in human airway epithelial cells. *Nat Commun* 2020; **11**: 3910 [PMID: 32764693]

- DOI: [10.1038/s41467-020-17796-z](https://doi.org/10.1038/s41467-020-17796-z)]
- 46 **Xu H**, Chitre SA, Akinyemi IA, Loeb JC, Lednický JA, McIntosh MT, Bhaduri-McIntosh S. SARS-CoV-2 viroporin triggers the NLRP3 inflammatory pathway. 2020 Preprint. Available from: [bioRxiv:2020.10.27.357731](https://doi.org/10.1101/2020.10.27.357731) [DOI: [10.1101/2020.10.27.357731](https://doi.org/10.1101/2020.10.27.357731)]
  - 47 **Li S**, Zhang Y, Guan Z, Li H, Ye M, Chen X, Shen J, Zhou Y, Shi ZL, Zhou P, Peng K. SARS-CoV-2 triggers inflammatory responses and cell death through caspase-8 activation. *Signal Transduct Target Ther* 2020; **5**: 235 [PMID: [33037188](https://pubmed.ncbi.nlm.nih.gov/33037188/) DOI: [10.1038/s41392-020-00334-0](https://doi.org/10.1038/s41392-020-00334-0)]
  - 48 **Qu Y**, Wang X, Zhu Y, Wang Y, Yang X, Hu G, Liu C, Li J, Ren S, Xiao Z, Liu Z, Wang W, Li P, Zhang R, Liang Q. ORF3a mediated-incomplete autophagy facilitates SARS-CoV-2 replication. 2020 Preprint. Available from: [bioRxiv:2020.11.12.380709](https://doi.org/10.1101/2020.11.12.380709) [DOI: [10.1101/2020.11.12.380709](https://doi.org/10.1101/2020.11.12.380709)]
  - 49 **Ramachandran P**, Onukogu I, Ghanta S, Gajendran M, Perisetti A, Goyal H, Aggarwal A. Gastrointestinal Symptoms and Outcomes in Hospitalized Coronavirus Disease 2019 Patients. *Dig Dis* 2020; **38**: 373-379 [PMID: [32599601](https://pubmed.ncbi.nlm.nih.gov/32599601/) DOI: [10.1159/000509774](https://doi.org/10.1159/000509774)]
  - 50 **Guan WJ**, Ni ZY, Hu Y, Liang WH, Ou CQ, He JX, Liu L, Shan H, Lei CL, Hui DSC, Du B, Li LJ, Zeng G, Yuen KY, Chen RC, Tang CL, Wang T, Chen PY, Xiang J, Li SY, Wang JL, Liang ZJ, Peng YX, Wei L, Liu Y, Hu YH, Peng P, Wang JM, Liu JY, Chen Z, Li G, Zheng ZJ, Qiu SQ, Luo J, Ye CJ, Zhu SY, Zhong NS; China Medical Treatment Expert Group for Covid-19. Clinical Characteristics of Coronavirus Disease 2019 in China. *N Engl J Med* 2020; **382**: 1708-1720 [PMID: [32109013](https://pubmed.ncbi.nlm.nih.gov/32109013/) DOI: [10.1056/NEJMoa2002032](https://doi.org/10.1056/NEJMoa2002032)]
  - 51 **Li LQ**, Huang T, Wang YQ, Wang ZP, Liang Y, Huang TB, Zhang HY, Sun W, Wang Y. COVID-19 patients' clinical characteristics, discharge rate, and fatality rate of meta-analysis. *J Med Virol* 2020; **92**: 577-583 [PMID: [32162702](https://pubmed.ncbi.nlm.nih.gov/32162702/) DOI: [10.1002/jmv.25757](https://doi.org/10.1002/jmv.25757)]
  - 52 **Jin X**, Lian JS, Hu JH, Gao J, Zheng L, Zhang YM, Hao SR, Jia HY, Cai H, Zhang XL, Yu GD, Xu KJ, Wang XY, Gu JQ, Zhang SY, Ye CY, Jin CL, Lu YF, Yu X, Yu XP, Huang JR, Xu KL, Ni Q, Yu CB, Zhu B, Li YT, Liu J, Zhao H, Zhang X, Yu L, Guo YZ, Su JW, Tao JJ, Lang GJ, Wu XX, Wu WR, Qv TT, Xiang DR, Yi P, Shi D, Chen Y, Ren Y, Qiu YQ, Li LJ, Sheng J, Yang Y. Epidemiological, clinical and virological characteristics of 74 cases of coronavirus-infected disease 2019 (COVID-19) with gastrointestinal symptoms. *Gut* 2020; **69**: 1002-1009 [PMID: [32213556](https://pubmed.ncbi.nlm.nih.gov/32213556/) DOI: [10.1136/gutjnl-2020-320926](https://doi.org/10.1136/gutjnl-2020-320926)]
  - 53 **Fang D**, Ma J, Guan J, Wang M, Song Y, Tian D, Li P. Manifestations of Digestive system in hospitalized patients with novel coronavirus pneumonia in Wuhan, China: a single-center, descriptive study. *Zhonghua Xiaohua Zazhi* 2020; **40**: E005-E005 [DOI: [10.3760/cma.j.issn.0254-1432.2020.0005](https://doi.org/10.3760/cma.j.issn.0254-1432.2020.0005)]
  - 54 **Xiao F**, Tang M, Zheng X, Liu Y, Li X, Shan H. Evidence for Gastrointestinal Infection of SARS-CoV-2. *Gastroenterology* 2020; **158**: 1831-1833. e3 [PMID: [32142773](https://pubmed.ncbi.nlm.nih.gov/32142773/) DOI: [10.1053/j.gastro.2020.02.055](https://doi.org/10.1053/j.gastro.2020.02.055)]
  - 55 **Parasa S**, Desai M, Thoguluva Chandrasekar V, Patel HK, Kennedy KF, Roesch T, Spadaccini M, Colombo M, Gabbiadini R, Artifon ELA, Repici A, Sharma P. Prevalence of Gastrointestinal Symptoms and Fecal Viral Shedding in Patients With Coronavirus Disease 2019: A Systematic Review and Meta-analysis. *JAMA Netw Open* 2020; **3**: e2011335 [PMID: [32525549](https://pubmed.ncbi.nlm.nih.gov/32525549/) DOI: [10.1001/jamanetworkopen.2020.11335](https://doi.org/10.1001/jamanetworkopen.2020.11335)]
  - 56 **Galanopoulos M**, Gkeros F, Doukatas A, Karianakis G, Pontas C, Tsoukalas N, Viazis N, Liatsos C, Mantzaris GJ. COVID-19 pandemic: Pathophysiology and manifestations from the gastrointestinal tract. *World J Gastroenterol* 2020; **26**: 4579-4588 [PMID: [32884218](https://pubmed.ncbi.nlm.nih.gov/32884218/) DOI: [10.3748/wjg.v26.i31.4579](https://doi.org/10.3748/wjg.v26.i31.4579)]
  - 57 **Wang D**, Hu B, Hu C, Zhu F, Liu X, Zhang J, Wang B, Xiang H, Cheng Z, Xiong Y, Zhao Y, Li Y, Wang X, Peng Z. Clinical Characteristics of 138 Hospitalized Patients With 2019 Novel Coronavirus-Infected Pneumonia in Wuhan, China. *JAMA* 2020; **323**: 1061-1069 [PMID: [32031570](https://pubmed.ncbi.nlm.nih.gov/32031570/) DOI: [10.1001/jama.2020.1585](https://doi.org/10.1001/jama.2020.1585)]
  - 58 **Han C**, Duan C, Zhang S, Spiegel B, Shi H, Wang W, Zhang L, Lin R, Liu J, Ding Z, Hou X. Digestive Symptoms in COVID-19 Patients With Mild Disease Severity: Clinical Presentation, Stool Viral RNA Testing, and Outcomes. *Am J Gastroenterol* 2020; **115**: 916-923 [PMID: [32301761](https://pubmed.ncbi.nlm.nih.gov/32301761/) DOI: [10.14309/ajg.0000000000000664](https://doi.org/10.14309/ajg.0000000000000664)]
  - 59 **Pan L**, Mu M, Yang P, Sun Y, Wang R, Yan J, Li P, Hu B, Wang J, Hu C, Jin Y, Niu X, Ping R, Du Y, Li T, Xu G, Hu Q, Tu L. Clinical Characteristics of COVID-19 Patients With Digestive Symptoms in Hubei, China: A Descriptive, Cross-Sectional, Multicenter Study. *Am J Gastroenterol* 2020; **115**: 766-773 [PMID: [32287140](https://pubmed.ncbi.nlm.nih.gov/32287140/) DOI: [10.14309/ajg.0000000000000620](https://doi.org/10.14309/ajg.0000000000000620)]
  - 60 **Redd WD**, Zhou JC, Hathorn KE, McCarty TR, Bazarbashi AN, Thompson CC, Shen L, Chan WW. Prevalence and Characteristics of Gastrointestinal Symptoms in Patients With Severe Acute Respiratory Syndrome Coronavirus 2 Infection in the United States: A Multicenter Cohort Study. *Gastroenterology* 2020; **159**: 765-767. e2 [PMID: [32333911](https://pubmed.ncbi.nlm.nih.gov/32333911/) DOI: [10.1053/j.gastro.2020.04.045](https://doi.org/10.1053/j.gastro.2020.04.045)]
  - 61 **Chen N**, Zhou M, Dong X, Qu J, Gong F, Han Y, Qiu Y, Wang J, Liu Y, Wei Y, Xia J, Yu T, Zhang X, Zhang L. Epidemiological and clinical characteristics of 99 cases of 2019 novel coronavirus pneumonia in Wuhan, China: a descriptive study. *Lancet* 2020; **395**: 507-513 [PMID: [32007143](https://pubmed.ncbi.nlm.nih.gov/32007143/) DOI: [10.1016/S0140-6736\(20\)30211-7](https://doi.org/10.1016/S0140-6736(20)30211-7)]
  - 62 **Mo P**, Xing Y, Xiao Y, Deng L, Zhao Q, Wang H, Xiong Y, Cheng Z, Gao S, Liang K, Luo M, Chen T, Song S, Ma Z, Chen X, Zheng R, Cao Q, Wang F, Zhang Y. Clinical characteristics of refractory COVID-19 pneumonia in Wuhan, China. *Clin Infect Dis* 2020 [PMID: [32173725](https://pubmed.ncbi.nlm.nih.gov/32173725/) DOI: [10.1093/cid/ciaa270](https://doi.org/10.1093/cid/ciaa270)]

- 63 **Leung WK**, To KF, Chan PK, Chan HL, Wu AK, Lee N, Yuen KY, Sung JJ. Enteric involvement of severe acute respiratory syndrome-associated coronavirus infection. *Gastroenterology* 2003; **125**: 1011-1017 [PMID: [14517783](#) DOI: [10.1016/j.gastro.2003.08.001](#)]
- 64 **Carvalho A**, Alqusairi R, Adams A, Paul M, Kothari N, Peters S, DeBenedet AT. SARS-CoV-2 Gastrointestinal Infection Causing Hemorrhagic Colitis: Implications for Detection and Transmission of COVID-19 Disease. *Am J Gastroenterol* 2020; **115**: 942-946 [PMID: [32496741](#) DOI: [10.14309/ajg.0000000000000667](#)]
- 65 **Pan Y**, Zhang D, Yang P, Poon LLM, Wang Q. Viral load of SARS-CoV-2 in clinical samples. *Lancet Infect Dis* 2020; **20**: 411-412 [PMID: [32105638](#) DOI: [10.1016/S1473-3099\(20\)30113-4](#)]
- 66 **Young BE**, Ong SWX, Kalimuddin S, Low JG, Tan SY, Loh J, Ng OT, Marimuthu K, Ang LW, Mak TM, Lau SK, Anderson DE, Chan KS, Tan TY, Ng TY, Cui L, Said Z, Kurupatham L, Chen MI, Chan M, Vasoo S, Wang LF, Tan BH, Lin RTP, Lee VJM, Leo YS, Lye DC; Singapore 2019 Novel Coronavirus Outbreak Research Team. Epidemiologic Features and Clinical Course of Patients Infected With SARS-CoV-2 in Singapore. *JAMA* 2020; **323**: 1488-1494 [PMID: [32125362](#) DOI: [10.1001/jama.2020.3204](#)]
- 67 **Peng L**, Liu J, Xu W, Luo Q, Chen D, Lei Z, Huang Z, Li X, Deng K, Lin B, Gao Z. SARS-CoV-2 can be detected in urine, blood, anal swabs, and oropharyngeal swabs specimens. *J Med Virol* 2020; **92**: 1676-1680 [PMID: [32330305](#) DOI: [10.1002/jmv.25936](#)]
- 68 **Wu Y**, Guo C, Tang L, Hong Z, Zhou J, Dong X, Yin H, Xiao Q, Tang Y, Qu X, Kuang L, Fang X, Mishra N, Lu J, Shan H, Jiang G, Huang X. Prolonged presence of SARS-CoV-2 viral RNA in faecal samples. *Lancet Gastroenterol Hepatol* 2020; **5**: 434-435 [PMID: [32199469](#) DOI: [10.1016/S2468-1253\(20\)30083-2](#)]
- 69 **Chen Y**, Chen L, Deng Q, Zhang G, Wu K, Ni L, Yang Y, Liu B, Wang W, Wei C, Yang J, Ye G, Cheng Z. The presence of SARS-CoV-2 RNA in the feces of COVID-19 patients. *J Med Virol* 2020; **92**: 833-840 [PMID: [32243607](#) DOI: [10.1002/jmv.25825](#)]
- 70 **Ling Y**, Xu SB, Lin YX, Tian D, Zhu ZQ, Dai FH, Wu F, Song ZG, Huang W, Chen J, Hu BJ, Wang S, Mao EQ, Zhu L, Zhang WH, Lu HZ. Persistence and clearance of viral RNA in 2019 novel coronavirus disease rehabilitation patients. *Chin Med J (Engl)* 2020; **133**: 1039-1043 [PMID: [32118639](#) DOI: [10.1097/CM9.0000000000000774](#)]
- 71 **Hikmet F**, Méar L, Edvinsson Å, Micke P, Uhlén M, Lindskog C. The protein expression profile of ACE2 in human tissues. *Mol Syst Biol* 2020; **16**: e9610 [PMID: [32715618](#) DOI: [10.15252/msb.20209610](#)]
- 72 **Zou X**, Chen K, Zou J, Han P, Hao J, Han Z. Single-cell RNA-seq data analysis on the receptor ACE2 expression reveals the potential risk of different human organs vulnerable to 2019-nCoV infection. *Front Med* 2020; **14**: 185-192 [PMID: [32170560](#) DOI: [10.1007/s11684-020-0754-0](#)]
- 73 **Zhang H**, Kang Z, Gong H, Xu D, Wang J, Li Z, Cui X, Xiao J, Zhan J, Meng T, Zhou W, Liu J, Xu H. Digestive system is a potential route of COVID-19: an analysis of single-cell coexpression pattern of key proteins in viral entry process. *Gut* 2020; **69**: 1010-1018 [DOI: [10.1136/gutjnl-2020-320953](#)]
- 74 **Bar-On YM**, Flamholz A, Phillips R, Milo R. SARS-CoV-2 (COVID-19) by the numbers. *Elife* 2020; **9** [PMID: [32228860](#) DOI: [10.7554/eLife.57309](#)]
- 75 **Sender R**, Bar-On YM, Flamholz A, Gleizer S, Bernsthein B, Phillips R, Milo R. The total number and mass of SARS-CoV-2 virions in an infected person. *medRxiv* 2020 [PMID: [33236021](#) DOI: [10.1101/2020.11.16.20232009](#)]
- 76 **Lamers MM**, Beumer J, van der Vaart J, Knoops K, Puschhof J, Breugem TI, Ravelli RBG, Paul van Schayck J, Mykytyn AZ, Duimel HQ, van Donselaar E, Riesebosch S, Kuijpers HJH, Schipper D, van de Wetering WJ, de Graaf M, Koopmans M, Cuppen E, Peters PJ, Haagmans BL, Clevers H. SARS-CoV-2 productively infects human gut enterocytes. *Science* 2020; **369**: 50-54 [PMID: [32358202](#) DOI: [10.1126/science.abc1669](#)]
- 77 **Bradley BT**, Maioli H, Johnston R, Chaudhry I, Fink SL, Xu H, Najafian B, Deutsch G, Lacy JM, Williams T, Yarid N, Marshall DA. Histopathology and ultrastructural findings of fatal COVID-19 infections in Washington State: a case series. *Lancet* 2020; **396**: 320-332 [PMID: [32682491](#) DOI: [10.1016/S0140-6736\(20\)31305-2](#)]
- 78 **Xiao F**, Sun J, Xu Y, Li F, Huang X, Li H, Zhao J, Huang J. Infectious SARS-CoV-2 in Feces of Patient with Severe COVID-19. *Emerg Infect Dis* 2020; **26**: 1920-1922 [PMID: [32421494](#) DOI: [10.3201/eid2608.200681](#)]
- 79 **Wurtz N**, Penant G, Jardot P, Duclos N, La Scola B. Culture of SARS-CoV-2 in a panel of laboratory cell lines, permissivity, and differences in growth profile. *Eur J Clin Microbiol Infect Dis* 2021; **40**: 477-484 [PMID: [33389257](#) DOI: [10.1007/s10096-020-04106-0](#)]
- 80 **Chu H**, Chan JF, Wang Y, Yuen TT, Chai Y, Shuai H, Yang D, Hu B, Huang X, Zhang X, Hou Y, Cai JP, Zhang AJ, Zhou J, Yuan S, To KK, Hung IF, Cheung TT, Ng AT, Hau-Yee Chan I, Wong IY, Law SY, Foo DC, Leung WK, Yuen KY. SARS-CoV-2 Induces a More Robust Innate Immune Response and Replicates Less Efficiently Than SARS-CoV in the Human Intestines: An Ex Vivo Study With Implications on Pathogenesis of COVID-19. *Cell Mol Gastroenterol Hepatol* 2021; **11**: 771-781 [PMID: [33010495](#) DOI: [10.1016/j.jcmgh.2020.09.017](#)]
- 81 **Lee S**, Yoon GY, Myoung J, Kim SJ, Ahn DG. Robust and persistent SARS-CoV-2 infection in the human intestinal brush border expressing cells. *Emerg Microbes Infect* 2020; **9**: 2169-2179 [PMID: [32969768](#) DOI: [10.1080/22221751.2020.1827985](#)]
- 82 **De Maio F**, Lo Cascio E, Babini G, Sali M, Della Longa S, Tilocca B, Roncada P, Arcovito A, Sanguinetti M, Scambia G, Urbani A. Improved binding of SARS-CoV-2 Envelope protein to tight

- junction-associated PALS1 could play a key role in COVID-19 pathogenesis. *Microbes Infect* 2020; **22**: 592-597 [PMID: 32891874 DOI: 10.1016/j.micinf.2020.08.006]
- 83 **Straight SW**, Shin K, Fogg VC, Fan S, Liu CJ, Roh M, Margolis B. Loss of PALS1 expression leads to tight junction and polarity defects. *Mol Biol Cell* 2004; **15**: 1981-1990 [PMID: 14718565 DOI: 10.1091/mbc.E03-08-0620]
- 84 **Guo Y**, Luo R, Wang Y, Deng P, Song T, Zhang M, Wang P, Zhang X, Cui K, Tao T, Li Z, Chen W, Zheng Y, Qin J. SARS-CoV-2 induced intestinal responses with a biomimetic human gut-on-chip. *Sci Bull (Beijing)* 2021; **66**: 783-793 [PMID: 33282445 DOI: 10.1016/j.scib.2020.11.015]
- 85 **Cao Y**, Yang R, Wang W, Lee I, Zhang R, Zhang W, Sun J, Xu B, Meng X. Computational Study of the Ion and Water Permeation and Transport Mechanisms of the SARS-CoV-2 Pentameric E Protein Channel. *Front Mol Biosci* 2020; **7**: 565797 [PMID: 33173781 DOI: 10.3389/fmolb.2020.565797]
- 86 **Barrett KE**, Keely SJ. Chloride secretion by the intestinal epithelium: molecular basis and regulatory aspects. *Annu Rev Physiol* 2000; **62**: 535-572 [PMID: 10845102 DOI: 10.1146/annurev.physiol.62.1.535]
- 87 **Ren Y**, Shu T, Wu D, Mu J, Wang C, Huang M, Han Y, Zhang XY, Zhou W, Qiu Y, Zhou X. The ORF3a protein of SARS-CoV-2 induces apoptosis in cells. *Cell Mol Immunol* 2020; **17**: 881-883 [PMID: 32555321 DOI: 10.1038/s41423-020-0485-9]
- 88 **Obukhov AG**, Stevens BR, Prasad R, Li Calzi S, Boulton ME, Raizada MK, Oudit GY, Grant MB. SARS-CoV-2 Infections and ACE2: Clinical Outcomes Linked With Increased Morbidity and Mortality in Individuals With Diabetes. *Diabetes* 2020; **69**: 1875-1886 [PMID: 32669391 DOI: 10.2337/dbi20-0019]
- 89 **Xu J**, Xu X, Jiang L, Dua K, Hansbro PM, Liu G. SARS-CoV-2 induces transcriptional signatures in human lung epithelial cells that promote lung fibrosis. *Respir Res* 2020; **21**: 182 [PMID: 32664949 DOI: 10.1186/s12931-020-01445-6]
- 90 **Jia HP**, Look DC, Tan P, Shi L, Hickey M, Gakhar L, Chappell MC, Wohlford-Lenane C, McCray PB Jr. Ectodomain shedding of angiotensin converting enzyme 2 in human airway epithelia. *Am J Physiol Lung Cell Mol Physiol* 2009; **297**: L84-L96 [PMID: 19411314 DOI: 10.1152/ajplung.00071.2009]
- 91 **Andring JT**, McKenna R, Stevens BR. Amino acid transporter B0AT1 influence on ADAM17 interactions with SARS-CoV-2 receptor ACE2 putatively expressed in intestine, kidney, and cardiomyocytes. 2020 Preprint. Available from: bioRxiv: 2020.10.30.361873 [DOI: 10.1101/2020.10.30.361873]
- 92 **Deretic V**, Saitoh T, Akira S. Autophagy in infection, inflammation and immunity. *Nat Rev Immunol* 2013; **13**: 722-737 [PMID: 24064518 DOI: 10.1038/nri3532]
- 93 **Sarkar S**. Regulation of autophagy by mTOR-dependent and mTOR-independent pathways: autophagy dysfunction in neurodegenerative diseases and therapeutic application of autophagy enhancers. *Biochem Soc Trans* 2013; **41**: 1103-1130 [PMID: 24059496 DOI: 10.1042/BST20130134]
- 94 **Delorme-Axford E**, Klionsky DJ. Highlights in the fight against COVID-19: does autophagy play a role in SARS-CoV-2 infection? *Autophagy* 2020; **16**: 2123-2127 [PMID: 33153403 DOI: 10.1080/15548627.2020.1844940]
- 95 **Shojaei S**, Suresh M, Klionsky DJ, Labouta HI, Ghavami S. Autophagy and SARS-CoV-2 infection: A possible smart targeting of the autophagy pathway. *Virulence* 2020; **11**: 805-810 [PMID: 32567972 DOI: 10.1080/21505594.2020.1780088]
- 96 **Siddiqi HK**, Mehra MR. COVID-19 illness in native and immunosuppressed states: A clinical-therapeutic staging proposal. *J Heart Lung Transplant* 2020; **39**: 405-407 [PMID: 32362390 DOI: 10.1016/j.healun.2020.03.012]
- 97 **Zhang L**, Han C, Zhang S, Duan C, Shang H, Bai T, Hou X. Diarrhea and altered inflammatory cytokine pattern in severe coronavirus disease 2019: Impact on disease course and in-hospital mortality. *J Gastroenterol Hepatol* 2021; **36**: 421-429 [PMID: 32602128 DOI: 10.1111/jgh.15166]
- 98 **Ma TY**, Iwamoto GK, Hoa NT, Akotia V, Pedram A, Boivin MA, Said HM. TNF-alpha-induced increase in intestinal epithelial tight junction permeability requires NF-kappa B activation. *Am J Physiol Gastrointest Liver Physiol* 2004; **286**: G367-G376 [PMID: 14766535 DOI: 10.1152/ajpgi.00173.2003]
- 99 **Al-Sadi R**, Ye D, Boivin M, Guo S, Hashimi M, Ereifej L, Ma TY. Interleukin-6 modulation of intestinal epithelial tight junction permeability is mediated by JNK pathway activation of claudin-2 gene. *PLoS One* 2014; **9**: e85345 [PMID: 24662742 DOI: 10.1371/journal.pone.0085345]
- 100 **Kuhn KA**, Manieri NA, Liu TC, Stappenbeck TS. IL-6 stimulates intestinal epithelial proliferation and repair after injury. *PLoS One* 2014; **9**: e114195 [PMID: 25478789 DOI: 10.1371/journal.pone.0114195]
- 101 **Kühn R**, Löhler J, Rennick D, Rajewsky K, Müller W. Interleukin-10-deficient mice develop chronic enterocolitis. *Cell* 1993; **75**: 263-274 [PMID: 8402911 DOI: 10.1016/0092-8674(93)80068-p]
- 102 **Lorén V**, Cabré E, Ojanguren I, Domènech E, Pedrosa E, García-Jaraquemada A, Mañosa M, Manyé J. Interleukin-10 Enhances the Intestinal Epithelial Barrier in the Presence of Corticosteroids through p38 MAPK Activity in Caco-2 Monolayers: A Possible Mechanism for Steroid Responsiveness in Ulcerative Colitis. *PLoS One* 2015; **10**: e0130921 [PMID: 26090671 DOI: 10.1371/journal.pone.0130921]
- 103 **Gu S**, Chen Y, Wu Z, Gao H, Lv L, Guo F, Zhang X, Luo R, Huang C, Lu H, Zheng B, Zhang J,

- Yan R, Zhang H, Jiang H, Xu Q, Guo J, Gong Y, Tang L, Li L. Alterations of the Gut Microbiota in Patients With Coronavirus Disease 2019 or H1N1 Influenza. *Clin Infect Dis* 2020; **71**: 2669-2678 [PMID: 32497191 DOI: 10.1093/cid/ciaa709]
- 104 **Zuo T**, Zhang F, Lui GCY, Yeoh YK, Li AYL, Zhan H, Wan Y, Chung ACK, Cheung CP, Chen N, Lai CKC, Chen Z, Tso EYK, Fung KSC, Chan V, Ling L, Joynt G, Hui DSC, Chan FKL, Chan PKS, Ng SC. Alterations in Gut Microbiota of Patients With COVID-19 During Time of Hospitalization. *Gastroenterology* 2020; **159**: 944-955. e8 [PMID: 32442562 DOI: 10.1053/j.gastro.2020.05.048]
- 105 **Mifsud EJ**, Hayden FG, Hurt AC. Antivirals targeting the polymerase complex of influenza viruses. *Antiviral Res* 2019; **169**: 104545 [PMID: 31247246 DOI: 10.1016/j.antiviral.2019.104545]
- 106 **Granata G**, Bartoloni A, Codeluppi M, Contadini I, Cristini F, Fantoni M, Ferraresi A, Fornabai C, Grasselli S, Lagi F, Masucci L, Puoti M, Raimondi A, Taddei E, Trapani FF, Viale P, Johnson S, Petrosillo N; On Behalf Of The CloVid Study Group. The Burden of Clostridioides Difficile Infection during the COVID-19 Pandemic: A Retrospective Case-Control Study in Italian Hospitals (CloVid). *J Clin Med* 2020; **9** [PMID: 33260943 DOI: 10.3390/jcm9123855]
- 107 **Hanna R**, Dalvi S, Sălăgean T, Pop ID, Bordea IR, Benedicenti S. Understanding COVID-19 Pandemic: Molecular Mechanisms and Potential Therapeutic Strategies. An Evidence-Based Review. *J Inflamm Res* 2021; **14**: 13-56 [PMID: 33447071 DOI: 10.2147/JIR.S282213]
- 108 **Gramlich L**, Kichian K, Pinilla J, Rodych NJ, Dhaliwal R, Heyland DK. Does enteral nutrition compared to parenteral nutrition result in better outcomes in critically ill adult patients? *Nutrition* 2004; **20**: 843-848 [PMID: 15474870 DOI: 10.1016/j.nut.2004.06.003]
- 109 **Blumenstein I**, Shastri YM, Stein J. Gastroenteric tube feeding: techniques, problems and solutions. *World J Gastroenterol* 2014; **20**: 8505-8524 [PMID: 25024606 DOI: 10.3748/wjg.v20.i26.8505]
- 110 **Li GF**, An XX, Yu Y, Jiao LR, Canarutto D, Yu G, Wang G, Wu DN, Xiao Y. Do proton pump inhibitors influence SARS-CoV-2 related outcomes? *Gut* 2020 [PMID: 33172925 DOI: 10.1136/gutjnl-2020-323366]
- 111 **Leonard J**, Marshall JK, Moayyedi P. Systematic review of the risk of enteric infection in patients taking acid suppression. *Am J Gastroenterol* 2007; **102**: 2047-56; quiz 2057 [PMID: 17509031 DOI: 10.1111/j.1572-0241.2007.01275.x]
- 112 **Tariq R**, Singh S, Gupta A, Pardi DS, Khanna S. Association of Gastric Acid Suppression With Recurrent Clostridium difficile Infection: A Systematic Review and Meta-analysis. *JAMA Intern Med* 2017; **177**: 784-791 [PMID: 28346595 DOI: 10.1001/jamainternmed.2017.0212]
- 113 **Hafiz RA**, Wong C, Paynter S, David M, Peeters G. The Risk of Community-Acquired Enteric Infection in Proton Pump Inhibitor Therapy: Systematic Review and Meta-analysis. *Ann Pharmacother* 2018; **52**: 613-622 [PMID: 29457492 DOI: 10.1177/1060028018760569]
- 114 **Moayyedi P**, Eikelboom JW, Bosch J, Connolly SJ, Dyal L, Shestakovska O, Leong D, Anand SS, Störk S, Branch KRH, Bhatt DL, Verhamme PB, O'Donnell M, Maggioni AP, Lonn EM, Piegas LS, Ertl G, Keltai M, Bruns NC, Muehlhofer E, Dagenais GR, Kim JH, Hori M, Steg PG, Hart RG, Diaz R, Alings M, Widimsky P, Avezum A, Probstfield J, Zhu J, Liang Y, Lopez-Jaramillo P, Kakkar AK, Parkhomenko AN, Ryden L, Pogossova N, Dans AL, Lanas F, Commerford PJ, Torp-Pedersen C, Guzik TJ, Vinereanu D, Tonkin AM, Lewis BS, Felix C, Yusuf K, Metsarinne KP, Fox KAA, Yusuf S; COMPASS Investigators. Safety of Proton Pump Inhibitors Based on a Large, Multi-Year, Randomized Trial of Patients Receiving Rivaroxaban or Aspirin. *Gastroenterology* 2019; **157**: 682-691. e2 [PMID: 31152740 DOI: 10.1053/j.gastro.2019.05.056]
- 115 **Amirian ES**. Potential fecal transmission of SARS-CoV-2: Current evidence and implications for public health. *Int J Infect Dis* 2020; **95**: 363-370 [PMID: 32335340 DOI: 10.1016/j.ijid.2020.04.057]
- 116 **Arslan M**, Xu B, Gamal El-Din M. Transmission of SARS-CoV-2 via fecal-oral and aerosols-borne routes: Environmental dynamics and implications for wastewater management in underprivileged societies. *Sci Total Environ* 2020; **743**: 140709 [PMID: 32652357 DOI: 10.1016/j.scitotenv.2020.140709]
- 117 **Hindson J**. COVID-19: faecal-oral transmission? *Nat Rev Gastroenterol Hepatol* 2020; **17**: 259 [PMID: 32214231 DOI: 10.1038/s41575-020-0295-7]
- 118 **Ahmed W**, Angel N, Edson J, Bibby K, Bivins A, O'Brien JW, Choi PM, Kitajima M, Simpson SL, Li J, Tschärke B, Verhagen R, Smith WJM, Zaugg J, Dierens L, Hugenholtz P, Thomas KV, Mueller JF. First confirmed detection of SARS-CoV-2 in untreated wastewater in Australia: A proof of concept for the wastewater surveillance of COVID-19 in the community. *Sci Total Environ* 2020; **728**: 138764 [PMID: 32387778 DOI: 10.1016/j.scitotenv.2020.138764]
- 119 **Medema G**, Heijnen L, Elsinga G, Italiaander R, Brouwer A. Presence of SARS-Coronavirus-2 RNA in sewage and correlation with reported COVID-19 prevalence in the early stage of the epidemic in the Netherlands. *Environ Sci Technol Lett* 2020; **7**: 511-516 [DOI: 10.1021/acs.estlett.0c00357]



Published by **Baishideng Publishing Group Inc**  
7041 Koll Center Parkway, Suite 160, Pleasanton, CA 94566, USA

**Telephone:** +1-925-3991568

**E-mail:** [bpgoffice@wjgnet.com](mailto:bpgoffice@wjgnet.com)

**Help Desk:** <https://www.f6publishing.com/helpdesk>

<https://www.wjgnet.com>

